POLITECNICO DI TORINO

Master's Degree in Chemical and sustainable process engineering

Master's Degree Thesis

SYNTHESIS AND ANTIBACTERIAL EVALUATION OF PHOTOCHROMIC MOLECULES

Supervisors

Prof. Francesca BOSCO

Prof. Estelle LEONARD

Candidate

Stefania RIESI

October 2024

Abstract

The ability of bacterial species to resist antimicrobial agents is an increasingly serious and widespread phenomenon in the 21st century. In hospital settings, this issue is even more severe and evident, capable of causing hospital-acquired infections (HAIs), particularly nosocomial infections (NIs) mainly contracted from contaminated hospital equipment. The main multidrug-resistant bacteria (MDR) involved include methicillin-resistant *Staphylococcus aureus* (MRSA), extended-spectrum β-lactamase (ESBL) producers, and *Mycobacterium tuberculosis*. The growing number of resistances developed by bacterial species highlights the need to find new, effective, and non-toxic alternatives to known antibacterial substances, capable of interacting innovatively with the microorganisms in question. In this context, the conformational switching of azobenzene has allowed for the observation of variations in the potency and efficacy of existing drugs modified with azocompounds, as well as the ability to modulate drug activity, thereby reducing the possibility of drug resistance occurring. From this perspective, this thesis aims to present the synthesis procedure, characterization, and evaluation of the antimicrobial activity of a group of analyzed azobenzenes.

Summary

Infezioni nosocomiali e batteri coinvolti

Le infezioni nosocomiali, o infezioni ospedaliere, rappresentano un grave problema di salute pubblica a livello mondiale. Circa l'8,7% dei pazienti ospedalizzati ne è affetto, secondo un'indagine dell'OMS. Tali infezioni vengono acquisite negli ambienti ospedalieri e possono essere trasmesse sia attraverso il personale sanitario che tramite superfici contaminate. I pazienti più vulnerabili, come anziani, immunodepressi e persone con patologie croniche, sono particolarmente esposti. Le infezioni ospedaliere sono per lo più causate da batteri, tra cui spiccano *Staphylococcus aureus*, *Escherichia coli*, *Pseudomonas aeruginosa*, e gli *Enterococcus*. Questi batteri possono sviluppare resistenze ai trattamenti antibiotici, trasformando infezioni comuni in condizioni difficili da trattare.

La resistenza antimicrobica è una delle principali sfide connesse alle infezioni nosocomiali. Essa può essere sia intrinseca che acquisita, tramite mutazioni genetiche o scambio di geni di resistenza tra batteri. Questo fenomeno è amplificato dalla pressione selettiva esercitata dall'uso eccessivo o inappropriato di antibiotici e biocidi. Esempi noti di batteri resistenti includono *Staphylococcus aureus* resistente alla meticillina (MRSA), la tubercolosi multiresistente (XDR-TB) e i batteri produttori di β-lattamasi a spettro esteso (ESBL), enzimi che rendono inefficaci molti antibiotici, specialmente le cefalosporine.

I meccanismi di resistenza dei batteri includono la produzione di enzimi che inattivano gli antibiotici, l'aumento dell'efflusso dei farmaci dalle cellule batteriche tramite pompe di efflusso, e le mutazioni nei target molecolari degli antibiotici, che rendono i farmaci meno efficaci. Una sfida cruciale è rappresentata dal trasferimento orizzontale di geni di resistenza, che avviene attraverso plasmidi, trasposoni e altri elementi genetici mobili. Questo fenomeno permette ai batteri resistenti di diffondersi rapidamente all'interno degli ambienti ospedalieri, complicando la gestione delle infezioni e richiedendo approcci terapeutici sempre più innovativi.

I batteri studiati in laboratorio nel contesto della ricerca descritta includono *Escherichia*

coli, *Pseudomonas fluorescens*, *Bacillus subtilis*, *Micrococcus luteus*, *Staphylococcus epidermidis*, ed *Erwinia persicina*. Questi batteri sono stati scelti per la loro rilevanza clinica e per la variabilità morfologica e fisiologica, offrendo modelli utili per lo studio della resistenza antimicrobica e dei meccanismi di sopravvivenza dei batteri in ambienti ostili come quelli ospedalieri.

In sintesi, le infezioni nosocomiali e la resistenza antimicrobica sono sfide cruciali nel campo della salute pubblica, richiedendo un'attenzione costante per prevenire la diffusione di ceppi resistenti e per sviluppare trattamenti efficaci.

Gli azobenzeni

L'aumento di ceppi batterici multi-resistenti (MDR) negli ospedali è una crescente preoccupazione, sottolineando la necessità urgente di sviluppare nuovi agenti antibatterici. Alcuni azobenzeni mostrano attività antimicrobica intrinseca, che varia in base al tipo e alla posizione dei sostituenti sui loro anelli aromatici.

Gli azobenzeni sono composti chimici caratterizzati da un legame -N=N- tra due anelli aromatici. Questi composti sono noti per le loro proprietà ottiche, dovute alla possibilità di isomerizzazione fotoindotta tra le forme trans e cis, che modifica le loro caratteristiche spettrali. Gli azobenzeni sono sintetizzati principalmente attraverso una reazione di accoppiamento azoico, che coinvolge un sale di diazonio e un fenolato. Questa reazione, utilizzata ampiamente nell'industria dei coloranti, è sensibile al pH e deve essere eseguita a basse temperature per evitare la decomposizione dei sali di diazonio, che sono instabili e potenzialmente esplosivi a temperature superiori a 5°C.

Dal punto di vista biologico, gli azobenzeni hanno guadagnato attenzione per le loro applicazioni in fotofarmacologia, grazie alla loro capacità di modulare l'attività biologica tramite isomerizzazione. Questo permette di influenzare processi come la neurotrasmissione o le proprietà anticancerogene, riducendo il rischio di resistenza ai farmaci. Diversi studi hanno dimostrato che gli azobenzeni possiedono attività antimicrobiche, antivirali, antiossidanti e antitumorali, ma la ricerca si concentra principalmente sulle loro proprietà antibatteriche. L'attività antimicrobica degli azobenzeni varia in funzione dei sostituenti presenti sugli anelli aromatici. Ad esempio, alcuni composti azobenzenici con gruppi nitro (NO_2) in posizioni specifiche sugli anelli aromatici hanno dimostrato una forte attività contro batteri come *Staphylococcus aureus* e *Candida krusei*.

Inoltre, i surfattanti basati sugli azobenzeni con teste polari a base di zucchero hanno

mostrato efficacia nel bloccare la crescita dei biofilm di *Pseudomonas aeruginosa*, mentre gli azobenzeni con minime funzionalizzazioni sono efficaci contro i biofilm di batteri gram-positivi, inibendo specifici processi metabolici come la sintesi di ATP e la proteina chinasi.

Un'altra interessante applicazione degli azobenzeni riguarda i derivati chinolonici, che sono agenti antibatterici ad ampio spettro. L'integrazione di un gruppo azobenzenico in questi composti consente di modulare la loro attività antimicrobica tramite isomerizzazione fotoindotta, mantenendo l'efficacia contro batteri sia gram-positivi che gram-negativi.

Alizarina

L'alizarina è un pigmento rosso derivato dalle radici delle piante di robbia, che presenta proprietà antiossidanti, antibatteriche e antimicrobiche. Essendo un composto di antrachinone con gruppi idrossilici (-OH) sostituiti nelle posizioni 1 e 2, l'alizarina è stata identificata come un indicatore colorimetrico o di pH altamente sensibile. Questo è dovuto alle sue proprietà colorimetriche che variano in funzione del pH, le quali sono state sfruttate anche nella tecnologia di imballaggio alimentare intelligente. Alcuni studi hanno dimostrato la sua efficacia contro i biofilm di *Staphylococcus aureus* e *Staphylococcus epidermidis*.

Reagenti, solventi e materiali usati nella sintesi organica

I reagenti organici e i solventi utilizzati provengono da Acros Organics, Sigma-Aldrich e SDS Carlo-Elba, usati senza trattamenti preliminari. L'acqua per la microbiologia è stata purificata con il sistema Veolia Elga Purelab Flex, mentre per le sintesi è stata utilizzata acqua di rubinetto non purificata. Le analisi di cromatografia su strato sottile sono state eseguite su piastre di alluminio Merck Kieselgel 60F254, mentre la purificazione delle miscele di reazione è avvenuta tramite un sistema di cromatografia Büchi Pure Flash 810. Le analisi NMR sono state eseguite con uno strumento Bruker UltraShield 400MHz/54 mm Ultra long hold.

Procedura generale di sintesi

Gli azobenzeni sono stati sintetizzati a partire da varie aniline e fenoli. Il fenolato viene preparato in una soluzione acquosa con aggiunta del carbonato di sodio e del fenolo selezionato. Il sale diazonio viene preparato separatamente dal fenolato, aggiungendo acido cloridrico e nitrito di sodio, mantenendo il tutto sotto i 5°C. Il fenolato viene poi lentamente aggiunto al sale diazonio, la miscela viene lasciata a temperatura ambiente per 3 ore sotto agitazione, e successivamente filtrata. Se il prodotto è oleoso, viene estratto con etil acetato, asciugato con $MgSO_4$, e l'acetato di etile viene evaporato.

Caratterizzazione dei prodotti

La cromatografia su strato sottile è stata eseguita su piastre di alluminio, utilizzando una fase mobile costituita da cicloesano ed etil acetato (Cicloesano/Acetato di etile, 7:3). La separazione dei composti si basa sulla competizione tra il soluto e la fase mobile per i siti di legame sulla fase stazionaria. Se la fase stazionaria è rappresentata dal gel di silice, che è considerato polare, un composto più polare avrà una maggiore affinità con la silice. Questo significa che il composto più polare sarà in grado di legarsi più facilmente alla fase stazionaria, restando più in basso sulla piastra al termine della procedura. La piastra viene successivamente esposta alla luce UV per verificare la migrazione dei composti.

Per la separazione e la purificazione dei composti delle miscele di reazione, è stato usato il sistema di cromatografia flash Büchi Pure Flash 810 con colonne di silice. Il prodotto secco è stato miscelato con gel di silice e acetone, poi evaporato e posto all'interno di una colonna vuota all'interno. La separazione è stata effettuata con il mix di solventi già utilizzato nella cromatografia su strato sottile (Cicloesano/Acetato di etile, 7:3). Il software controlla un sistema automatizzato che raccoglie le frazioni contenenti il composto target e aiuta a localizzare il materiale purificato all'interno del collettore di frazioni. Inoltre, salva il cromatogramma risultante dal processo per archivio e consultazioni future.

La spettroscopia di risonanza magnetica nucleare (RMN) è stata utilizzata per determinare la struttura molecolare degli azobenzeni. Uno dei vantaggi principali della tecnologia RMN è la sua capacità di servire da strumento analitico primario, permettendo la valutazione quantitativa della purezza del composto senza l'esigenza di uno standard di riferimento specifico. Le analisi sono state eseguite su campioni preparati in cloroformio o metanolo. Il solvente deve essere adatto alla sostanza da analizzare per evitare che i picchi del solvente nello spettro RMN interferiscano con quelli del campione. L'azobenzene deve essere solubile nel solvente prescelto per garantire che la soluzione sia limpida e priva di particelle solide che potrebbero interferire con il segnale RMN. Ciò contribuisce

a garantire una buona qualità del segnale e una scansione uniforme.

Il test di isomerizzazione ha coinvolto l'esposizione degli azobenzeni alla luce UVA per convertire la conformazione trans in cis. L'assorbimento spettrale è stato misurato prima e dopo l'esposizione per verificare la corretta isomerizzazione e determinare il tempo necessario per la transizione. In condizioni sperimentali, l'assorbanza è stata monitorata usando una soluzione di azobenzene in un mix di solventi (DMSO ed etanolo), seguita da misurazioni cicliche per analizzare il passaggio tra le forme isomeriche.

Risultati

Sono stati ottenuti in totale 8 prodotti dalle reazioni di accoppiamento azoico realizzate. Per verificare la presenza dell'azobenzene desiderato all'interno del prodotto di reazione, è necessario eseguire uno step di purificazione tramite cromatografia flash con colonne di silice. Dopo aver eseguito la cromatografia flash sui prodotti di sintesi, sono stati analizzati alcuni campioni per identificare i picchi corrispondenti ai prodotti desiderati. Ogni cromatogramma ottenuto è stato sottoposto a una successiva verifica tramite cromatografia su strato sottile per confermare la presenza dell'azobenzene. Nei casi in cui i prodotti risultavano puri, veniva evaporata la miscela solvente usata nella cromatografia, ottenendo un prodotto secco per ulteriori analisi.

Per i primi 4 prodotti sintetizzati, sono stati identificati facilmente i campioni contenenti l'azobenzene desiderato. Dopo l'evaporazione del solvente, è stato confermato tramite NMR che i prodotti erano effettivamente gli azobenzeni attesi.

Il quinto prodotto ha mostrato una complicazione significativa: l'analisi tramite cromatografia su strato sottile e RMN ha rivelato che, oltre all'azobenzene, il campione conteneva una grande quantità di alizarina residua, un sottoprodotto non desiderato. Ciò ha sollevato dubbi sul fatto che il picco osservato nel cromatogramma corrispondesse effettivamente all'azobenzene. Per migliorare la resa, è stata ripetuta la reazione con il doppio della quantità di nitrito di sodio e anilina, mantenendo costante la quantità di alizarina. Nonostante un aumento dell'intensità dei punti sulla piastra di cromatografia su strato sottile indicasse una maggiore quantità di prodotto desiderato, l'analisi RMN ha successivamente confermato che il prodotto ottenuto era principalmente alizarina residua e prodotti di scarto di reazione, non l'azobenzene.

L'analisi RMN del prodotto ottenuto dalla reazione con alizarina ha rivelato che non si trattava dell'azobenzene atteso. Il motivo principale potrebbe essere la reattività elevata dei due gruppi ossidrilici presenti nell'alizarina, che possono aver partecipato a reazioni collaterali, riducendone la quantità disponibile per la reazione di accoppiamento azoico

con l'anilina. Inoltre, la struttura dell'alizarina potrebbe aver creato un ingombro sterico, impedendo un efficace avvicinamento del sale di diazonio, e quindi riducendo l'efficienza della formazione di azobenzene.

A causa di questi problemi, solo i primi quattro composti sintetizzati, che hanno mostrato spettri RMN coerenti con la struttura attesa dell'azobenzene, sono stati considerati validi e utilizzati per ulteriori analisi e test successivi.

Il test di isomerizzazione è stato condotto sui primi quattro composti sintetizzati per valutare la loro capacità di cambiare conformazione sotto l'influenza della luce UVA, un aspetto cruciale per controllare le proprietà biologiche delle molecole di azobenzene. Il processo di isomerizzazione avviene tra le configurazioni trans e cis, con un cambiamento visibile attraverso le variazioni delle bande di assorbimento nello spettro UV. Durante l'isomerizzazione da trans a cis, si osserva una diminuzione dell'intensità della banda di assorbimento intorno ai 350-400 nm (corrispondente alla transizione $\pi \Rightarrow \pi^*$ dell'azobenzene) e un aumento a circa 450 nm (corrispondente alla transizione n $\Rightarrow \pi^*$ dell'azobenzene). Ciò è dovuto alla geometria più planare e simmetrica della conformazione trans, che permette una migliore delocalizzazione degli elettroni π, causando l'assorbimento a lunghezze d'onda maggiori (350-400 nm). L'illuminazione UVA a queste lunghezze d'onda maggiori, promuove la transizione $\pi \Rightarrow \pi^*$, inducendo il passaggio alla conformazione cis, che, essendo più piegata, mostra una minore delocalizzazione degli elettroni e un assorbimento a lunghezze d'onda più corte (280-300 nm). In questo caso, l'assorbimento della luce a queste lunghezze d'onda può anch'essa promuovere l'isomerizzazione, ma verso la conformazione trans. Inoltre, l'illuminazione UVA può indurre la transizione n $\Rightarrow \pi^*$, meno energetica, che facilita l'isomerizzazione da trans a cis.

Per tre dei quattro azobenzeni testati, l'isomerizzazione è risultata rapida ed efficace, mentre per il quarto composto il passaggio è stato meno evidente e più lento, richiedendo 10 minuti di esposizione alla luce UVA senza grandi cambiamenti di intensità di banda. Questo risultato potrebbe essere attribuito alla presenza del gruppo azotato nella struttura, che potrebbe destabilizzare la delocalizzazione degli elettroni π e rendere l'isomerizzazione meno efficiente. Inoltre, la maggiore stabilità termodinamica della forma trans, potenziata dal gruppo azotato attraverso legami idrogeno, potrebbe ostacolare ulteriormente la transizione alla forma cis.

Materiali, mezzi di coltura e tecniche per le proprietà biologiche

I ceppi batterici impiegati sono *Escherichia coli* ATCC 25922, *Micrococcus luteus* CRBIP 107660, *Bacillus subtilis* ATCC 6051, *Staphylococcus epidermidis* ATCC 35984, *Erwinia persicina* e *Pseudomonas fluorescens*. Questi batteri sono coltivati su Agar Trypticase Soy (TSA) solido e incubati a 30°C al buio per 24 ore. Dopo l'incubazione, le piastre vengono conservate a 4°C o utilizzate per inoculare 20 mL di terreno liquido per i test su micropiastre o i test di inibizione.

I batteri sono coltivati su terreno TSA (Tryptic Soy Agar) con una concentrazione di 40 g/L, sterilizzato in autoclave a 120°C per 15 minuti a 2,2 bar. Il terreno viene versato in capsule Petri, e i batteri sono inoculati sulla superficie dell'agar in condizioni sterili. Le piastre inoculate sono incubate a 30°C per 24 ore, poi conservate a 4°C, o utilizzate per inoculare terreno liquido 24 ore prima dei test.

Il terreno di coltura minerale MM2 è specifico per i metanotrofi, contenente sali minerali e nutrienti. Due versioni sono utilizzate: una senza e una con estratto di lievito, sterilizzate in autoclave a 120°C per 15 minuti. Prima dei test di resistenza ai raggi UVA o dei test antimicrobici, viene aggiunta una soluzione di glucosio al terreno liquido per ottenere una concentrazione finale di glucosio di 10 g/L.

Test di resistenza ai raggi UVA

Prima di eseguire i test antimicrobici, è necessario determinare se i batteri sono sensibili alla luce UVA. Questo è fondamentale perché l'esposizione alla luce UVA potrebbe mascherare l'effetto dell'azobenzene. Il test è stato condotto su *Erwinia persicina*, *Pseudomonas fluorescens* e *Staphylococcus epidermidis*. Per coltivare i batteri in un terreno liquido, si lavora in condizioni sterili utilizzando una cappa a flusso laminare. Il terreno MM2 senza estratto di lievito è utilizzato per *Erwinia persicina* e *Pseudomonas fluorescens*, mentre il terreno MM2 con estratto di lievito è usato per *Staphylococcus epidermidis*. I batteri sono raccolti dalle capsule Petri e trasferiti nei tubi con all'interno terreno liquido e soluzione di glucosio. I tubi sono sigillati e incubati a 30°C sotto agitazione per 24 ore. Successivamente, si misura la densità ottica (DO) a 600 nm. I campioni vengono diluiti per raggiungere una DO di 0,2 in 10 mL. Successivamente i campioni vengono divisi in due tubi più piccoli, uno dei quali è esposto alla luce UVA, mentre l'altro è ricoperto con alluminio per evitare l'esposizione. Le lampade UVA hanno una potenza di 6W e una lunghezza d'onda di 385-405 nm. La DO viene misurata ogni ora o dopo 24 ore per verificare l'influenza della luce UVA sulla crescita batterica.

Risultati

I test di resistenza ai raggi UVA hanno mostrato che tutte i batteri analizzati, tranne *E.persicina*, continuano a crescere anche sotto l'esposizione alla luce UVA. La crescita batterica è stata verificata tramite misurazione della densità ottica (DO) a 600 nm, sia in presenza che in assenza di luce UVA.

La crescita è stata determinata confrontando la differenza tra DO_{max} - DO_{min} dei batteri e DO_{max} - DO_{min} del mezzo liquido sterile su un periodo di 24 ore. Per ogni batterio, sono stati condotti tre test con e senza UVA, per un totale di sei provette per batterio. La misurazione del mezzo liquido sterile è stata effettuata per verificare l'assenza di contaminazioni da microorganismi esterni. Una significativa differenza DO_{max} - DO_{min} in presenza di UVA indica che i batteri non sono sensibili all'azione inattivante della luce UVA. Le deviazioni standard sono state calcolate a partire dalle tre misurazioni di DO per ogni batterio.

Test antimicrobici

Il test in piastre multipozzetto è una tecnica essenziale per valutare l'efficacia dei composti antibatterici contro diversi ceppi batterici. Essa consente di analizzare rapidamente l'impatto di varie concentrazioni di un composto su numerosi campioni simultaneamente. Inizialmente, si preparano concentrazioni diverse di azobenzeni da testare successivamente in microplacche. In seguito, si coltivano i batteri su un mezzo solido e si lasciano tutta la notte nell'incubatore a 30°C. Il giorno successivo si trasferiscono in un mezzo liquido e, anche questa volta, si mettono sotto agitazione a 30°C. Il terzo giorno si può procedere con la distribuzione dei due azobenzeni da testare su ogni piastra e all'inoculazione dei batteri. Le piastre multipozzetto vanno inserite nell'incubatore a 30°C sotto agitazione moderata per evitare fuoriuscite. Dopo 24 ore, si verifica l'inibizione tramite misurazione di densità ottica a 600 nm per verificare l'effetto degli azobenzeni con e senza esposizione a luce UVA.

Il test di inibizione è una tecnica microbiologica semplice e visivamente chiara per valutare l'efficacia degli agenti antimicrobici. Si utilizza sia il metodo di diffusione su disco che quello su agar. Nel primo caso, dei dischi di carta filtro vengono impregnati con diverse concentrazioni di azobenzeni e successivamente posizionati su capsule Petri. Di seguito, avviene l'inoculazione del batterio in modo uniforme su tutta la capsula. Nel secondo caso, si creano dei fori sulla superficie dell'agar e si riempiono con la soluzione

di azobenzene. Entrambi i metodi determinano la zona di inibizione, ossia l'area in cui i batteri non crescono grazie all'azione dell'antibiotico, consentendo la misurazione della concentrazione minima inibitoria (MIC).

Facendo un confronto tra le due metodologie, i test in piastre multipozzetto richiedono attrezzature specializzate e sono più costosi, mentre i test di inibizione offrono risultati qualitativi, possono essere meno precisi e influenzati dalle proprietà dell'agar.

Risultati

Nello studio sull'attività antimicrobica degli azobenzeni, è stato utilizzato il test in piastre multipozzetto per valutare l'effetto antimicrobico dei due azobenzeni A1 e A3 su diversi batteri, valutando la crescita batterica prima e dopo 24 ore di esposizione alla luce UVA, o in sua assenza. I batteri testati includono *Staphylococcus epidermidis*, *Escherichia coli*, *Micrococcus luteus* e *Bacillus subtilis*.

Il primo batterio testato è stato *S.epidermidis*, un batterio gram-positivo che tende a formare aggregati, che potrebbero potenzialmente causare problemi di diffusione uniforme della sostanza antimicrobica all'interno della massa.

Confrontando i due composti antibatterici utilizzati, è evidente che l'azobenzene A3 è molto più efficace nell'inibire la crescita di *S.epidermidis*. In particolare, il composto A3 ha mostrato un'inibizione del 46.6% sotto esposizione UVA rispetto al 15% in sua assenza, con una propagazione della deviazione standard rispettivamente del 9.6% e 8.4%. Il composto A1, invece, ha mostrato un'inibizione del 25.5% sotto UVA e del 14.8% senza UVA, con una propagazione della deviazione standard rispettivamente del 3.8 % e 6%.

In generale, i test hanno dimostrato che l'esposizione alla luce UVA aumenta l'efficacia degli azobenzeni nell'inibire i batteri. La configurazione cis degli azobenzeni sembra quindi più efficace, probabilmente grazie alla sua struttura più compatta e reattiva, che facilita l'interazione con le membrane cellulari batteriche. Tuttavia, alcune discrepanze nei dati, specialmente a basse concentrazioni, suggeriscono la possibilità di errori strumentali o di manipolazione.

E.coli è un batterio gram-negativo con una complessa struttura della parete cellulare, che rende più difficile l'interazione da parte delle sostanze antimicrobiche. In generale, i risultati mostrano che i tassi di inibizione di *Escherichia coli* sono superiori a quelli di *Staphylococcus epidermidis*, nonostante la complessità della parete cellulare di *E.coli*. Ciò potrebbe essere dovuto al fatto che *E.coli* non tende a formare aggregati

cellulari come *S.epidermidis*, permettendo una migliore diffusione della sostanza antimicrobica e, di conseguenza, tassi di inibizione più elevati. La formazione di aggregati in *S.epidermidis* impedisce all'azobenzene di penetrare completamente, lasciando una parte di cellule batteriche non inibite e riducendo così il tasso medio di inibizione.

Confrontando i due composti antibatterici utilizzati, A3 ha mostrato risultati più consistenti ed affidabili rispetto ad A1, ottenendo un massimo di inibizione del 65,5% a 5 g/L sotto UVA, con una deviazione standard del 11,8%. Al contrario, A1 ha raggiunto un'inibizione del 79% a una concentrazione di 2,5 g/L, ma con una propagazione della deviazione standard elevata (37,9%), indicando una minore affidabilità ed un'incoerenza nel risultato a concentrazione maggiore. Le discrepanze nei risultati di A1 potrebbero essere attribuite alla formazione di precipitati dovuti a una scarsa solubilità dell'azobenzene nel solvente utilizzato (DMSO), compromettendo l'omogeneità del test.

Micrococcus luteus è un batterio gram-positivo a forma di cocco che tende a formare gruppi irregolari, simili a quelli di *S.epidermidis*. Questa disposizione può ostacolare la diffusione uniforme delle sostanze antimicrobiche. Nei test in piastre multipozzetto, si utilizzano controlli positivi, che dovrebbero mostrare crescita dopo le 24 ore, e negativi, che non dovrebbero mostrare alcuna crescita batterica dopo le 24 ore per garantire la validità dei risultati. Tuttavia, durante l'esperimento, il controllo negativo ha mostrato crescita batterica dopo 24 ore, segnalando una possibile contaminazione del terreno di coltura. Di conseguenza, i risultati ottenuti con *M.luteus* non sono considerati validi.

Analogamente, nei test su *Bacillus subtilis*, i risultati non sono ritenuti affidabili, probabilmente a causa della formazione di biofilm, che ha impedito un'adeguata azione inibitoria da parte degli azobenzeni. Sebbene i controlli abbiano confermato la correttezza del test, la bassa solubilità degli azobenzeni o errori durante la manipolazione automatizzata dei liquidi potrebbero aver compromesso i risultati. Pertanto, anche i risultati su *B.subtilis* non possono essere considerati validi per trarre conclusioni sull'attività degli azobenzeni analizzati.

In sintesi, lo studio ha evidenziato l'importanza della configurazione cis degli azobenzeni, ottenuta tramite foto isomerizzazione tramite luce UVA, nell'aumentare l'efficacia antimicrobica, in particolare l'isomero cis dell'azobenzene A3 che ha mostrato i risultati migliori. Tuttavia, i problemi sperimentali incontrati indicano la necessità di ulteriori approfondimenti per convalidare i risultati, soprattutto per quanto riguarda l'affidabilità delle misurazioni e la gestione delle variabili sperimentali.

Nel test delle zone di inibizione, è stata utilizzata inizialmente la tecnica con i dischi di diffusione, ma i risultati non sono stati soddisfacenti poiché non si sono formate zone di inibizione. Questo fallimento è stato attribuito alla scarsa diffusione della sostanza

antimicrobica attraverso il gel di agar a partire dai dischi di diffusione. Per ovviare a questo problema, è stato proposto un metodo alternativo senza l'uso di dischi di carta, che ha dato risultati più coerenti. Questo metodo alternativo prevede la creazione di fori nell'agar in cui viene inserita direttamente la soluzione di azobenzene. I risultati ottenuti con questo approccio sono stati più soddisfacenti, ma hanno fornito solo dati qualitativi o semi-quantitativi, non comparabili con la precisione dei test in piastre multipozzetto.

È stata proposta un'analisi quantitativa basata sul valore MIC (concentrazione minima inibente) per valutare l'efficacia degli antibiotici, utilizzando modelli di diffusione "libera" (modello quadratico) e "dissipativa" (modello lineare). I risultati hanno mostrato che il modello di diffusione dissipativa, che considera la perdita della sostanza antimicrobica durante la diffusione, si adatta meglio ai dati ottenuti, soprattutto per sostanze relativamente idrofobiche come gli azobenzeni. Confrontando i due modelli, si è osservato che i valori di MIC sono inferiori con il modello lineare, suggerendo una maggiore attività antimicrobica.

I test hanno anche rivelato che l'esposizione alla luce UVA migliora l'attività inibitoria degli azobenzeni, confermando i risultati ottenuti in piastre multipozzetto. Nello specifico, l'azobenzene A3 ha mostrato una maggiore efficacia contro *E.coli* rispetto ad A1, mentre per *S.epidermidis* A1 è risultato più efficace. Tuttavia, le differenze tra i due batteri possono essere attribuite alle loro strutture cellulari e al comportamento in diversi ambienti.

In sintesi, i test hanno evidenziato che gli azobenzeni sono più efficaci contro *S.epidermidis* su terreno di coltura solido rispetto a *E.coli*, probabilmente a causa della minore complessità della parete cellulare di *S.epidermidis* e dell'assenza di agglomerati nel mezzo solido. Tuttavia, le discrepanze tra i risultati in piastre multipozzetto e su agar richiedono ulteriori verifiche per stabilire conclusioni definitive.

Acknowledgements

This work was carried out at the Microbial Activities and Bioprocesses (MAB) laboratory at one of the campuses of the Université de Technologie de Compiègne during my mobility experience abroad. I would like to thank all the members of the laboratory team who welcomed me into their big family from the beginning, helping me and teaching me so much. In particular, I would like to thank my co-supervisor, Estelle Leonard, who allowed me to carry out this work as part of a larger project. I am grateful to her for guiding me through this journey and teaching me all the necessary chemical and microbiological procedures for the work, always giving me the space to learn and try things firsthand.
I would also like to thank my supervisor, Francesca Bosco, for supporting me from Italy and always being available to provide clarifications and corrections to the manuscript.

I would like to thank my friends, my boyfriend, and especially my parents, who have always supported me throughout this experience.
In general, I thank all the people who were close to me during this wonderful experience abroad, which allowed me to discover and learn many things both from an academic perspective and a human and social point of view.

Table of Contents

List of Tables

List of Figures

Acronyms

HAIs
Hospital-acquired infections

NIs
Nosocomial infections

WHO
World Health Orgnization

RNA
Ribonucleic acid

DNA
Deoxyribonucleic acid

MDR
Multidrug-resistant

XDR
Extensively drug-resistant

PDR
Pandrug-resistant

PGA
Poly-y-glutamic acid

AMPs
Antimicrobial peptides

TLC

Thin layer chromatography

NMR

Nuclear magnetic resonance

DMSO

Dimethyl sulfoxide

ATCC

American Type Culture Collection

TSA

Trypticase Soy Agar

CRBIP

Biological Resource Center of Institut Pasteur

MM2

Mineral Medium

OD

Optical density

MIC

Minimum inhibitory concentration

MRSA

Methicillin-resistant Staphylococcus aureus

Chapter 1

State of the art

1.1 Nosocomial infections

Hospital-acquired infections (HAIs) are one of the most serious public health problems of the 21st century. Globally, over 1.4 million people worldwide suffer from infectious complications acquired in hospitals. An epidemiological investigation implemented by the World Health Organization (WHO) in 55 hospitals of 14 countries from 4 WHO Regions (Europe, Eastern Mediterranean, South-East Asia, and Western Pacific) revealed an average of 8.7% of hospital patients had a nosocomial infection [1].

Nosocomial infection is a kind of infection contracted from the environment or staff of a healthcare facility. Infection happens in the clinical setting through contaminated equipment, bedding articles, or aerosols, staff also can spread infection. The infections acquired by the workers and the staff during duty in the occupational environment are also included as nosocomial infections [2].
These infections majorly affect hospitalized patients. In particular, the patient's susceptibility state has effects on the risk of developing various nosocomial infections. Older people are at greater risk of developing HAIs due to immune senescence and decline in the immune system with increasing age. In addition to the causative agents and environmental factors, host susceptibility is a crucial factor in the occurrence of nosocomial infections. Key aspects of host susceptibility include age, chronic diseases, immune status, diagnostic and therapeutic procedures, as well as environmental conditions [3].

Nosocomial infections are caused by many microbes and each one can cause infection in healthcare settings. Bacteria account for approximately ninety percent of infections, while protozoans, fungi, viruses, and mycobacteria contribute less significantly compared to bacterial infections. Hospital-acquired infections are commonly caused by agents such as *Streptococcus* species, *Acinetobacter* species, enterococci, *Pseudomonas aeruginosa*,

coagulase-negative staphylococci, *Staphylococcus aureus*, *Bacillus cereus*, *Legionella*, and members of the *Enterobacteriaceae* family including *Proteus mirabilis*, *Klebsiella pneumoniae*, *Escherichia coli*, and *Serratia marcescens*. Among these, enterococci, *Pseudomonas aeruginosa*, *Staphylococcus aureus*, and *Escherichia coli* play particularly significant roles [4].

Hospital environments are settings where a variety of microorganisms from different sources interact, but these environments are also regularly cleaned and disinfected with various biocides. As a result, there is a high potential for horizontal gene transfer and strong selective pressure that promotes the emergence of resistant strains.

1.1.1 The phenomenon of antibacterial resistance

Mechanism of action of antimicrobial agents

In order to appreciate the mechanisms of resistance, it is important to understand how antimicrobial agents act. Antimicrobial agents target essential microbial functions with minimal or no impact on host functions. These agents operate through various mechanisms shown in figure 1.1, and understanding both these mechanisms and the chemical nature of the agents is key to comprehending how resistance to them develops [5].

The distinction between bactericidal and bacteriostatic antibiotics is an effective way to differentiate between those that kill bacteria, known as 'bactericidal,' and those that inhibit bacterial growth, referred to as 'bacteriostatic'. Bacteriostatic antimicrobial agents work by inhibiting the growth or reproduction of bacteria, giving the host's immune system time to eliminate them. As a result, the complete removal of bacteria depends on the immune system's effectiveness. In contrast, bactericidal agents directly kill bacteria, ensuring their elimination regardless of the host's immune response. Antimicrobial agents can also be classified based on the specific bacterial structures or functions they target, including inhibiting cell wall synthesis, RNA synthesis, DNA replication, protein synthesis, enzymatic activity, and cell membrane function.

Figure 1.1: Antibacterial activity mechanism [6]

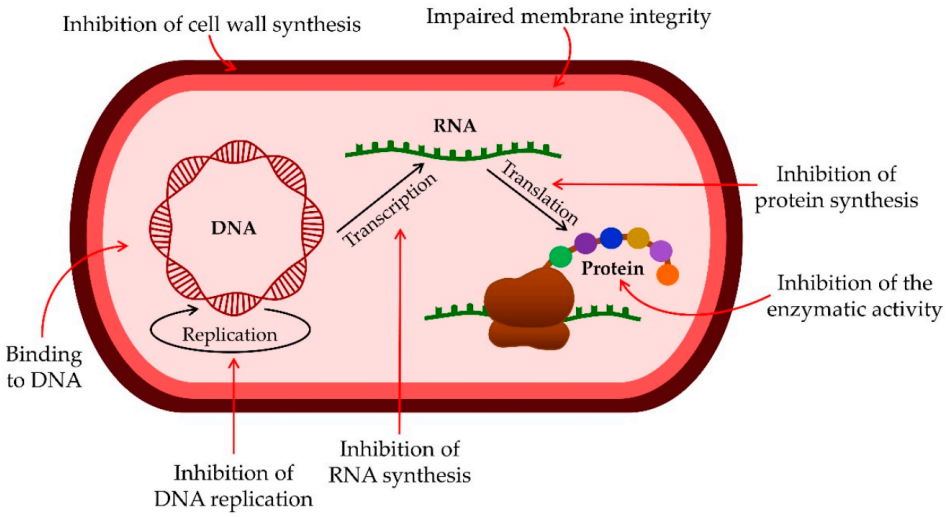

Mechanism of antimicrobial resistance

Antibiotic resistance can be either intrinsic or acquired. Intrinsic, natural, or passive resistance occurs when microorganisms inherently lack the target sites needed for a drug to be effective or when they naturally have low permeability to the drug. This low permeability is often due to differences in the drug's chemical nature and the microbial membrane's structure, especially in cases where the drug needs to enter the microbial cell to be effective.

Acquired or active resistance, the primary mechanism behind antimicrobial resistance, arises when bacteria develop countermeasures against a specific antimicrobial or class of antimicrobials due to evolutionary pressure. This leads previously sensitive bacterial populations to become resistant. This form of resistance occurs through changes in the bacterial genome. Bacteria can acquire resistance through mutations, which are then passed down to daughter cells through selection. More commonly, resistance is gained through the horizontal transfer of resistance genes between different strains and species. This gene exchange can occur via transformation, transduction, or conjugation.

There are several mechanisms through which bacteria achieve resistance to antibiotics: qualitative alteration of the target that reduces the affinity for antibiotics either by mutation or by target modification; inactivation of antibiotics by enzymic modification; post-transcriptional or post-translational modification of the antimicrobial agent's target, which reduces binding of the antimicrobial agent; overproduction of the target of the antimicrobial agent; synthesis of an additional drug-resistant enzyme; synthesis of

an additional enzyme that inactivates the antimicrobial agent; increased efflux of the antimicrobial agent; reduced uptake of the antimicrobial agent into the cell [7] [8].

1.1.2 The microorganisms responsible for nosocomial infections

Multidrug-resistant bacteria (MDR) result from the proliferation of bacteria that have acquired one or more genes conferring resistance to antibiotics. Specifically, non-susceptibility to at least one agent in three or more antimicrobial categories. In this category, we can distinguish extensively drug-resistant (XDR) and pandrug-resistant (PDR) bacteria. The category XDR is defined as non-susceptibility to at least one agent in all but two or fewer antimicrobial categories, meaning the bacterial isolates are susceptible to only one or two categories. The category PDR is defined as non-susceptibility to all agents in all antimicrobial categories, meaning no tested agents are effective against that organism [9].

Some types of MDR have proven to be very threatening in recent years. The first case is methicillin-resistant *Staphylococcus aureus* (MRSA), which is resistant to methicillin as well as other types of antibiotics, e.g. aminoglycosides. In this instance, resistance was caused by the modification of penicillin-binding proteins (PBP2a), encoded by the chromosomal mecA gene located on a mobile genetic element known as the staphylococcal cassette chromosome mec (SCCmec). This change in the target site renders the bacteria resistant to all β-lactams and their derivatives [10].

The second case involves multidrug-resistant or extensively drug-resistant (XDR) tuberculosis caused by *Mycobacterium tuberculosis*. This strain was responsible for the tuberculosis epidemic in 2017, which resulted in 558,000 new cases. The epidemic was classified as XDR due to its resistance to isoniazid, rifampicin, fluoroquinolones, and aminoglycosides such as amikacin, kanamycin, and capreomycin [11].

The last case involves extended-spectrum β-lactamase (ESBL) producers, which include *Enterobacteriaceae* family. One of the most significant antibiotic resistance mechanisms in *Enterobacteriaceae* is the production of enzymes capable of hydrolyzing penicillins, cephalosporins, and monobactams. These enzymes are known as extended-spectrum β-lactamases (ESBLs). Some bacteria in this family that employ this drug-resistance mechanism include *Klebsiella pneumoniae*, *Escherichia coli*, and *Enterobacter spp.* [12].

1.2 Microorganisms tested in the context of the thesis

The equipment for handling microorganisms in the laboratory is classified as BSL1, so Class 1 strains were chosen. For this thesis, a non-pathogenic strain of *Escherichia coli* was selected, along with *Micrococcus luteus*, *Bacillus subtilis*, *Erwinia persicina*, *Pseudomonas fluorescens* and *Straphylococcus epidermidis*. These six bacteria were selected for their clinical relevance and morphological and physiological variability. They provided useful models for studying antimicrobial resistance and bacterial survival mechanisms in hostile environments such as hospital settings.
The main characteristic that distinguishes these bacteria is their cell wall structure. The figure 1.2 below highlights the structural differences between gram-positive and gram-negative bacteria. The two main factors responsible for the distinct staining properties of these species are the thickness of the peptidoglycan layer and the presence or absence of an outer lipid membrane. Gram-positive bacteria possess cell walls composed of a thick peptidoglycan layer. In contrast, gram-negative bacteria have a thinner peptidoglycan layer and an outer membrane, which is not present in gram-positive bacteria.

Figure 1.2: Gram-positive and gram-negative cell wall structure [13]

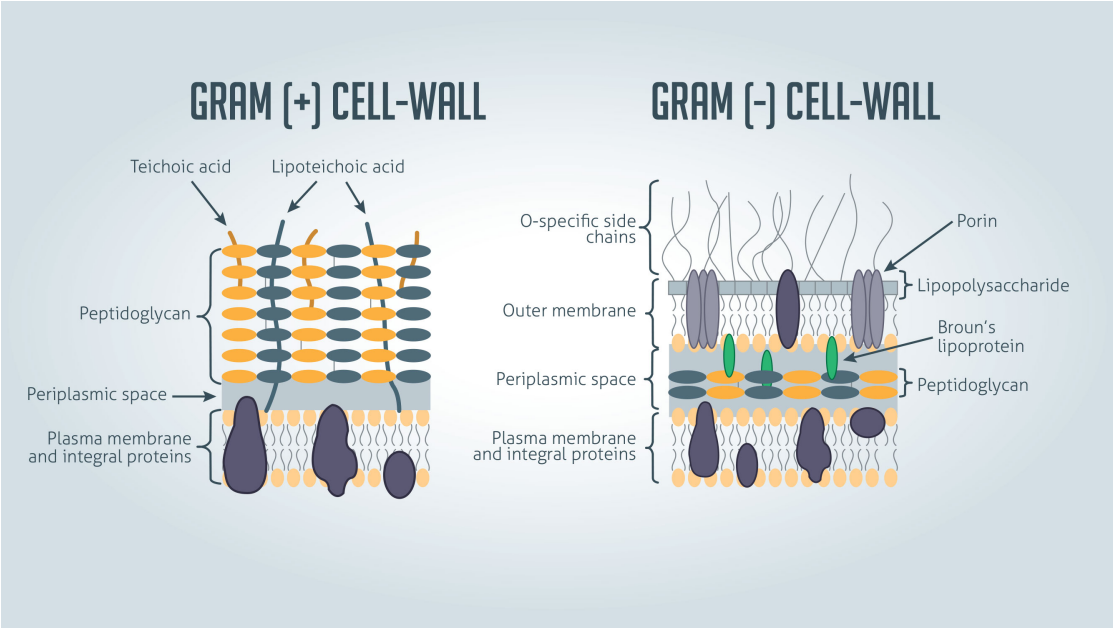

Escherichia coli is a gram-negative bacillus that is facultatively anaerobic, catalase-positive, and oxidase-negative. It is the most extensively studied bacterium by microbiologists, belonging to the *Enterobacteriaceae* family. *E.coli* makes up about 80 % of

the human intestinal flora and is generally non-pathogenic. However, pathogenic strains can cause gastroenteritis, meningitis, septicemia, and urinary tract infections. In recent years, there has been an increase in diarrhea cases in developing countries caused by pathogenic strains of *E.coli* [14]. In humans, *E.coli* infections primarily occur via the gastrointestinal route, with 90 % of urinary tract infections being attributed to *E.coli* [15]. There is growing evidence that the clonal lineage of *E.coli* sequence type ST131, which is resistant to β-lactams and carbapenems, has greater epidemic potential [16]. *Pseudomonas aeruginosa*, a bacterium frequently found in nosocomial infections, shares similarities with *E.coli*. *P.aeruginosa* is already highly resistant due to its physiological traits, such as the relative impermeability of its outer membrane and its efficient efflux pump system. As a result, it continues to develop new antibiotic resistances [17].

Micrococcus luteus is a saprotrophic, gram-positive, cocci-shaped bacterium. The cells are typically arranged in irregular clusters. *M.luteus* is oxidase-positive and strictly aerobic. The *Micrococcus* genus is found in dust, soil, water, and air [18]. These bacteria are part of the natural flora on the skin of mammals and also colonize mucous membranes, the mouth, and human respiratory tracts. *M.luteus* is considered an opportunistic pathogen. This bacterium is of particular interest because it is closely related to *Staphylococcus aureus* in terms of morphology and phylogeny. *S.aureus* is one of the leading causes of nosocomial infections. Therefore, *S.aureus* holds a unique position among antibiotic-resistant species due to its high virulence and remarkable adaptability to various environmental conditions. *S.aureus* strains have developed resistance mechanisms to nearly all antimicrobial drugs used in treatment. The most significant resistances are to the drugs commonly used for treating gram-positive infections, such as β-lactams, glycopeptides, and oxazolidinones [19].

Bacillus subtilis is a gram-positive, rod-shaped bacterium belonging to the *Bacillaceae* family. It is catalase-positive and moves using a flagellum. While non-pathogenic, it serves as an effective model for mimicking *Bacillus anthracis*, the bacterium responsible for anthrax, and *Bacilluscereus*, which causes food poisoning. This bacterium is also of interest because the *Bacillus* genus has developed a mechanism for antibiotic resistance through the use of ribosomal protection proteins, which can make them resistant to streptogramin A or lincomycin [20]. Moreover, the bacterium caused a batch of amoxicillin to be withdrawn from the market in august 2024 in France.

Staphylococcus epidermidis is a coagulase-negative, gram-positive cocci that forms clusters. It is also a catalase-positive and facultative anaerobe. It is usually a symbiont that is harmless in its natural environment (human skin or mucosa). However, it is an opportunistic pathogen that can cause virulence once it invades the human body via medical and prosthetic devices. One of the crucial factors allowing coagulase-negative species to survive in a harsh environment is the production of the biofilm. Biofilm

formation occurs with initial adhesion to a foreign surface, which leads to accumulation into multicellular structures. The biofilm production helps to protect them from host defense or antimicrobials via protective exopolymers called poly-y-glutamic acid (PGA). The pseudo peptide polymer PGA, produced by the gene products of the cap locus, plays a crucial role in *S.epidermidis* resistance to neutrophil phagocytosis and antimicrobial peptides (AMPs). It is reported that *S.epidermidis* is one of the most common causes of nosocomial infection, with infection rates as high as those of *S.aureus*. *S.epidermidis* is particularly notable as the most frequent source of infections related to indwelling medical devices. This is likely due to its permanent and widespread presence on human skin, which increases the likelihood of device contamination during insertion [21].

Erwinia persicina is a facultative anaerobe, a gram-negative plant pathogen that is a member of the family Enterobacteriaceae. It is known to produce a soluble pink pigment and it was first isolated from healthy tomato, banana, and cucumber. In grain legumes, it is possible that *E.persicina* may not be easily eliminated because of the protection afforded by the biofilm or the seed coat. Once *E.persicina* enters into a new region, it may represent a new and permanent threat to forage or grain legume production within its farming systems [22]. *Erwinia persicina* has been identified as a soft rot agent that causes pink-pigmented soft rot on a small range of plant hosts, including garlic, onions, lettuce, mushrooms, barley, and parsley root [23]. Detailed antibiotic resistance patterns are available for only seven strains of *E.persicina* [24]. Reports of *Erwinia* species as human pathogens are limited, as most isolates previously identified in clinical microbiology are now classified under the *Pantoea* group. The phytopathogen *E.persicina* [25] has been isolated from human urinary tract infections. *E.chrysanthemi* has been shown to kill human gastrointestinal cells in culture and expresses virulence factors similar to those of other well-known enterobacterial pathogens [26].

Pseudmonas fluorescens is a gram-negative, nonsporulating, motile unicellular rod which is primarily aerobic, unable to ferment glucose, and chemoorganotrophic. Quorum sensing and biofilm formation are integral to the many environmental niches occupied by *P.fluorescens*, and allow it to colonize surfaces such as hospital equipment and food-grade stainless steel. This highly heterogeneous species includes virulent and sub-clinical strains involved in opportunistic nosocomial infections. It has been demonstrated that this bacterium exhibits resistance to nisin Z and pediocin PA-1/AcH at concentrations up to 100 mg/mL [27]. Therefore, *Pseudomonas fluorescens* is a regular contaminant of ready-to-eat foods. These microscopic organisms show a wide choice of growth temperature, and contamination is a key issue in ordinary and refrigerated food items [28].

1.3 The azobenzenes

The rise of nosocomial multi-drug resistant (MDR) bacterial strains is an increasing concern in hospitals, highlighting the urgent need to develop new antibacterial agents [29]. Certain azobenzenes display intrinsic antimicrobial activity in this context, which varies based on the type and position of substituents on their aromatic rings.

1.3.1 Properties

Azo compounds are defined by the presence of a -N=N- double bond, with two substituents—typically aromatic rings—attached. The strong electronic absorption band of azobenzene can be adjusted by substituting different groups on the ring, allowing the color to be fine-tuned across the spectrum from ultraviolet to red-visible regions. Coupled with the robustness and chemical stability of azo groups, this has led to extensive research into azobenzene-based structures as dyes and colorants [30].

Figure 1.3: Trans-to-cis azobenzene isomerization

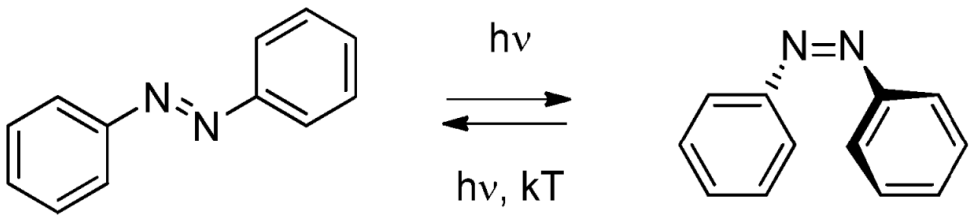

Azobenzene can adopt two conformations, trans and cis, which interconvert through isomerization when exposed to UV light or thermal activation, as shown in figure 1.3 [31]. Cis-to-trans retro-isomerization can happen naturally in the dark because the trans isomer is more stable, or it can be triggered by exposure to visible light or heat.
In figure 1.4 we can find four mechanisms—rotation, inversion, concerted inversion, and inversion-assisted rotation— that have been suggested as potential pathways for azobenzene photoisomerization. The rotational pathway is characterized by breaking the N=N π-bond, permitting free rotation around the N–N bond and consequently altering the C–N–N–C dihedral angle while maintaining the N–N–C angle at roughly 120°. In the inversion mechanism, one N=N–C angle extends to 180°, keeping the C–N=N–C dihedral angle fixed at 0°, which results in a transition state with one nitrogen atom adopting sp hybridization. For the concerted inversion pathway, both N=N–C bond angles increase to 180°, leading to a linear transition state. Meanwhile, in the inversion-assisted rotation, both the C–N=N–C dihedral angle and the N=N–C bond angles undergo simultaneous

and significant changes. Notably, the transition state in concerted inversion lacks a net dipole moment, unlike the other three pathways, which involve polar transition states [32].

Figure 1.4: Isomerization mechanisms [32]

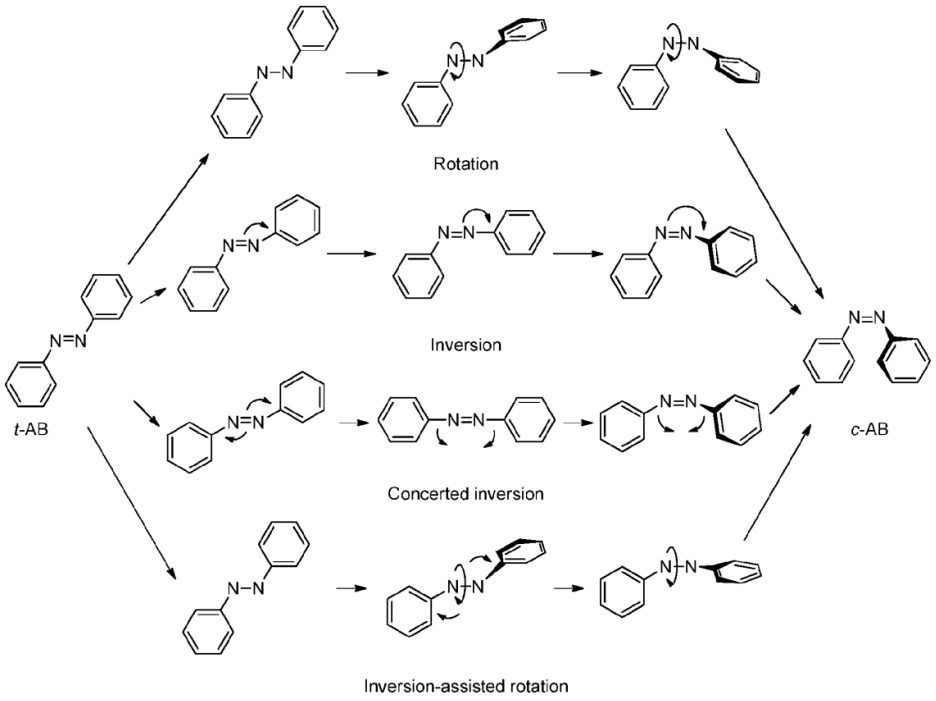

The change in geometry upon isomerization modifies the spectroscopic properties. The absorption spectrum of trans isomers features two distinct bands in the UV-visible region: a strong band around 350–400 nm corresponding to the $\pi \Rightarrow \pi^*$ transition and a weaker visible band, max.450 nm, from the $n \Rightarrow \pi^*$ transition. Conversely, the cis isomer shows weaker $\pi \Rightarrow \pi^*$ transitions but a stronger $n \Rightarrow \pi^*$ absorption [32].

1.3.2 Synthesis

Azobenzene is mainly obtained through an azo-coupling reaction between a diazonium salt and a phenolate. Azo coupling is the most widely used industrial reaction in producing dyes, lakes, and pigments. In this reaction shown in figure 1.5, aromatic diazonium ions function as electrophiles and react with activated aromatic compounds like anilines or phenols. The substitution typically takes place at the para position unless it is occupied, in which case the ortho position becomes more favorable.

Figure 1.5: General scheme of the azo coupling reaction [31]

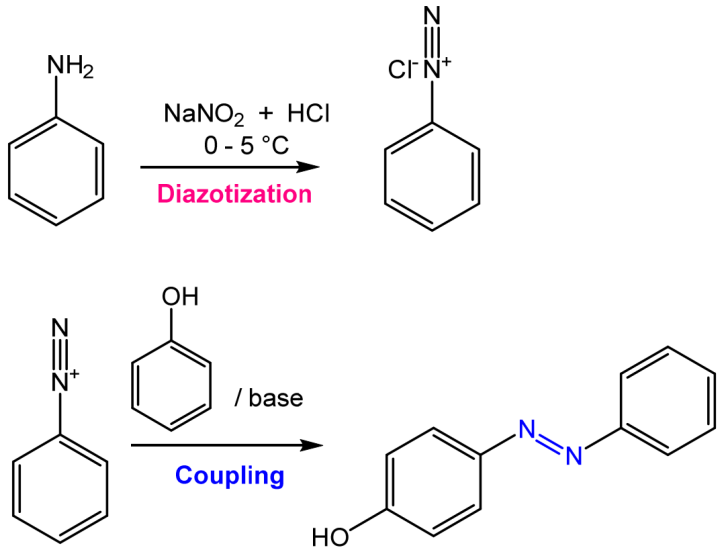

The pH of the solution plays a crucial role, needing to be mildly acidic or neutral, as the reaction does not occur if the pH is too low [33].

Diazonium salt formation

In aqueous solution, diazonium salts decompose at temperatures above 5°C, and the solid form is explosive. For this reason, they are prepared in ice-cold solutions and used immediately.

Diazonium salts are synthesized through a diazotization reaction in two reaction steps as shown by equations 1.1 and 1.2, where a cold solution of sodium nitrite is added to an arylamine solution in concentrated hydrochloric acid, kept below 5°C.

Firstly, sodium nitrite ($NaNO_2$) is dissolved in water, where it dissociates into sodium ions (Na^+) and nitrite ions (NO_2^-). Hydrochloric acid (HCl) is added to the solution. The acid dissociates into hydrogen ions (H^+) and chloride ions (Cl^-), which are also essential in forming the final diazonium salt

The nitrite ion (NO_2^-) from sodium nitrite reacts with the hydrogen ions (H^+) from hydrochloric acid to form nitrous acid (HNO_2), which is an unstable intermediate:

$$NO_2^- + H^+ \rightarrow HNO_2 \tag{1.1}$$

Nitrous acid is always generated during the reaction due to its instability, typically by the action of hydrochloric acid (HCl) on sodium nitrite ($NaNO_2$). The hydrochloric acid used to generate nitrous acid provides the anion for the diazonium salt.

The nitrous acid (HNO_2) then reacts with the arylamine ($C_6H_5NH_2$) to form diazonium salt:

$$C_6H_5NH_2 + HNO_2 + HCl \rightarrow C_6H_5N_2^+Cl^- + 2H_2O \tag{1.2}$$

The amine group (NH_2) is protonated by HCl, and nitrous acid converts it into a diazonium ion (N_2^+).
While diazonium salts can be isolated in crystalline form, they are typically kept in solution and used immediately, as they tend to decompose even when stored in cold conditions [34].

Phenolate formation
The formation of phenolate is the process by which a phenol molecule loses a proton H^+ from its hydroxyl group -OH, leading to the formation of a phenolate ion ($C_6H_5O^-$). In the presence of sodium carbonate, phenol is converted into its conjugate base (phenolate) through a series of reactions shown in equations 1.3, 1.4 and 1.5.
The first step is the sodium carbonate dissociation in water into sodium ions (Na^+) and carbonate ions (CO_3^{2-}):

$$Na_2CO_3 \rightarrow 2Na^+ + CO_3^{2-} \tag{1.3}$$

The sodium ions remain as spectator ions, while the carbonate ions react with water to form bicarbonate ions (HCO_3^-) and hydroxide ions (OH^-) as shown in equation 1.4. The hydroxide ions are the key to forming phenolate.

$$CO_3^{2-} + H_2O \rightarrow HCO_3^- + OH^- \tag{1.4}$$

Phenol (C_6H_5OH) is a weak acid and in the presence of the hydroxide ions (OH^-) from the previous step, it loses a proton (H^+). This deprotonation creates a phenolate ion ($C_6H_5O^-$), the conjugate base of phenol:

$$C_6H_5OH + OH^- \rightarrow C_6H_5O^- + H_2O \tag{1.5}$$

The phenolate ion ($C_6H_5O^-$) pairs with the sodium ions (Na^+) from the dissociated sodium carbonate to form sodium phenolate ($C_6H_5O^-\ Na^+$).

1.3.3 Biologic properties

In recent years, there has been growing interest in azobenzenes due to their biological properties, particularly in the field of photopharmacology, where they are amongst the most commonly used chemical functions [35]. The $cis/trans$ photoisomerization of these compounds allows for the modulation of processes such as neurotransmission [36] or the anticancer properties of molecules [37]. In this context, the conformational switching of azobenzene has allowed for the observation of variations in the potency and efficacy of existing drugs modified with azocompounds, as well as the ability to modulate drug activity, thereby reducing the possibility of drug resistance occurring [38].

Recently, various studies have explored the synthesis of azo compounds, highlighting their potential in biomedical applications. These compounds are known to possess various biological activities, such as antioxidant [39], antiviral[40][41], antimicrobial [42], anticancer [43], and antidiabetic effects [44]. However, the focus will be exclusively on the antibacterial properties of molecules containing diazo motifs.

The mechanism of action of azo dyes against different microbes in figure 1.6 begins with the inhibition of protein synthesis, which starts to impair cellular processes, eventually leading to the destruction of the cell wall. This is followed by the inhibition of nucleic acid synthesis through the generation of reactive oxygen species within microbial cells, causing oxidative stress. Finally, the interaction of azo dyes with the cell membrane results in its destruction, leading to altered permeability and integrity. In particular, it has been reported that the isomerization of azo compounds leads to changes in their dipole moment and shape, which can cause specific disturbances in biological environments, including alterations in the permeability of bacterial cell membranes [45].

Figure 1.6: Mechanism of azo dyes against different microbes [45]

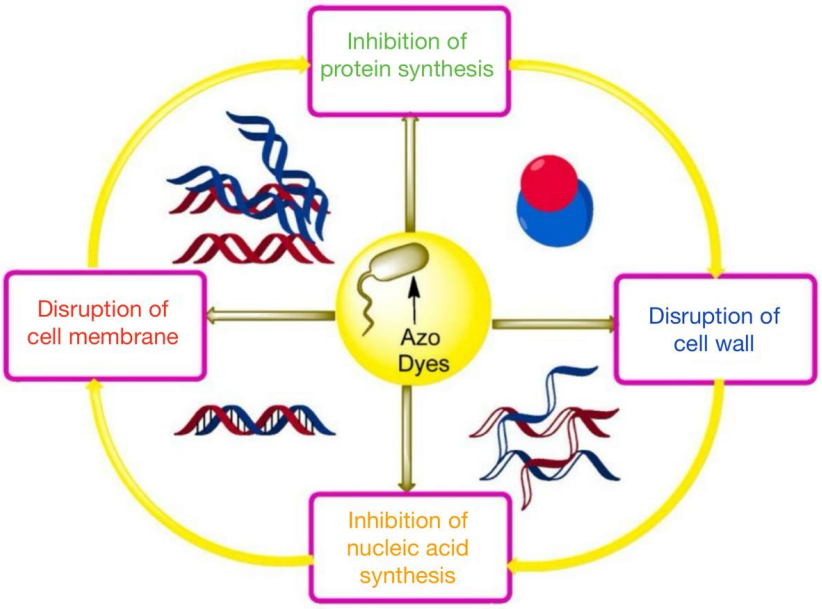

Electron-accepting groups in azo dyes play a role in inhibiting bacterial growth. Experimental evidence has demonstrated that azo dyes are genotoxic to bacteria, causing damage to bacterial DNA through N-hydroxylation and esterification. Specifically, the aromatic amine component of azo dyes is reduced to generate oxygen radicals, which then contribute to N-hydroxylation and esterification processes that harm bacterial DNA. Additionally, ortho-hydroxy aromatic amines with an azo linkage are particularly known for their preferential damage to bacteria [46].

Certain azobenzenes display inherent antimicrobial properties that vary based on the type and location of substituents on the aromatic rings. The literature includes a limited number of studies detailing the synthesis and investigation of variously substituted azobenzenes with antimicrobial and genotoxic effects on bacteria.

A team of researchers synthesized and studied three azo compounds shown in figure 1.7, in which the NO_2 group occupies an ortho, meta, or para position with the -N=N- double bond on one of the two aromatic rings. The antimicrobial activity *in vitro* was assessed using the solid agar diffusion test, which revealed that all three azo dyes exhibited strong antimicrobial effects. Notably, the molecule with the NO_2 group positioned at the meta site demonstrated the highest activity against *S.aureus*, with an inhibition zone measuring 39 mm. Conversely, the molecule with the NO_2 group at the ortho position showed superior activity against *C.krusei*, achieving an inhibition zone of 42 mm [47].

Figure 1.7: Nitro-substituted azobenzenes [47]

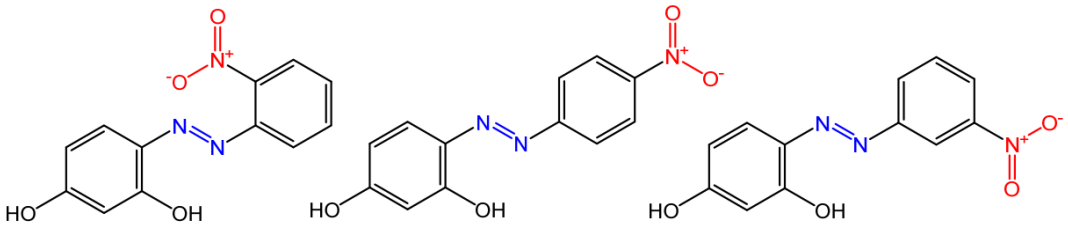

In the field of surfactants, it has been demonstrated that non-ionic surfactants based on azobenzene with sugars as polar heads can inhibit the growth of *P.aeruginosa* biofilms [48]. On the other hand, the growth of biofilms formed by gram-positive bacteria can be effectively inhibited by small, minimally functionalized azobenzenes shown in figure 1.8 [49][50]. The metabolic targets in this case are the inhibition of adenosine triphosphate (ATP) synthase and protein kinase. The antibacterial activity of these compounds is maintained even when they are incorporated into a polymer matrix [51].

Figure 1.8: Basic structure of the small azobenzene that inhibits the growth of biofilms formed by gram-positive bacteria [49]

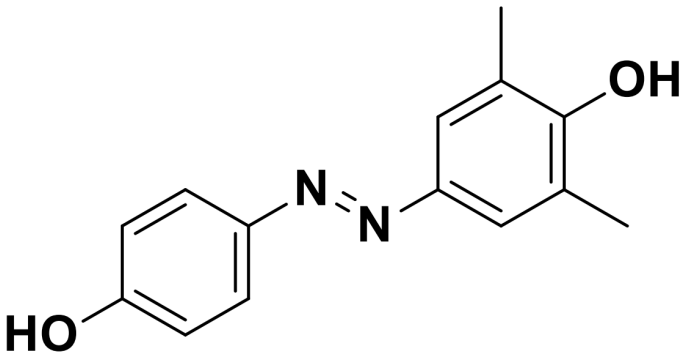

An additional important aspect concerns how photoisomerization affects the antimicrobial activity of azobenzene derivatives. These derivatives are based on quinolones, which are broad-spectrum antibacterial agents that work by binding to DNA gyrase, an essential enzyme in DNA replication. Quinolones used clinically typically have piperazine and fluorine atoms on the benzene ring, contributing to their antimicrobial properties. In this research, the quinolone component is attached to a photoresponsive azobenzene

molecule, replacing the piperazine group. Various azo-quinolone compounds with different substituents in figure 1.9 were synthesized and examined to assess how photoinduced isomerization of the azobenzene residue influences their antimicrobial activity [52].

Figure 1.9: Chemical structure of azoquinolones [52]

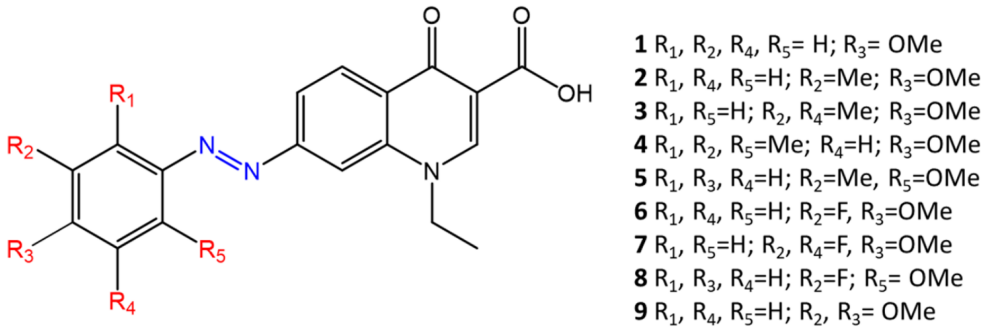

The cis isomer exhibited strong antimicrobial activity, whereas converting back to the trans form resulted in reduced activity for the tested compounds. This variation in antibacterial effectiveness was noted in both gram-negative and gram-positive bacteria, suggesting that the photosensitive quinolone maintains its broad-spectrum activity. Molecule 2, with R2 = Me and R3 = OMe, demonstrated a notable difference in antimicrobial effectiveness between the two isomers. For *E.coli* , the MIC for the trans isomer was greater than 64 μg/mL, while the cis isomer had a MIC of 16 μg/mL. In contrast, for *M.luteus*, the MIC was 16 μg/mL for the trans isomer and 2 μg/mL for the cis isomer.

1.3.4 Alizarin

Alizarin (1,2-dihydroxyanthraquinone; $C_{14}H_8O_4$) is a red pigment derived from the roots of madder plants, commonly used as an analytical reagent and for data recording purposes [53]. As an anthraquinone compound with hydroxyl (-OH) group substitutions at the 1 and 2 positions, alizarin has been identified as a highly sensitive colorimetric or pH indicator [54]. Alizarin undergoes a color change from yellow in acidic conditions to red at neutral pH, and to a reddish-purple in alkaline environments, making it a suitable natural colorant for use in food freshness indicator systems [55]. The color variation is linked to the formation of phenolic oxygen anions on its structure. Both the hydroxyl and quinone groups can act as proton acceptors, facilitating electrochemical catalysis and enhancing electron transfer between the sensor and the test sample [56]. As a natural

dye, alizarin could be considered safer or pose fewer risks than synthetically produced dyes currently used in smart food packaging systems.

Figure 1.10: Chemical structure of alizarin

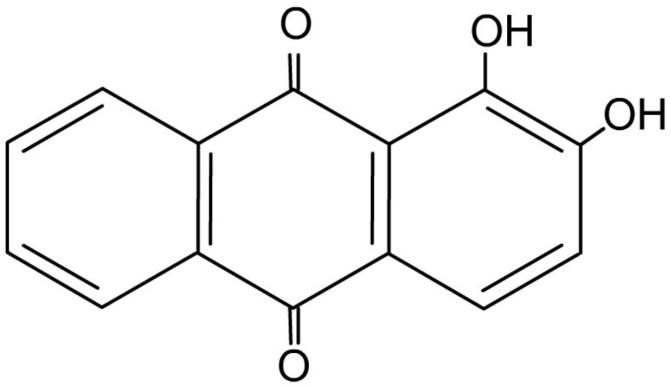

Furthermore, alizarin, a naturally occurring hydroxyanthraquinone, exhibits a range of biological activities including anti-leukemia and anti-HIV effects, as well as antioxidant and antimicrobial properties [57][58][59][60].

Antimicrobial activity

The antibiofilm properties of 560 purified phytochemicals are examined, and it was found that alizarin (at concentrations of 0, 1, 2, 5, 10, 50, and 100 μ g/mL) effectively inhibited biofilm formation by an *S.epidermidis* strain and three *S.aureus* strains. Specifically, alizarin at 10 μg/mL reduced biofilm formation by $\geq$ 90% in all three *S.aureus* strains (MSSA 6538, MRSA MW2, and MSSA 25923), while at 50 μg/mL, it decreased biofilm formation by $\geq$ 70% in *S.epidermidis*. These findings highlight that anthraquinones, particularly alizarin, are highly effective in controlling the growth of *S.aureus* [61] .

Another study found that acid hydrolysis of *Rubia tinctorum* significantly increased the concentration of alizarin in the extract, thereby enhancing its antimicrobial efficacy. Their study tested the antimicrobial activity of both hydrolyzed and non-hydrolyzed *R.tinctorum* extracts (containing alizarin) against two gram-positive bacteria (*Listeria monocytogenes* ATCC 11120 and *S.aureus* ATCC 25923), five gram-negative bacteria (*Pseudomonas aeruginosa* ATCC 9027, *Escherichia coli* ATCC 25922, *S.enteritidis* ATCC 14028, *Klebsiella pneumoniae* ATCC 13833, and *Aeromonas hydrophila* ATCC 1943), and two fungi (*Aspergillus ochraceus* and *A.niger*). The study showed that both extracts were effective against all strains, with inhibition zones ranging from 9 to 21 mm. Notably, increasing the concentration of *R.tinctorum* extracts enlarged the inhibition

zones. Fungi were more sensitive than bacteria, and gram-positive bacteria were more affected than gram-negative ones. The acid-hydrolyzed extract exhibited a stronger antibacterial effect compared to synthetic alizarin and the non-hydrolyzed extract [62].

Chapter 2

Materials and methods

2.1 Reagents, solvents, and materials used in organic synthesis

The organic reagents and solvents come from Acros Organics (a division of Fisher Bioblock Scientific), Sigma-Aldrich, and SDS Carlo-Elba. The reagents were used without any prior treatment. The water used for microbiology came from a Veolia Elga Purelab Flex system to ensure it qualified as Ultra Pure Water 18.2 $M\Omega$. It was sterilized before use. Water for syntheses was used from a tap without any purification. TLC analyses were performed on aluminum plates (Merck Kieselgel 60F254, silica thickness: 0.2 mm). The crude reaction mixtures were purified using a Büchi Pure Flash 810 chromatography system with silica gel cartridges (40 g). The NMR analyses of the compounds were performed on a Bruker UltraShield 400MHz/54 mm Ultra long hold instrument.

2.2 General protocols and characterization of the obtained compounds

2.2.1 General procedure for the synthesis of azobenzenes

The azobenzene syntheses were done for a group of anilines and phenols listed below in table 2.1. The steps of the azo-coupling reaction are shown in figure 2.1:

Table 2.1: Quantities of reagents used for the syntheses

	M[$\frac{g}{mol}$]	**n** [mol]	**m**[g]	**d**[$\frac{mg}{L}$]	**v**[mL]
ANILINE					
4-bromoaniline	172.02	0.01	1.72		
4-nitroaniline	138.12	0.01	1.38		
3,4-dichloroaniline	162.01	0.01	1.62		
2,4-dichloroaniline	162.02	0.01	1.62		
PHENOL					
Thymol	150.22	0.01	1.50		
Alizarin	240.21	0.01	2.40		
p-Xylenol	122.16	0.01	1.22		
OTHERS					
Sodium carbonate	105.99	0.02	2.12		
Hydrochloric acid	36.5	0.043		12	3.57
Sodium nitrite	69	0.0105	0.72		

Figure 2.1: Azo-coupling reaction

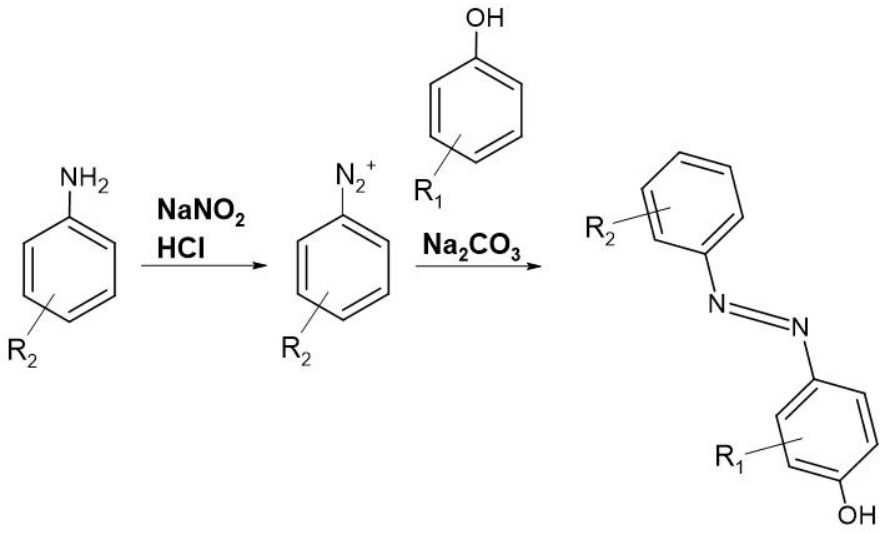

• **Preparation of phenolate (Erlenmeyer 1):** Sodium carbonate (2.12 g) is placed in 45 mL of water in an Erlenmeyer flask, then the chosen phenol is added (1.50 g Thymol; 2.40 g Alizarine; 1.22 g p-Xylenol).

• **Preparation of diazonium salt (Three-neck round-bottom flask):** In a 250 mL three-neck round-bottom flask fitted with a thermometer and a dropping funnel, the

chosen aniline (1.72 g 4-bromoaniline; 1.38 g 4-nitroaniline; 1.62 g 3,4-dichloroaniline; 1.62 g 2,4-dichloroaniline) is placed in 20 mL of water. Concentrated hydrochloric acid (3.57 mL at 12 mol/L) is then added. The mixture is left under stirring for at least 10 minutes. The temperature is lowered to below 5°C. In the dropping funnel, 10 mL of an aqueous solution of sodium nitrite (0.72 g) is introduced. This solution is slowly dripped into the three-neck round-bottom flask without exceeding 5°C. The mixture is left under stirring for 10 minutes.

• **Formation of azobenzene:** Using a pipette, the phenolate from Erlenmeyer 1 is added very slowly to the diazonium salt in the three-neck round-bottom flask without exceeding 5°C. The mixture is then allowed to return to room temperature and left under stirring for at least 3 hours.

• **Filtration:** Using a Kitasato flask, a Buchner funnel, filter paper, and a vacuum pump, a vacuum filtration system is set up if the product has precipitated. The mixture formed after the reaction is passed through the filtration system to separate the suspended solids from the liquid. The mixture is poured gradually to prevent a long filtration time. Once the entire mixture has been poured, it can be rinsed with a little water to recover as much solid as possible. The filtered solid is left to air dry for at least 1 hour to allow all the remaining liquid in the solid mass to evaporate. It is important not to carry out the procedure in an oven, as the compound may be heat-sensitive. The filter paper with the entire filtered mass can be placed inside a large beaker for the final drying phase. If the product is oily, it is extracted with 40 mL of ethyl acetate, dried with MgSO4, and the ethyl acetate is evaporated.

2.2.2 Product characterization

Thin Layer Chromatography

The principle of TLC is the distribution of a compound between a solid fixed phase (thin layer) applied to an aluminum plate and a liquid mobile phase (eluting solvent) that is moving over the solid phase.
In a jar with a lid, the solvent mixture is prepared consisting of 7 mL (70%) cyclohexane and 3 mL (30%) ethyl acetate. The mobile phase is chosen according to the properties of the components in the mixture. In our case, a mobile phase with a standard composition was used, given the presence of a compound with medium polarity. The lid is securely placed on the jar to prevent evaporation of the volatile solvent and ensure that the amount remains consistent throughout the procedure. A horizontal line is drawn 1 cm from the base of the plate with a pencil to mark the application point of the three substances. The three substances are applied using a very fine glass rod. Specifically, phenol is placed in

spot 1, followed by aniline in spot 2, and azobenzene in spot 3. Subsequently, the TLC plate is inserted into the jar containing the solvent mixture and closed with the lid. It is important that the plate remains vertically positioned during the operation as shown in figure 2.2, and the solvent level is kept below 1 cm, below the application point of the compounds. When the solvent has migrated approximately 0.5-1 cm from the top edge, the jar can be opened, and the aluminum plate can be removed, ensuring it is taken from the upper, solvent-free portion. After quickly drying the plate, it is placed under UV light at a wavelength of 254 nm to verify the compound migration.

Figure 2.2: Thin Layer Chromatography procedure (created with BioRender.com)

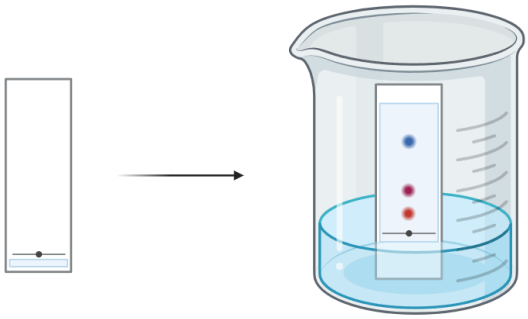

The separation of compounds is based on the competition of the solute and the mobile phase for binding places on the stationary phase. If the normal phase silica gel is used as the stationary phase, it can be considered polar. Given two compounds that differ in polarity, the more polar compound has a stronger interaction with the silica and is, therefore, more capable of dispelling the mobile phase from the binding places. Consequently, the less polar compound moves higher up the plate [63]. This allows verification of the presence of starting aniline and phenol in the reaction product, to subsequently purify through a flash chromatography system with silica columns. The presence of other spots at different heights must be verified to ensure that the reaction has indeed occurred and not merely residual aniline and phenol.

Flash Chromatography

Flash chromatography is a technique used to separate mixtures of molecules into their constituents. It is an air-pressure instrument combining medium pressure and shorter column chromatography, optimized for particularly rapid separation. The crude reaction mixtures were purified using a Büchi Pure Flash 810 system with silica columns (40g) shown in figure 2.3. To prepare the sample for purification, silica gel (ultrapure, 60-200 micrometers) should be added at twice the weight of the dry product. Acetone is then added to thoroughly homogenize the two components, and the mixture is evaporated

using a rotary evaporator. The resulting dry product is placed into a specific sample, ensuring it is compacted as much as possible.
The sample to be purified is placed on top of a cartridge containing solid support of silica gel. The rest of the column is then filled with a mixture of solvents (30% ethyl acetate, 70% cyclohexane) which then runs through the solid support. The software controls an automated system that collects the fractions containing the target compound and helps locate the resulting purified material within the fraction collector [64]. The software also saves the resulting chromatograph from the process for archival and later recall purposes.

Figure 2.3: Flash chromatoghraph [65]

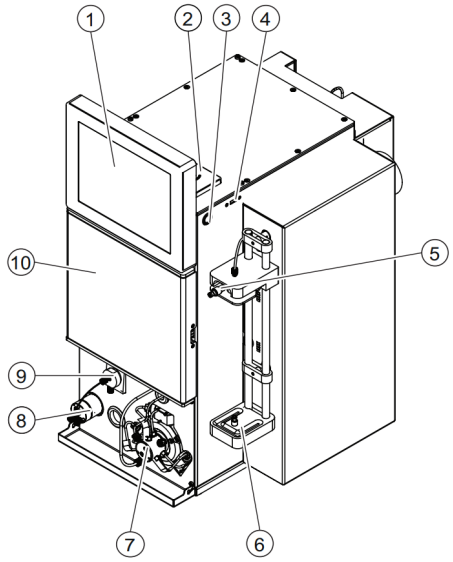

1. **Screen**
2. **RFID Reader**
3. **On/Off Switch**
4. **USB Port**
5. **Liquid sample injection port**
6. **Injection port**
7. **Injection valve**
8. **Flow divider**
9. **UV Detector**
10. **Tube holder**

Nuclear magnetic resonance spectroscopy

Nuclear magnetic resonance (NMR) spectroscopy is a well-known analytical technique for the structure elucidation of small and macro molecules. One of the key benefits of

NMR is its ability to serve as a primary analytical tool, allowing for the quantitative assessment of compound purity without the need for a specific reference standard [66]. It exploits the magnetic properties of certain atomic nuclei, which exhibit nuclear spins that align with an external magnetic field. When these nuclei are exposed to radiofrequency radiation, they undergo transitions between different spin states, producing signals that are detected and analyzed. An NMR spectrum can be detected only for nuclei that have a net spin. In this regard, hydrogen, the most prevalent nucleus in organic molecules, is particularly suitable because its most common isotope (^{1}H) has a spin of $\frac{1}{2}$ [67]. Similarly, the carbon isotope (^{13}C) has a nuclear spin of $\frac{1}{2}$, which allows it to be studied using NMR. Although (^{13}C) has a relatively low natural abundance compared to the more common isotope (^{12}C) (which has a nuclear spin of zero and thus cannot be detected by NMR), modern technologies, such as high-resolution nuclear magnetic resonance, enable the detection and analysis of signals from (^{13}C). The integration of (^{1}H) and (^{13}C) NMR data provides a comprehensive view of a molecule's structure, identifying not only the arrangement of atoms but also their interactions and connectivity within the molecule.
The preparation of the sample for NMR spectroscopy involved adding a small amount of purified azobenzene to an NMR tube containing chloroform or methanol. The solvent must be suitable for the substance being analyzed to prevent the solvent peaks from interfering with those of the sample in the NMR spectrum. The azobenzene should be soluble in the chosen solvent to ensure that the solution is clear and free of solid particles that could interfere with the NMR signal. The solvent quantity should be sufficient to fill more than half of the height of the NMR tube. This helps to ensure good signal quality and uniform scanning. The sample concentration should be sufficient to obtain a clear NMR signal, but not so high as to cause signal overlap.

Isomerization test

Exposing the sample to UVA light enables the isomerization of azobenzene from the trans conformation to the cis conformation. Cis to trans retro-isomerization can occur spontaneously in the dark, due to the higher stability of the trans isomer, or by exposure to visible light or heating. The two isomers differ in their absorbance profile. Therefore, the absorbance spectra are measured in the presence and absence of UVA light to verify correct isomerization and to determine the time required for the transition from one isomer to the other.
In the trans conformation, the molecule is planar, linear, and symmetric, with the two benzene rings positioned opposite each other relative to the nitrogen-nitrogen double bond (N=N). This conformation allows for greater delocalization of π-electrons along the entire molecule, resulting in two well-separated bands in the UV-visible region: an intense band around 350–400 nm corresponding to the $\pi \Rightarrow \pi^*$ transition and a weaker band in the visible region, max. 450 nm, which corresponds to the n $\Rightarrow \pi^*$ transition. The cis isomer has a bent and less symmetric structure, with the two benzene rings

closer together. This leads to a lesser delocalization of π-electrons, resulting in a weaker $\pi \Rightarrow \pi^*$ transition, while the band corresponding to the n $\Rightarrow \pi^*$ transition is strong.
Experimentally, given a volume of 10 milliliters of pure ethanol, 10 microliters of a dimethyl sulfoxide (DMSO, Thermo Scientific) and azobenzene solution at a concentration of 5g/L are added. This results in a solution with a concentration of 5 mg/L of azobenzene in a solvent mix of DMSO and ethanol. The solution is then poured into a test tube where a probe is inserted for absorbance measurement. The measurement software conducts a cycle of measurements, each lasting 1 minute. To verify the transition from the trans form to the cis form, the sample needs to be exposed to UVA light at 385-405 nm (60 watts), ensuring a well-irradiated environment by surrounding the sample with aluminum foil. A subsequent measurement can be conducted for the transition from the cis form back to the trans form in the absence of UVA light to better understand the isomerization timings.

2.3 Materials, culture media, and techniques for biological properties

2.3.1 Bacteria

The bacterial strains used are *Escherichia coli* ATCC 25922TM (American Type Culture Collection, USA), *Micrococcus luteus* CRBIP 107660 (Institut Pasteur, France), *Bacillus subtilis* ATCC 6051 (American Type Culture Collection, USA), *Straphylococcus epidermidis* ATCC 35984 (American Type Culture Collection, USA), *Erwinia persicina* (UTC laboratory), and *Pseudomonas fluorescens*. They are cultured on solid Trypticase Soy Agar (TSA, CONDA, Madrid) and incubated at 30°C in the dark in an incubator (SANYO, MIR-253 incubator) for 24 hours. Culture plates are then stored in a cold room at 4°C or used to inoculate 20 mL of liquid medium 24 hours before microplate tests or zone of inhibition tests.

2.3.2 Bacteria in solid medium protocol

Bacteria are cultured on a solid tryptic soy agar medium (TSA, Sigma) with a concentration of 40 g/L. The medium is sterilized in an autoclave at a temperature of 120°C, maintained for 15 minutes at a pressure of 2.2 bars, then poured into Petri dishes (25 mL for each dish). The bacteria are cultured on Petri dishes by streaking as shown in figure 2.4. During the procedure, it is necessary to work in a sterile environment (biological safety cabinet) and to avoid passing over the items that need to remain sterile (sterility is ensured if objects remain vertically positioned under the biological safety cabinet). The agar surface of the plate must be dry without visible moisture such as condensation drops. Traditionally, inoculated plates are incubated with the agar side up to prevent condensed

moisture from falling onto the agar surface, compromising isolation by allowing bacteria to move across the moist surface and create areas of confluent growth.

In a streak plate, dilution is achieved by spreading the sample on the surface of the agar in the Petri dish. A sterile disposable loop is streaked through the initial sector, and organisms are carried into the second sector where they are spread with a zig-zag motion. Similarly, the third sector is streaked in the same manner [68].

Figure 2.4: Bacteria in solid medium (created with BioRender.com)

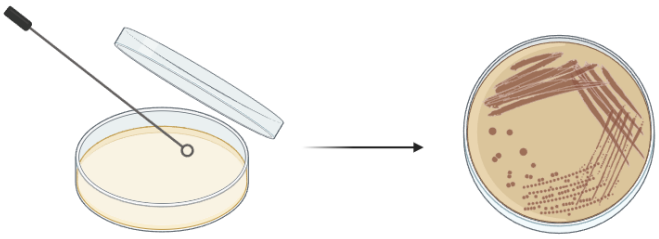

The Petri dishes are subsequently sealed with a strip of paraffin film to transport them outside the biological safety cabinet. They are then incubated at 30°C for 24 hours. Afterward, they are stored in the refrigerator at 4°C or used to inoculate 20 mL of liquid medium 24 hours before microplate tests or zone of inhibition tests.

2.3.3 Liquid medium

The MM2 culture medium is a specialized formulation used for the cultivation of certain bacteria, particularly methanotrophs. It contains a specific combination of mineral salts and nutrients to support the growth of these microorganisms under controlled laboratory conditions. The oligo-element and liquid mineral media compositions, with and without yeast extract, are shown in the following tables 2.4, 2.2 and 2.3:

Table 2.2: MM2 composition for 1L solution

Component	**Quantity** [gr]	**Volume** [mL]
KCl	0.250	
NaH_2PO_4	6.46	
$Na_2HPO_4.2H_2O$	10.408	
$MgSO_4.7H_2O$	0.244	
NO_3NH_4	1	
$Oligoelements$		10

Table 2.3: MM2 composition with yeast extract for 1L solution

Component	**Quantity** [gr]	**Volume** [mL]
KCl	0.250	
NaH_2PO_4	6.46	
$Na_2HPO_4.2H_2O$	10.408	
$MgSO_4.7H_2O$	0.244	
NO_3NH_4	1	
$Oligoelements$		10
$Yeast\ extract$	5	

Table 2.4: Oligo-element composition for 1L solution

Component	**Quantity** [gr]
$ZnSO_4.7H_2O$	0.1
$MnCl_2.4H_2O$	0.01
$FeSO_4.7H_2O$	0.1
$CuSO_4.5H_2O$	0.05
$CaCl_2.2H_2O$	0.1
MoO_3	0.2

The media are sterilized in an autoclave at a temperature of 120°C maintained for 15 minutes at a pressure of 2.2 bars, then they are stored in the refrigerator at 4°C. The liquid medium will be used to cultivate the bacteria before the UVA resistance tests, microplate tests, or zone of inhibition tests, after adding, in proportion, 400 μL of glucose solution (500 g/L) to 20 mL of the liquid medium, to obtain a final concentration of 10 g/L.

2.3.4 UVA resistance test: *E.persicina*, *P.fluorescens*, *S.epidermidis*

Before proceeding with the antimicrobial tests, it is necessary to determine if the bacteria being considered are sensitive to UVA light. If they are, it will not be possible to assess the effect of azobenzene through microplates, as exposure to UVA light may obscure whether the observed inhibition is caused by the UVA light or the azobenzene produced. For this reason, the UVA resistance test was carried out for the three bacteria: *E.persicina*, *P.fluorescens*, and *S.epidermidis*. Regarding *E.coli*, *M.luteus*, and *B.subtilis*, it is already known from previous laboratory experiments that they are not sensitive to the UVA light effect.
It is necessary to work under sterile conditions to cultivate bacteria in a liquid medium, thus using a biological safety cabinet. For *E.persicina* and *P.fluorescens*, MM2 without yeast extract is used, and for *S.epidermidis*, MM2 with yeast extract is used (necessary for cocci). The bacterium is collected from the Petri dish and inserted into the test tube with the liquid mineral medium and glucose solution as shown in figure 2.5. The test tubes are closed with stoppers, sealed with a paraffin film, and placed inside the incubator at 30°C overnight under agitation with an orbital shaker at a speed of 1800 rpm to ensure homogenization.

Figure 2.5: Culture preparation (created with BioRender.com)

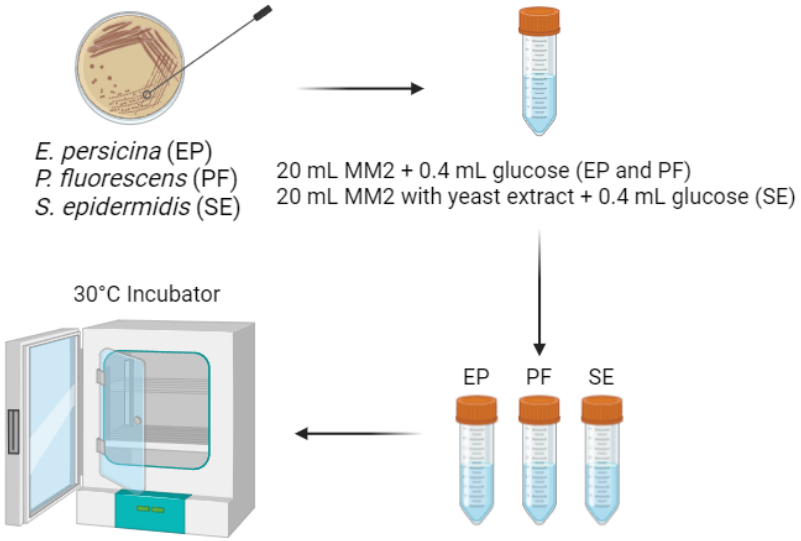

After 24 hours, a small sample is collected from each test tube, and the optical density (OD) is measured at 600 nm (figure 2.6). For this measurement, a blank with the same proportion of glucose and MM2 as the starting culture medium (with and without yeast extract) needs to be prepared.

Figure 2.6: OD measurement (created with BioRender.com)

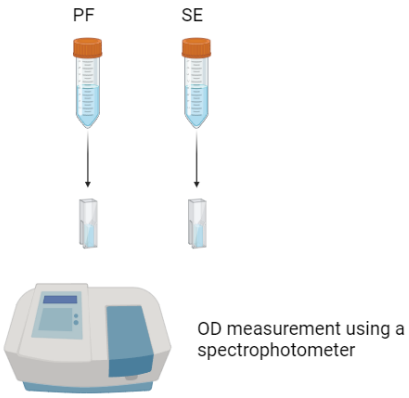

It is necessary to dilute the test tubes to achieve an optical density of 0.2 in a final volume of 10 mL.

$$Initial\ volume\ x\ initial\ OD = final\ volume\ x\ final\ OD \tag{2.1}$$

The initial volume has to be calculated depending on the initial measured OD.
Thus, the starting test tube is divided into two smaller test tubes with a volume of 10 mL and an OD of 0.2. One of them is covered with aluminum to avoid the UVA effect, while the other is exposed to UVA light (figure 2.7). The UVA light lamps have a power of 6W and a wavelength range of 385-405 nm. In the current experiment, these lamps are used in the 30°C incubator to verify how bacterial development changes under the effect of UVA light. The OD has to be measured each hour, or after 24 hours, to verify the UVA light influence.

Figure 2.7: OD evolution with and without UVA light exposure (created with BioRender.com)

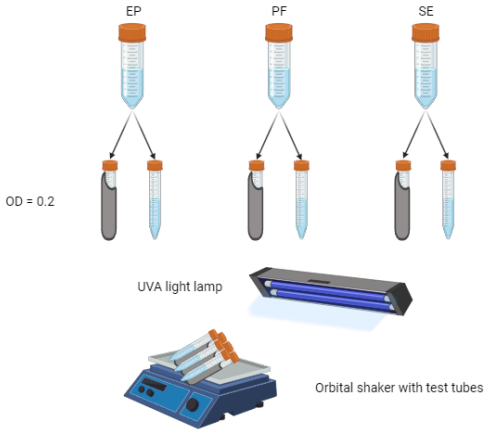

2.3.5 Microplate test

Microplate tests are essential for evaluating the efficacy of inhibitory antibacterial compounds on different bacterial strains. This technique allows rapid and accurate analysis of the impact of various concentrations of a compound on a large number of samples simultaneously. Due to their precision and the potential for automation, microplate tests are widely used in microbiological and pharmacological fields for the development and validation of new antibiotics and for the search for more effective antimicrobial agents. Microplate tests, on the other hand, require specialized equipment and can be more expensive and complex to perform.

The test is conducted using two azobenzenes for one microplate. Five milligrams of each azobenzene from purified samples are inserted into a small tube containing one milliliter of DMSO. For each azobenzene, seven tubes with different concentrations are prepared as shown in figure 2.8. For the first tube, labeled as A, a concentration of 5 g/L is achieved; for the second tube, labeled as B or A/2, a concentration of 2.5 g/L is achieved. For subsequent dilutions, 500 μL from the previous tube are taken and mixed with 500 μL of DMSO to achieve a halved concentration for each successive tube (5 g/L, 2.5 g/L, 1.25 g/L, 0.625 g/L, 0.313 g/L, 0.156 g/L, 0.078 g/L).

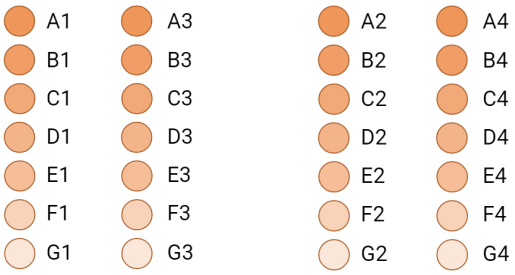

Figure 2.8: Azobenzenes concentrations (created with BioRender.com)

The initial step involves culturing bacteria on a solid medium. After 24 hours in the 30°C incubator, the bacteria are transferred to a liquid mineral medium and they are placed back in the 30°C incubator under agitation. The following day, the liquid culture is diluted to reach an optical density of 0.2. The distribution of substances and inoculation of bacteria on microplates were performed using automated liquid handling Eppendorf epMotion 5070 (figure 2.9), remotely controlled by the epBlue software.

Figure 2.9: Eppendorf epMotion 5070 [69]

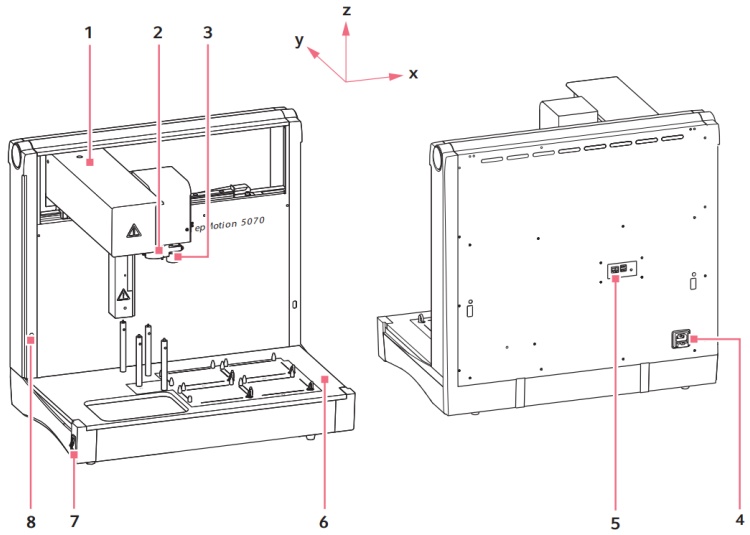

1. **Carrier**: the carrier moves in X-direction, Y-direction, and Z-direction
2. **Tool holder**: holds dispensing tools
3. **Optical sensor**: detects filling levels, tips, and labware
4. **Mains/power connection**
5. **Interfaces**
6. **Worktable**: work surface for placing tools and labware
7. **Mains/power switch**
8. **Light barrier**: The light reflectors are located on the inside of the front screen of the Cleanbench

Two microplates are required for each bacterium used, one to be exposed to UVA light and one not. At the end of the automated procedure, an OD measurement of the freshly inoculated plates is taken. Subsequently, they are placed in the incubator at 30°C overnight, under agitation with an orbital shaker to ensure homogenization. After 24 hours, the inhibition percentage is measured, as shown in equation 2.2, to verify the azobenzenes effect with and without UVA light exposure.

$$\%_{inhibition} = \left(1 - \frac{OD_{var\ test}}{OD_{var\ control}}\right) x100 \tag{2.2}$$

where $OD_{var\ test}$ is the difference of optical density between the highest point and the lowest point of the growth curve of the bacterium for a test. $OD_{var\ control}$ is the difference in optical density between the highest point and the lowest point of the growth curve of the bacterium in the control without an antimicrobial compound.

2.3.6 Zone of inhibition test

The zone of inhibition test is a widely used method in microbiology to evaluate the effectiveness of antimicrobial agents against specific bacteria. This technique offers several advantages over microplate tests, including simplicity, cost-effectiveness, and clear visual results. However, it is less precise and quantitative, offering only qualitative or semi-quantitative results. Moreover, the results can be influenced by the component diffusion in the agar and the agar composition and thickness.

Disk diffusion method

The procedure begins by adding 20 mg of each azobenzene from purified samples to a small tube containing one milliliter of pure ethanol. For each azobenzene, six tubes with different concentrations are prepared. The first tube, labeled A, contains a concentration of 20 g/L. The second tube, labeled B (or A/2), contains a concentration of 10 g/L. For subsequent dilutions, 500 μL from the previous tube are mixed with 500 μL of ethanol to achieve a halved concentration for each successive tube (20 g/L, 10 g/L, 5 g/L, 2.5 g/L, 1.25 g/L, 0.625 g/L).

Ten microliters of each sample are applied to 6 mm diameter filter paper discs and they are left to dry for a few hours. Ethanol was used for dilutions due to its high volatility, a necessary characteristic to allow the discs to dry after the application of the substances at different concentrations.

Each Petri dish contains six filter paper discs with different concentrations of the same substance, as shown in figure 2.10. Four different antimicrobial substances are tested for each bacterium, with six Petri dishes used for each substance: three exposed to UVA light and three not exposed to UVA light. In total, 24 Petri dishes are tested for each bacterium.

Figure 2.10: Example of Petri dish configuration

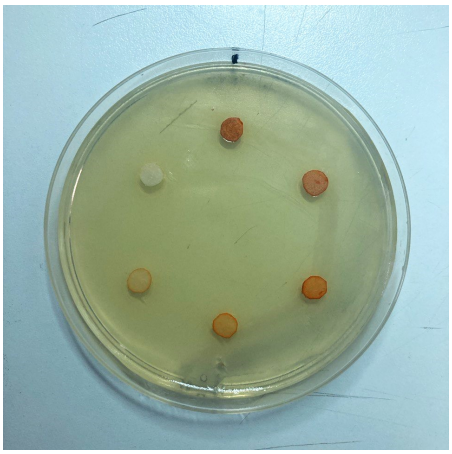

The initial step of the microbiological procedure involves culturing bacteria on a solid medium. After 24 hours in the 30°C incubator, the bacteria are transferred to a liquid mineral medium, and they are placed back in the 30°C incubator under agitation. The following day, the sample is diluted to reach an optical density of 0.063 (corresponding to Mc Farland latex standard of 0.5).
One hundred microliters of the collected sample are uniformly applied to a Petri dish. Filter paper discs impregnated with different azobenzene concentrations are then placed on the dish. This setup is finally placed in agar. It is important that the height of the agar inside the Petri dish is 4 mm to ensure an optimal diffusion of the antimicrobial substance. The antibiotic diffuses into the agar, with its concentration radially decreasing from the spot where the antibiotic was applied outward. If the antibiotic is effective against the bacteria at a particular concentration, the bacteria will not grow where the agar concentration exceeds the effective concentration. This region of no bacterial growth is called the zone of inhibition. [70]

Agar diffusion method
The microbiological procedure remains unchanged. Compared to the disk diffusion method, the differences involve the concentrations obtained for the dilutions, the solvent used, and the configuration of the petri dish without using filter paper discs. In particular, DMSO was used as the solvent for the dilutions, and the prepared concentrations were as follows: 5 g/L, 2.5 g/L, 1.25 g/L, 0.625 g/L, 0.313 g/L, and 0.156 g/L.
Instead of discs, 6 mm holes were punched with a glass capillary on the agar surface and filled with 20 μL of azobenzene solution.
DMSO has intrinsic toxicity, so this contribution must also be assessed, unlike the previous method where the solvent evaporated. To do this, an additional circular hole was made in the center of the Petri dish to evaluate the effect of the solvent on bacterial inhibition.
Diffusion distances were calculated as half of the inhibition zone diameter minus the diameter of the well. Each plate was analyzed individually to determine the minimum inhibitory concentration (MIC), and the final MIC was determined by averaging the values from three repetitions. This approach was taken to ensure that all inhibition zones in each experiment were obtained under consistent experimental conditions. [71]

Chapter 3

Results and discussion

ATTEMPT 1
Using the general procedure described earlier, 4-bromoaniline and p-Xylenol were used for the first synthesis. After filtration under vacuum, the solvent was evaporated. The residue was purified by silica gel chromatography (Cyclohexane/EtOAc, 7:3) to obtain the compound in figure 3.1:

Figure 3.1: 4-[(E)-(4-bromophenyl)diazenyl]-2,5-dimethylphenol

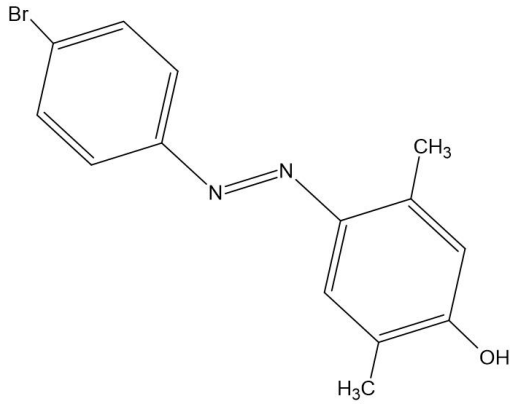

^{1}H *NMR* (400 MHz, MeOD) : δ 7.77 (d, J= 8.8Hz, 2H, CHAr) ; 7.68 (d, J= 8.8Hz, 2H, CHAr) ; 7.56 (s, 1H, CHAr) ; 6.74 (s, 1H, CHAr) ; 2.63 (s,3H, CH_3) ; 2.20 (s,3H, CH_3).
^{13}C *NMR* (1400 MHz, MeOD) : δ 133.34 ; 125.05; 118.84; 117.47; 17.27; 15.96.

ATTEMPT 2
Using the general procedure described earlier, 4-bromoaniline and Thymol were used for the second synthesis. After filtration under vacuum, the solvent was evaporated. The residue was purified by silica gel chromatography (Cyclohexane/EtOAc, 7:3) to obtain the compound in figure 3.2:

Figure 3.2: 4-[(E)-(4-bromophenyl)diazenyl]-5-methyl-2-(propan-2-yl)phenol

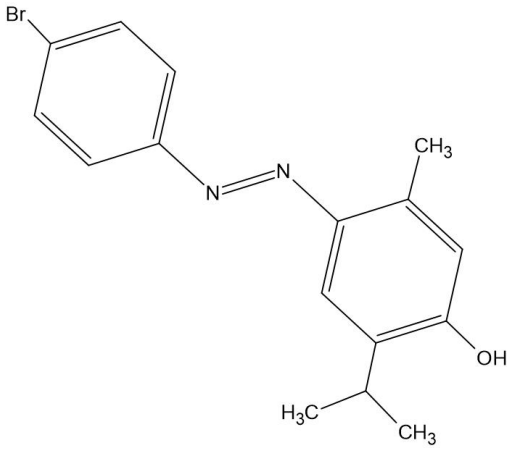

^1H *NMR* (400 MHz, MeOD) : δ 7.78 (d, J= 8.78Hz, 2H, CHAr) ; 7.69 (d, J= 8.78Hz, 2H, CHAr) ; 7.65 (s, 1H, CHAr) ; 6.74 (s, 1H, CHAr) ; 3.28 (d, J= 6.86Hz, 1H, CH); 2.63 (s,3H, CH_3); 1.25 (s, J= 6.92Hz, 3H, CH_3) ; 1.24 (s, J= 6.92Hz, 3H, CH_3).

ATTEMPT 3

Using the general procedure described earlier, 3,4-dichloroaniline and Thymol were used for the third synthesis. After filtration under vacuum, the solvent was evaporated. The residue was purified by silica gel chromatography (Cyclohexane/EtOAc, 7:3) to obtain the compound in figure 3.3.

Figure 3.3: 4-[(E)-(3,4-dichlorophenyl)diazenyl]-5-methyl-2-(propan-2-yl)phenol

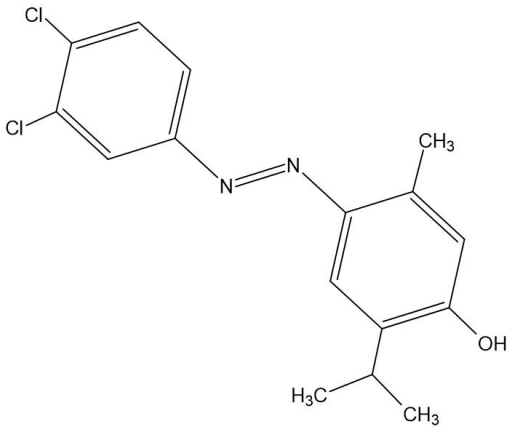

^1H *NMR* (400 MHz, $CDCl_3$) : δ 7.99 (d, J= 2.22Hz, 1H, CHAr) ; 7.80 (dd, J= 2.25Hz, J'= 2.25Hz, 1H, CHAr) ; 7.71 (s, 1H, CHAr) ; 7.58 (d, J= 8.55Hz, 1H, CHAr) ; 6.75 (s,

1H, CHAr) ; 3.2 (m, J= 6.87Hz, 1H, CH) ; 2.58 (s, 3H, CH_3) ; 1.19 (s, 3H, CH_3) ; 1.16 (s, 3H, CH_3). ^{13}C *NMR*: δ 171.46 ; 157.60 ; 151.46 ; 144.39 ; 140.11 ;?; 130.79 ; 123.50 ; 122.48 ; 117.40 ; 114.58 ; 60.54 ; 27.15 ; 22.43 ; 21.11 ; 17.18 ; 14.20.

ATTEMPT 4

Using the general procedure described earlier, 4-nitroaniline and p-xylenol were used for the fourth synthesis. After filtration under vacuum, the solvent was evaporated. The residue was purified by silica gel chromatography (Cyclohexane/EtOAc, 7:3) to obtain the compound in figure 3.4:

Figure 3.4: 2,5-dimethyl-4-[(E)-(4-nitrophenyl)diazenyl]phenol

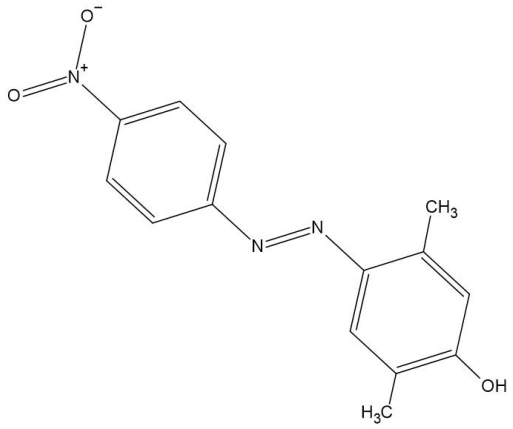

^1H *NMR* (400 MHz, $CDCl_3$) : δ 8.41 (d, J= 9.12Hz, 2H, CHAr) ; 8.01 (d, J= 9.05Hz, 2H, CHAr) ; 7.64 (s, 1H, CHAr) ; 6.76 (s, 1H, CHAr) ; 2.67 (s,3H, CH_3) ; 2.17 (s,3H, CH_3)

ATTEMPT 5

Using the general procedure described earlier, 3,4-dichloroaniline and Alizarin were used for the third synthesis. The desired product should have been the one shown in the figure 3.8:

Figure 3.5: 2-[(E)-(3,4-dichlorophenyl)diazenyl]-1,4-dihydroxyanthracene-9,10-dione

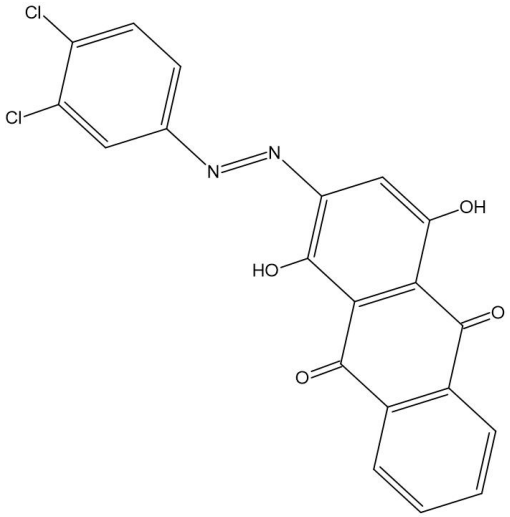

No product was obtained.

ATTEMPT 6

Using the general procedure described earlier, 2,4-dichloroaniline and Alizarin were used for the third synthesis. The desired product should have been the one shown in the figure 3.6:

Figure 3.6: 2-[(E)-(2,4-dichlorophenyl)diazenyl]-1,4-dihydroxyanthracene-9,10-dione

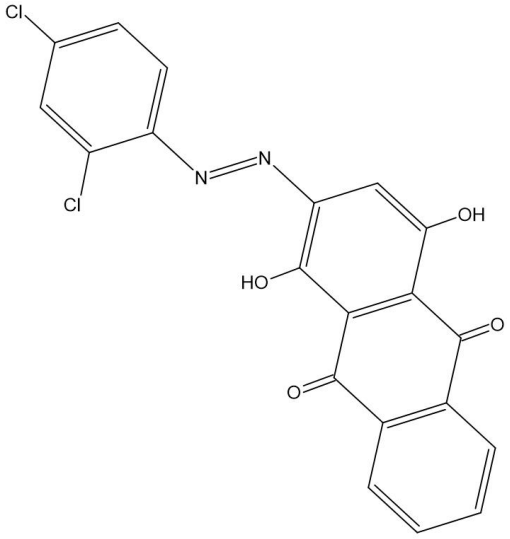

No product was obtained.

ATTEMPT 7

Using the general procedure described earlier, 4-bromoaniline and Alizarin were used for the third synthesis. The desired product should have been the one shown in the figure 3.7:

Figure 3.7: 2-[(E)-(4-bromophenyl)diazenyl]-1,4-dihydroxyanthracene-9,10-dione

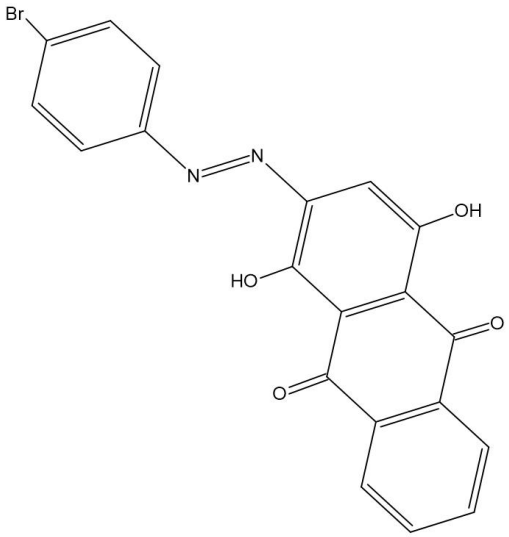

No product was obtained.

ATTEMPT 8

Using the general procedure described earlier, 2,4-dichloroaniline and Alizarin were used for the third synthesis. Twice the amount of aniline and sodium nitrite was used to try to improve the yield of the final product. The desired product should have been the one shown in the figure 3.8:

Figure 3.8: 2-[(E)-(3,4-dichlorophenyl)diazenyl]-1,4-dihydroxyanthracene-9,10-dione

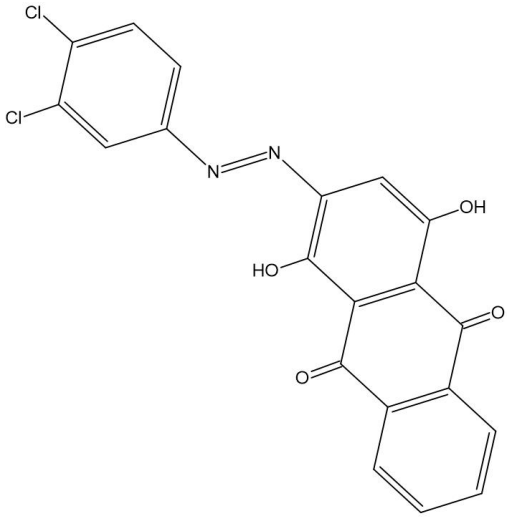

No product was obtained.

3.1 Product characterisation

3.1.1 Purification

The purification phase of the obtained products involves performing flash chromatography on the crude reaction mixtures and identifying the chromatogram peaks corresponding to the desired products. A chromatogram is a graph obtained during a chromatographic separation that shows the detector response as a function of time. The peaks in the chromatogram represent the different components of the mixture being eluted from the column. Each peak corresponds to a different compound, and the position of the peak (retention time) and its height can provide information about the identity and relative quantity of the compound.

Figure 3.9: Chromatogram 1

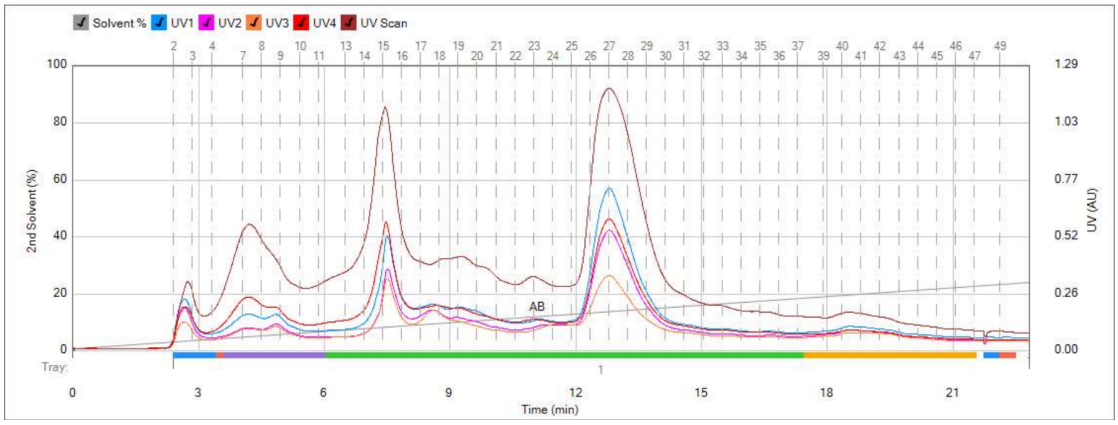

After analyzing the resulting chromatograms from the flash chromatography, further TLCs were performed to determine which peak in the chromatogram corresponded to the desired product. For the first product obtained, tubes 26 to 28 were considered. It was necessary to evaporate the solvent mixture (Cyclohexane/EtOAc, 7:3) used during flash chromatography to obtain a dry product. Subsequently, further verification was conducted through NMR spectroscopy to confirm that the purified product was indeed the desired azobenzene.

Figure 3.10: Purification TLC 1

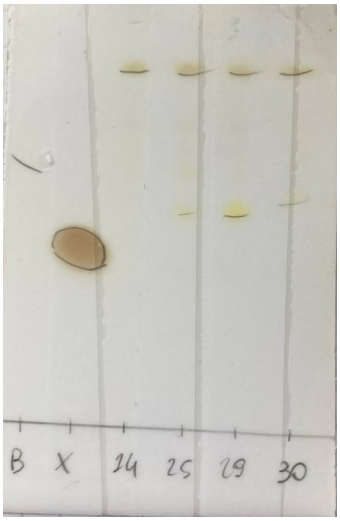

Figure 3.11: Chromatogram 2

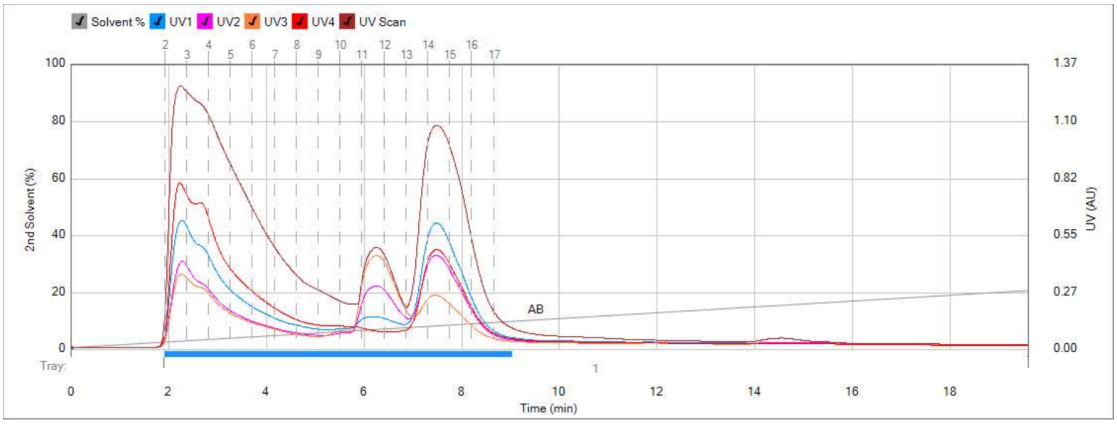

Figure 3.12: Purification TLC 2

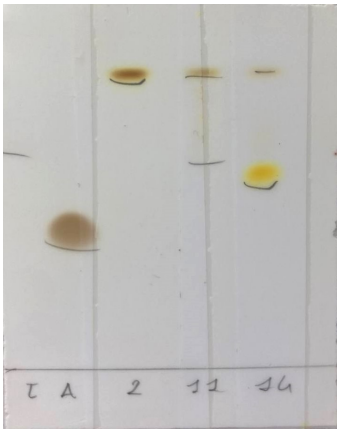

For the second product obtained, tubes 14 to 16 were considered.

Figure 3.13: Chromatogram 3

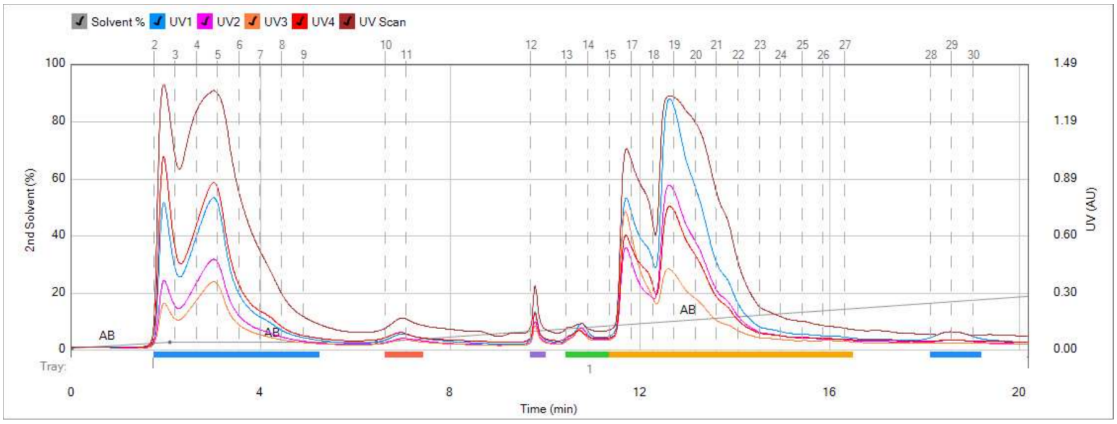

Figure 3.14: Purification TLC 3

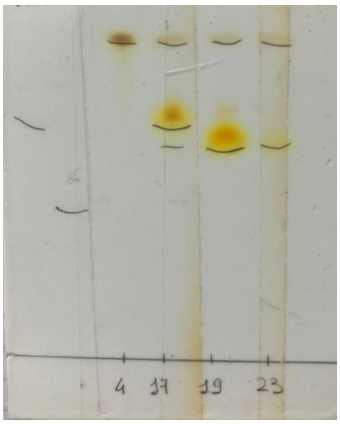

For the third product obtained, tubes 18 to 22 were considered.

Figure 3.15: Chromatogram 4

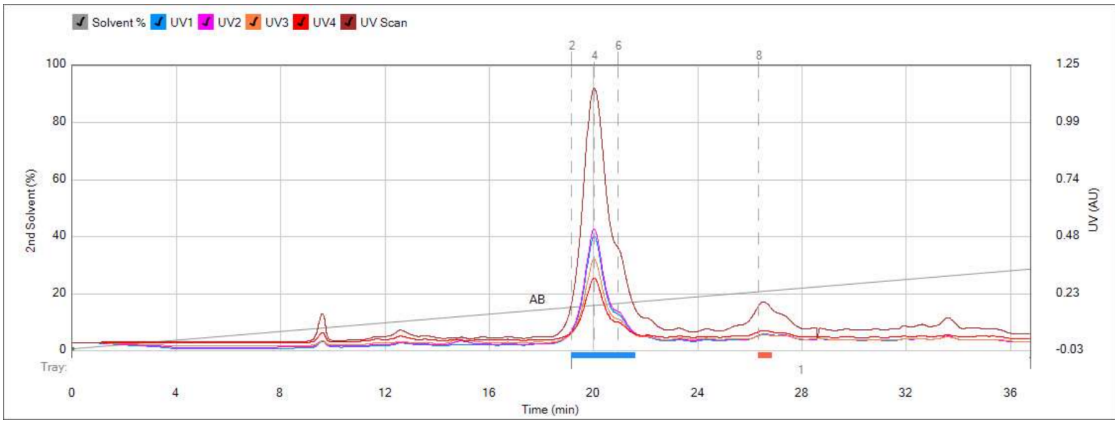

Figure 3.16: Purification TLC 4

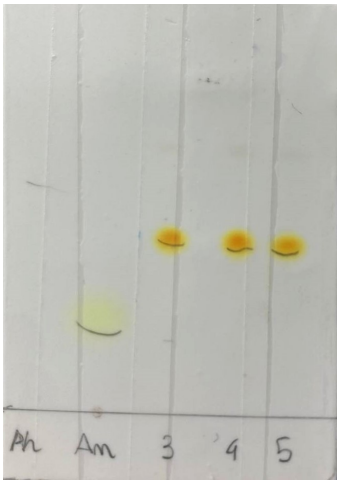

For the fourth product obtained, tubes 3 to 6 were considered.

Figure 3.17: Chromatogram 4.1

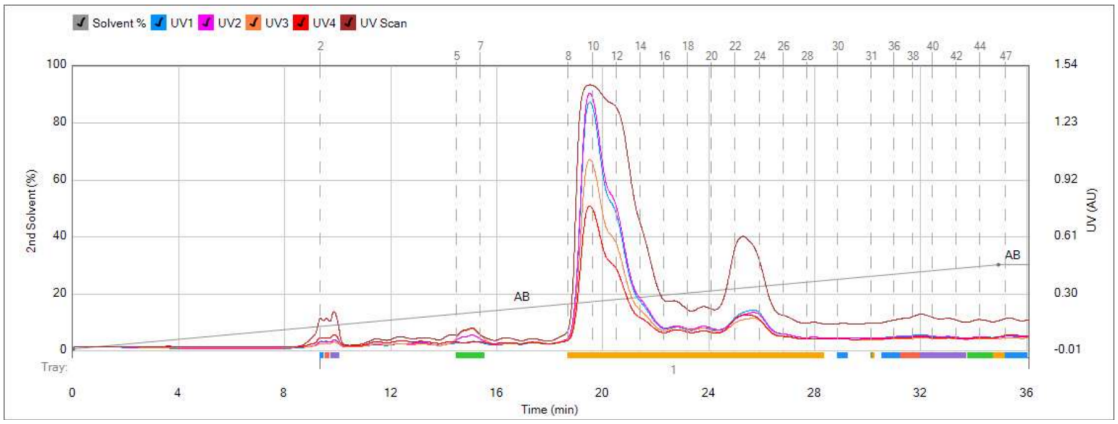

An additional flash chromatography was performed for the fourth product since its yield was higher, and therefore, the reaction product was in excess quantity to be processed in a single flash chromatography.

Figure 3.18: Purification TLC 4.1

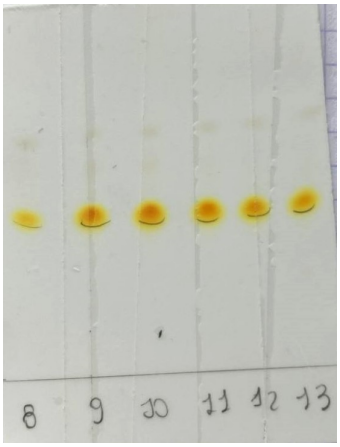

For the fourth product obtained, tubes 9 to 13 were considered.

Figure 3.19: Chromatogram 5

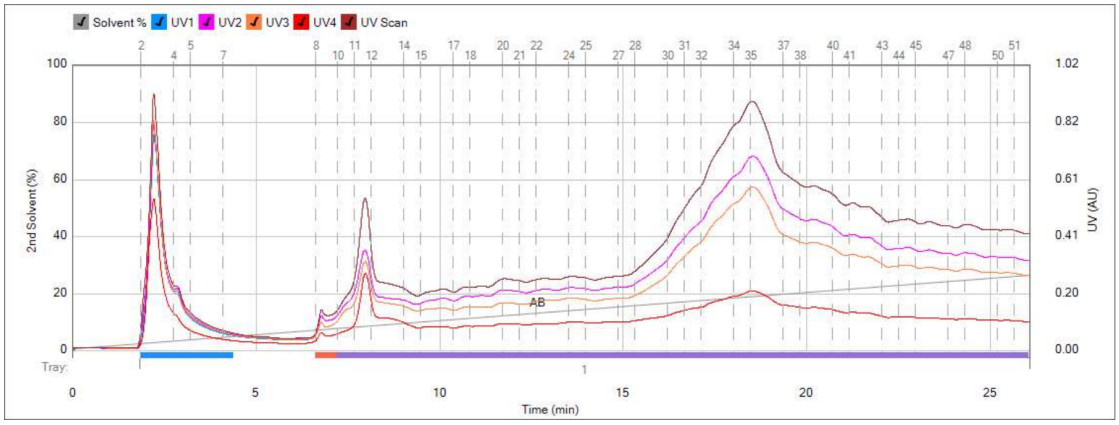

Figure 3.20: Purification TLC 5

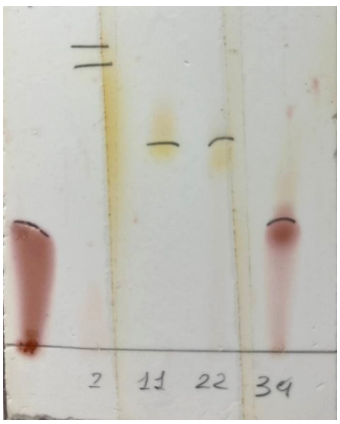

For the fifth product obtained, tubes 11 to 24 were considered.

Regarding this chromatogram, there were initial doubts about whether peak 34 could be residual alizarin or the desired azobenzene, given the large amount present in the obtained product. It was concluded that peak 34 was indeed alizarin, and peak 11 was likely the desired product in small quantities. Therefore, the reaction product contained a large amount of residual alizarin and a minimal amount of the desired azobenzene. Consequently, another reaction (reaction 8) was initiated with double the amount of sodium nitrite and aniline while keeping the same amount of alizarin to try to improve the yield of the final product.

Figure 3.21: Chromatogram 8

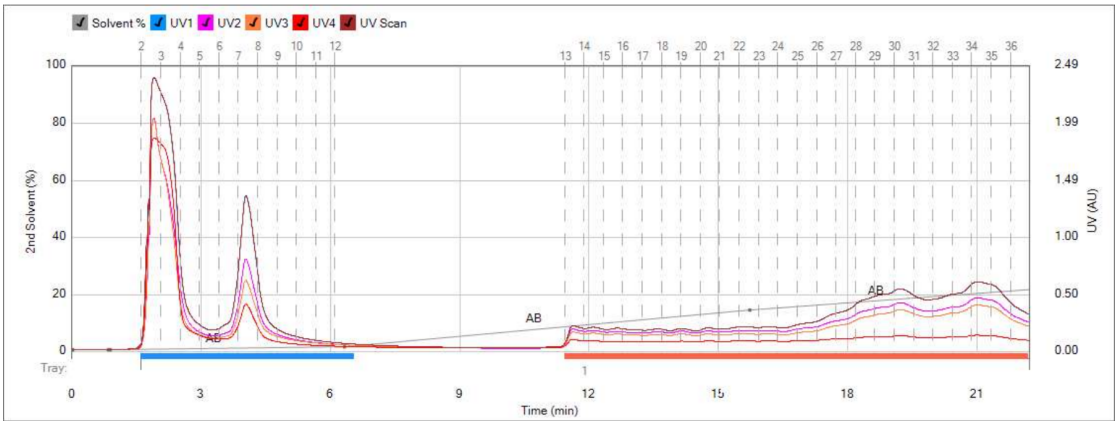

Figure 3.22: Purification TLC 8

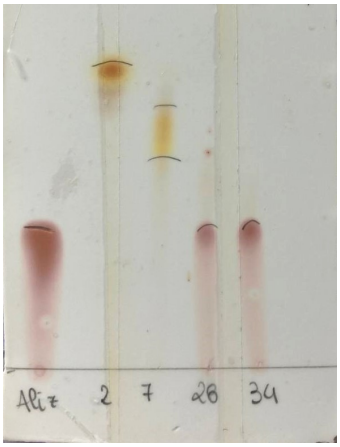

For the eighth product obtained, tubes 2 to 4 were considered.

It can be observed that the yield of the presumed desired product has significantly increased, as indicated by the intensity of the spots on the TLC sheet. Despite this, a large amount of residual alizarin is still clearly present in the final product. In conclusion, it is possible that the reaction product is not the desired azobenzene, but rather just residual alizarin and byproducts from the reaction. To gain more information about the structure, it is necessary to perform an NMR spectrum analysis of the purified product. This analysis will confirm whether the desired azobenzene is present.

3.1.2 NMR spectroscopy

The NMR spectrum of the eighth substance confirmed that the purified product obtained using alizarin does not correspond to the desired azobenzene. The ^{1}H spectrum presented numerous peaks that did not match the hydrogens in the desired structure. This can be explained by the fact that the two hydroxyl groups of alizarin are highly reactive. These groups could participate in side reactions, reducing the amount of alizarin available for the azo-coupling reaction with aniline, which is necessary to form azobenzene. Another explanation could be related to the structure of alizarin. The structure might create a steric hindrance that prevents the effective approach of aniline or diazonium salt, thereby reducing the efficiency of the azobenzene formation reaction.

Following this result, only the first four synthesized compounds were considered for all subsequent tests and analyses. These compounds showed consistent NMR spectra, confirming that they corresponded to the desired azobenzenes.

3.1.3 Isomerization test

The first four synthesized compounds were subjected to the isomerization test, as previously described, after purification.

A rapid isomerization of azobenzene via UVA light is particularly important because it allows for precise and immediate control of the molecule's biological properties. The importance of this test lies in the ability of azobenzene to change conformation quickly, allowing for the modification of antibacterial activity when needed. Assuming that the antibacterial action is more effective in the cis conformation, a molecule active against bacteria can be obtained in a short time if the isomerization rate is high. This approach allows for the creation of a molecule that is generally inactive against bacteria but can be activated quickly under UVA light, or in the absence of UVA light if the antibacterial action is more effective in the trans form.

Figure 3.23: Absorption spectrum trans-cis of the azobenzene A1. In red, the trans configuration, and in blue, the cis configuration, after UVA illumination at 385-405 nm (60 watts) for 1 minute.

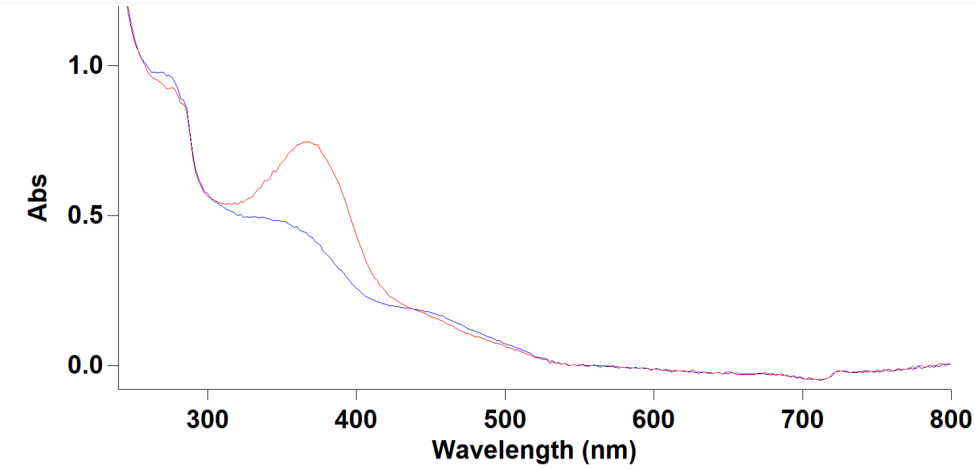

Figure 3.24: Absorption spectrum cis-trans of the azobenzene A1. In red, the cis configuration, and in blue, the trans configuration, after stopping UVA illumination for 1 minute.

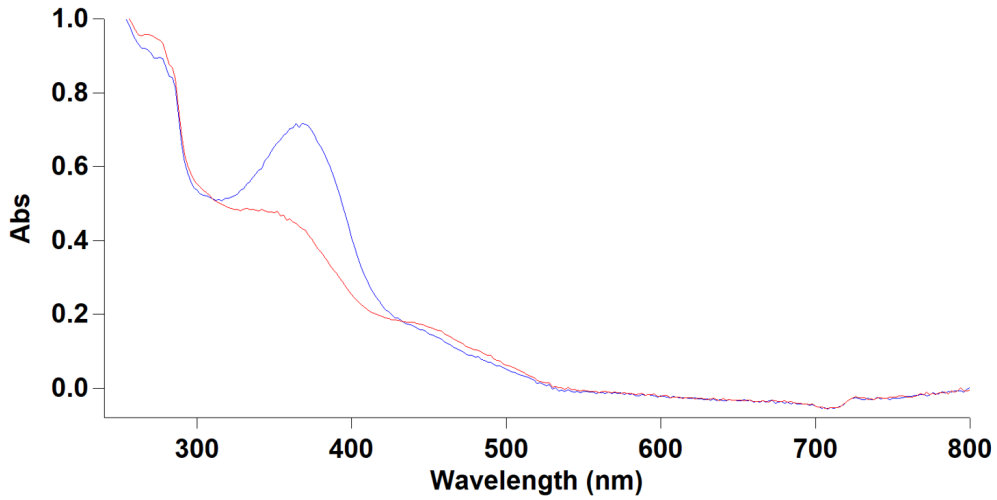

Band 1 = 273 nm : $\pi \Rightarrow \pi^*$ (benzene)
Band 2 = 366 nm : $\pi \Rightarrow \pi^*$ (azobenzene)
Band 3 = 435 nm : n $\Rightarrow \pi^*$ (nitrogen)

Figure 3.25: Absorption spectrum trans-cis of the azobenzene A2. In red, the trans configuration, and in blue, the cis configuration, after UVA illumination at 385-405 nm (60 watts) for 1 minute.

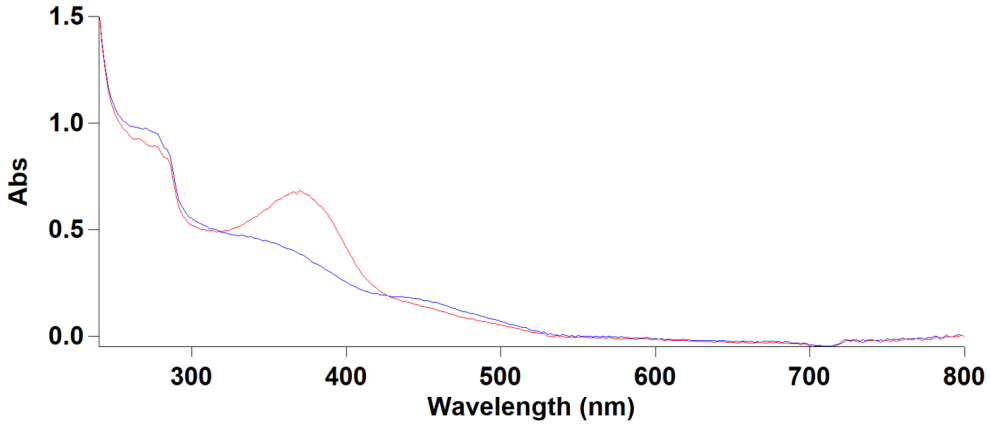

Figure 3.26: Absorption spectrum cis-trans of the azobenzene A2. In red, the cis configuration, and in blue, the trans configuration, after stopping UVA illumination for 1 minute.

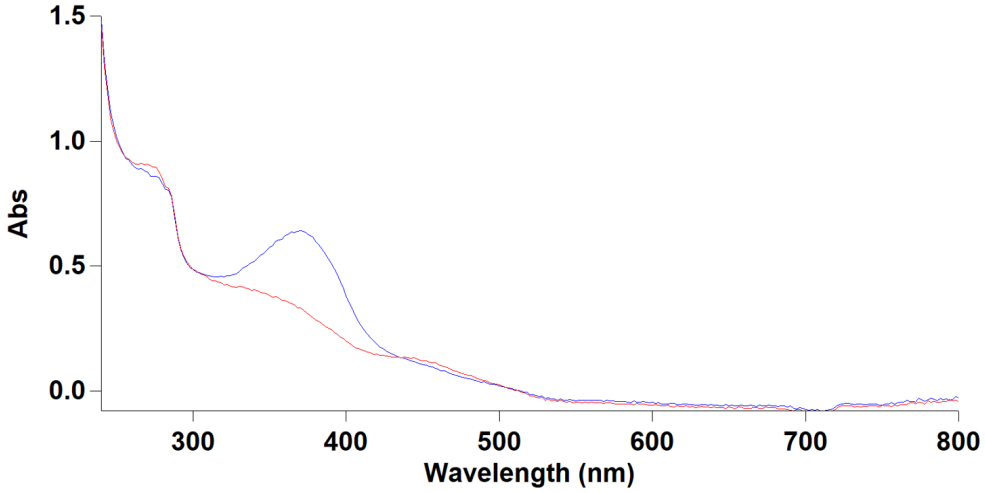

Band 1 = 270 nm : $\pi \Rightarrow \pi^*$ (benzene)
Band 2 = 368 nm : $\pi \Rightarrow \pi^*$ (azobenzene)
Band 3 = 433 nm : n $\Rightarrow \pi^*$ (nitrogen)

Figure 3.27: Absorption spectrum trans-cis of the azobenzene A3. In red, the trans configuration, and in blue, the cis configuration, after UVA illumination at 385-405 nm (60 watts) for 1 minute.

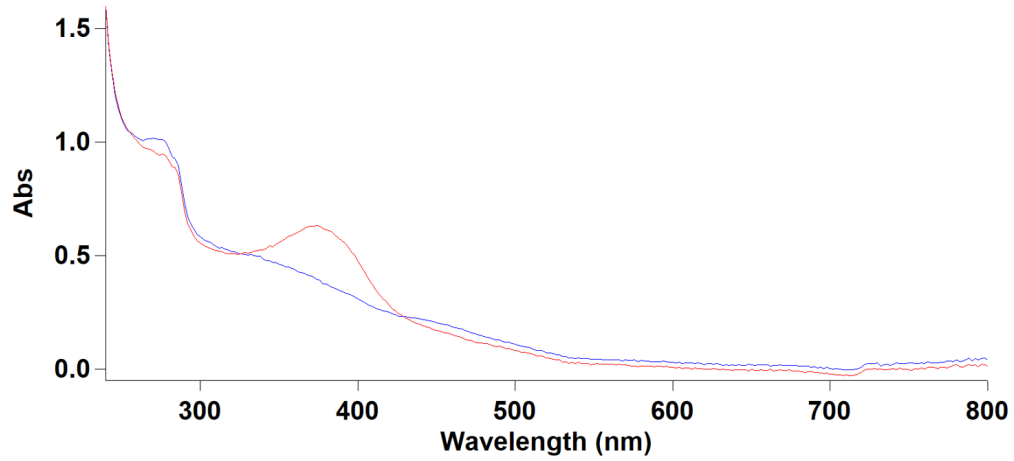

Figure 3.28: Absorption spectrum cis-trans of the azobenzene A3. In red, the cis configuration, and in blue, the trans configuration, after stopping UVA illumination for 1 minute.

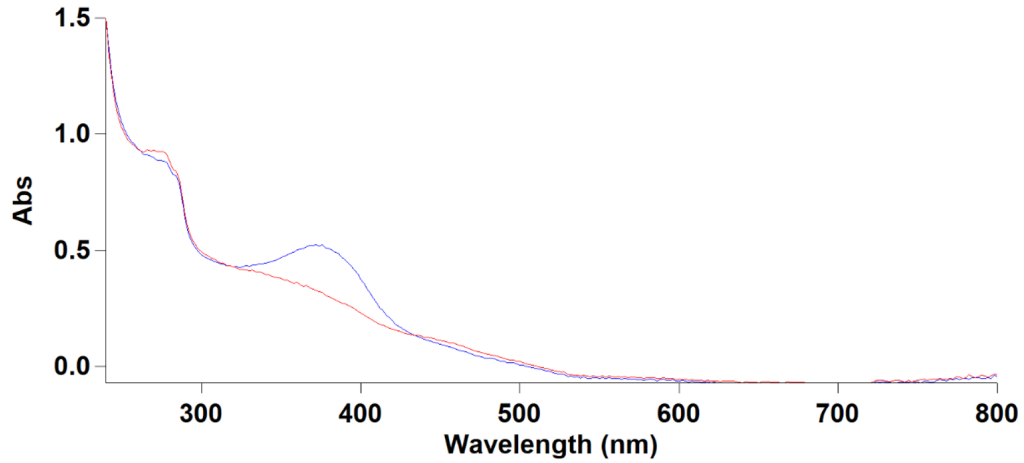

Band 1 = 275 nm : $\pi \Rightarrow \pi^*$ (benzene)
Band 2 = 374 nm : $\pi \Rightarrow \pi^*$ (azobenzene)
Band 3 = 439 nm : n $\Rightarrow \pi^*$ (nitrogen)

For all three azobenzenes, the isomerization between the trans and cis forms occurs

effectively and within very short time frames. Specifically, during the trans-to-cis isomerization, a decrease in the absorption band intensity around 350-400 nm (corresponding to the $\pi \Rightarrow \pi^*$ transition of azobenzene) and an increase in the band around 450 nm (corresponding to the n $\Rightarrow \pi^*$ transition) are observed. Additionally, an increase in absorption is noted around 280-300 nm, which corresponds to the $\pi \Rightarrow \pi^*$ transition of benzene.

This behavior can be explained by the more planar and symmetric geometry of the trans conformation, which allows for better delocalization of π-electrons, resulting in absorption at longer wavelengths (350-400 nm). The absorption of UVA light at these wavelengths promotes the $\pi \Rightarrow \pi^*$ transition, inducing the shift to the cis conformation.

The cis conformation, being more bent, exhibits less electron delocalization, leading to absorption at shorter wavelengths (280-300 nm). In this case, absorption of light at these wavelengths can also promote isomerization, but towards the trans conformation.

Additionally, UVA illumination can induce the n $\Rightarrow \pi^*$ transition, which is less energetic compared to the $\pi \Rightarrow \pi^*$ transition, but can still facilitate the trans-to-cis isomerization. This process is crucial as it allows the molecule to change configuration with minimal energy consumption, enabling control of isomerization via UVA light. When UVA illumination is halted, the molecule tends to revert to the trans conformation, often through the absorption of UV-visible light.

Figure 3.29: Absorption spectrum trans-cis of the azobenzene A4. In red, the trans configuration, and in blue, the cis configuration, after UVA illumination at 385-405 nm (60 watts) for 10 minutes.

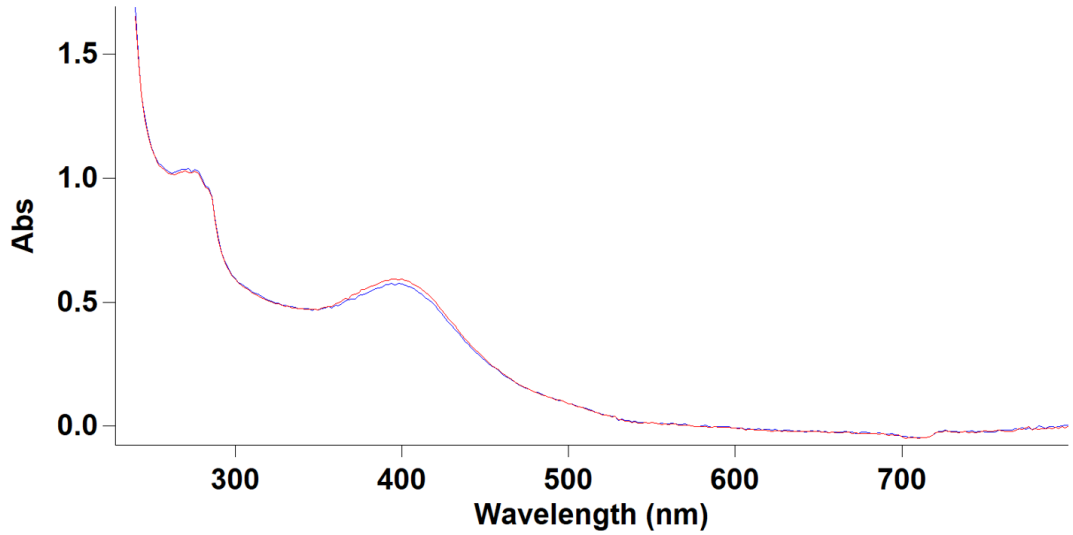

Figure 3.30: Absorption spectrum cis-trans of the azobenzene A4. In red, the cis configuration, and in blue, the trans configuration, after stopping UVA illumination for 10 minutes.

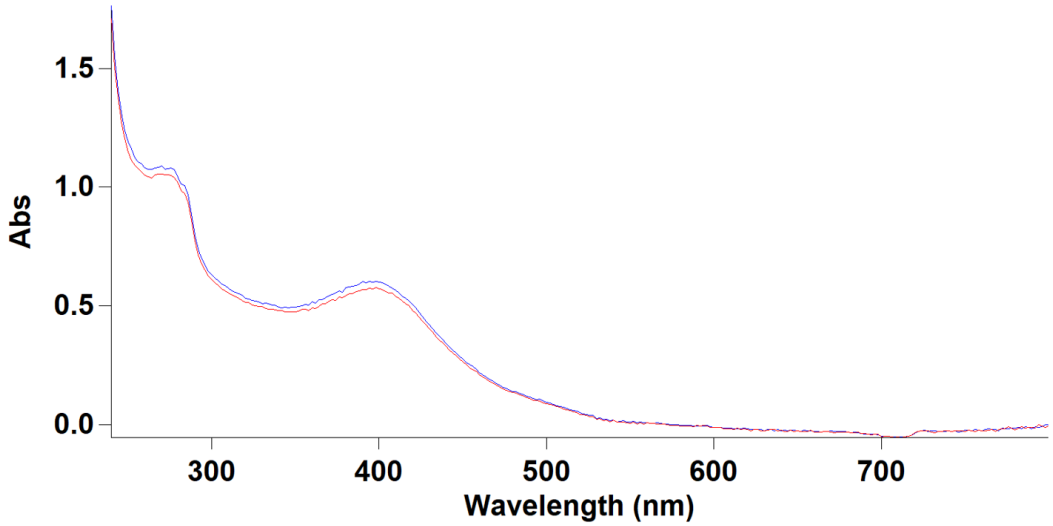

Band 1 = 274 nm : $\pi \Rightarrow \pi^*$ (benzene)
Band 2 = 400 nm : $\pi \Rightarrow \pi^*$ (azobenzene)
Band 3 = - nm : n $\Rightarrow \pi^*$ (nitrogen)

The isomerization of azobenzene 4 is not as immediate and evident as for the other three azobenzenes obtained. It can be observed that, after 10 minutes of UVA light exposure, the transition to the cis form is minimal, with an absorbance peak at 400 nm decreasing very slightly. This phenomenon can be explained by the presence of the nitrogen group, which may influence the electronic distribution of the molecule, destabilizing the delocalization of π-electrons. This could reduce the efficiency of photoisomerization, as the molecule might not properly absorb the UVA light required for the process.

Another explanation could be the greater thermodynamic stability of the trans form compared to the cis form, which may hinder the isomerization process. The presence of the nitrogen group might increase this stability. Additionally, this group could form hydrogen bonds with other parts of the molecule or with nearby molecules, further stabilizing the trans form and making the transition to the cis form more difficult.

3.2 Bacteria characterisation

The UVA resistance tests demonstrate that all analyzed bacteria, except for *E.persicina*, exhibit growth even under UVA light. In figure 3.31, bacterial growths measured by optical density at 600 nm, both in the presence and absence of UVA light, are shown along with their respective standard deviations.

Figure 3.31: Bacteria growth measurement with and without UVA light

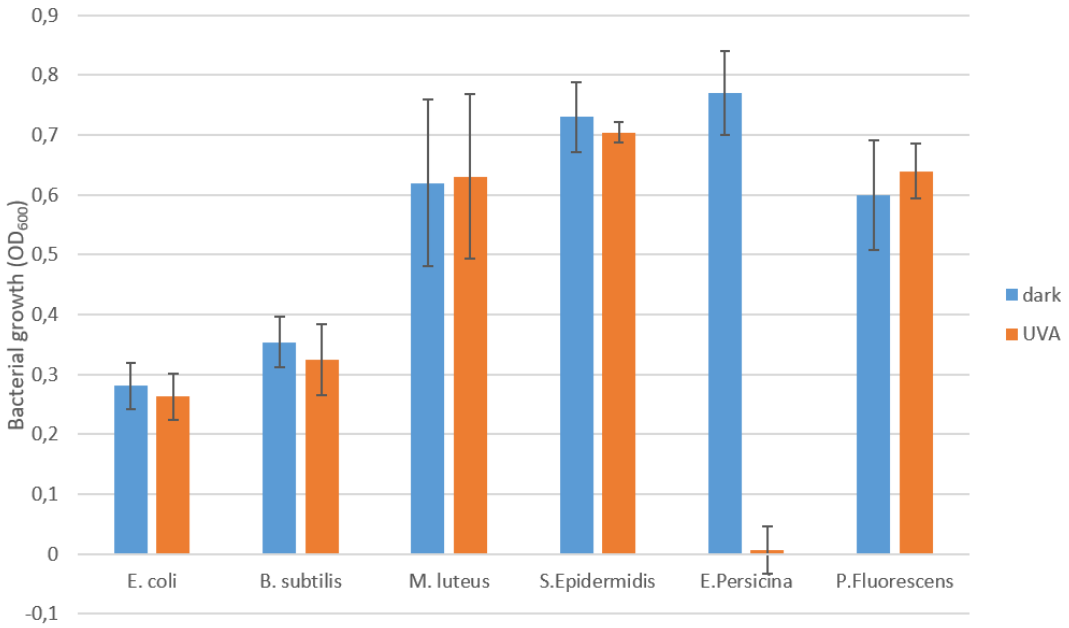

The bacterial growth measurement is determined by the difference between the OD_{max} - OD_{min} of the bacteria over 24 hours and the OD_{max} - OD_{min} of the liquid medium in which they are cultured during the same period. Therefore, an OD measurement is taken before the tests start and again after 24 hours. Measurements are averaged over three values, requiring three tests to be conducted in both the presence and absence of UVA light, resulting in six tubes for each bacterium tested.
The OD measurement of sterile liquid medium at the beginning and end of the tests is conducted to check for potential contamination. Therefore, if the difference OD_{max} - OD_{min} of the liquid medium remains null over 24 hours, no organisms were contaminating the fluid medium. The difference OD_{max} - OD_{min} of the analyzed bacteria over 24 hours in the presence of UVA light will be significant if the bacteria are not sensitive to the inactivating effect of UVA light.
The standard deviation of the growth rate is calculated from the three OD_{max} - OD_{min} values of the bacteria over 24 hours.

3.3 Antimicrobial activity of azobenzenes

3.3.1 Microplate test

As outlined in the procedure detailed in the previous chapter, optical density values are obtained after a few minutes from the bacterial inoculation and after 24 hours of exposure to UVA light or in the absence of it. For each inoculated microplate, it is possible to analyze the effect of two azobenzenes simultaneously on a bacterium.

The results from the microplate tests are processed using an Excel spreadsheet. The calculations were previously described in the 'Bacteria characterization' section, with the addition of the formula 2.2 for the inhibition rate found in the 'Materials and methods' chapter. Another important aspect to consider is the standard deviation propagation, which is useful for determining the reliability of the results. The formula 3.3 indicates the propagation of the standard deviation in percentage:

$$\%_{\sigma} = \left| \frac{100}{\bar{m}\Delta OD_{control}} \; x \; \sigma\Delta OD_{test} \right| + \left| \frac{\bar{m}\Delta OD_{test} \; x \; 100}{\bar{m}\Delta OD_{control} \; x \; \bar{m}\Delta OD_{control}} \; x \; \sigma\Delta OD_{control} \right| \quad (3.1)$$

$\%_{\sigma}$ represents the standard deviation propagation. $\bar{m}\Delta OD_{test}$ denotes the average of three measurements of the difference OD_{max} - OD_{min} over 24 hours for a test. $\bar{m}\Delta OD_{control}$ indicates the average of three measurements of the difference OD_{max} - OD_{min} over 24 hours in the control without an antimicrobial compound. $\sigma\Delta OD_{test}$ refers to the standard deviation of the three measurements of the difference OD_{max} - OD_{min} over 24 hours for a test. $\sigma\Delta OD_{control}$ denotes the standard deviation of the three measurements of the difference OD_{max} - OD_{min} over 24 hours in the control without an antimicrobial compound.

The graphs below show the inhibition caused by the substances used at different concentrations on each bacterium analyzed. The x-axis represents the various concentrations of the two azobenzenes, in this case, A1 and A3, expressed in mg/L. The y-axis displays the percentage inhibition calculated using the formula 2.2 for the different concentrations, both under UVA light exposure and in its absence. Additionally, the percentage inhibition of the solvent used (DMSO) is indicated both with and without UVA light exposure. This inhibition value is also calculated because DMSO has its own intrinsic toxicity that needs to be verified. The graph also includes the standard deviation propagation values for each inhibition percentage.

Figure 3.32: *S.epidermidis* inhibition by A1 (left) and A3 (right) using microplate assays

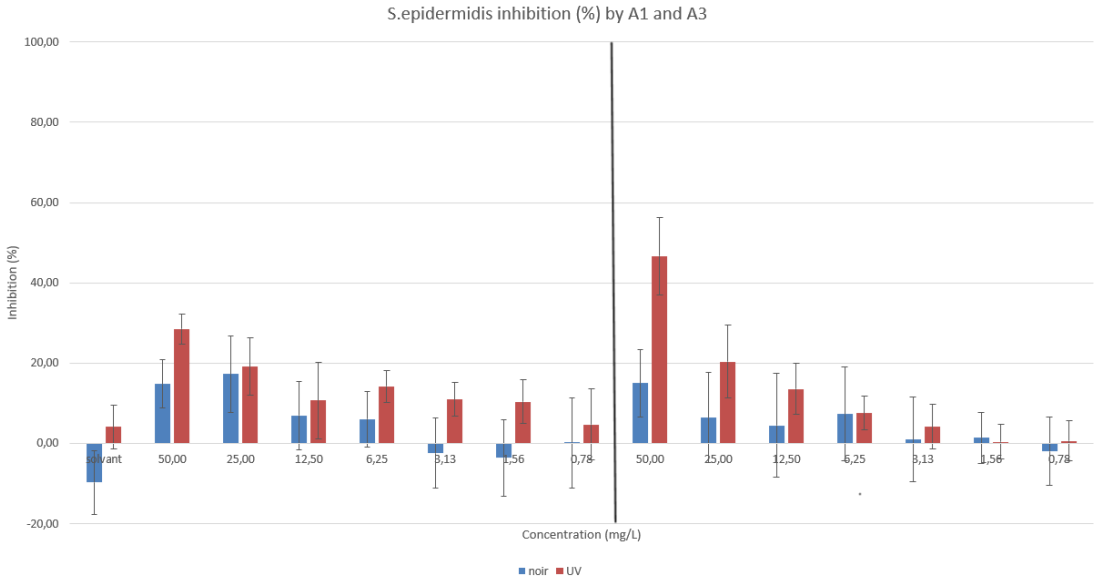

The first bacterium tested in microplates was *S.epidermidis*. It is a gram-positive bacterium belonging to the Staphylococcus genus, which often tends to form clusters. These clusters could potentially cause issues with the uniform diffusion of the antimicrobial substance within the aggregate.
From the graph 3.32, we can first observe the consistency of the results across the analyzed concentrations. As the concentrations decrease, the inhibition percentages gradually decrease as well. This indicates that the substance used did not encounter any diffusion issues and has successfully interacted with the bacterial cell walls.
In general, we can observe that under UVA light, the inhibition values are higher compared to those in its absence. This indicates that the cis conformation of azobenzenes A1 and A3 is more active and effective in inhibiting *S.epidermidis* than the trans conformation. This is a significant advantage because having the ability to modulate bacterial activity, through a conformational change via an immediate process like UVA irradiation, can reduce the likelihood of drug resistance phenomena. The greater inhibition might be attributed to the more compact and less planar structure of the cis isomer, which may facilitate the insertion of the molecule into bacterial cell membranes, thereby enhancing its interaction with membrane lipids and its ability to disrupt membrane function. Another explanation could be the higher reactivity of the cis conformation, which may lead to more effective or faster reactions with bacterial cell components.
Looking at the propagation of standard deviations for the inhibition values, the only consistent results are at a concentration of 50 mg/L for both azobenzenes analyzed.

Specifically, for these two results, the lower $\%_\sigma$ margin of the values under UVA light is higher than the upper $\%_\sigma$ margin of the values without UVA exposure. Therefore, these large $\%_\sigma$ values might be attributed to a lack of accuracy in the optical density measurement instrument or to minor errors during the automated pipetting and inoculation process.
Comparing the two antibacterial compounds used, it is evident that azobenzene A3 is much more effective in inhibiting *S.epidermidis* growth, with an inhibition rate of 46.6% under UVA light and 15% in the absence of UVA light. The respective standard deviation propagation values are 9.6% and 8.4%. In contrast, azobenzene A1 shows an inhibition rate of 25.5% under UVA light and 14.8% without UVA light, which is significantly lower than the values obtained for azobenzene A3. The respective standard deviation propagation values are 3.8% and 6%.

Figure 3.33: *E.coli* inhibition by A1 (left) and A3 (right) using microplate assays

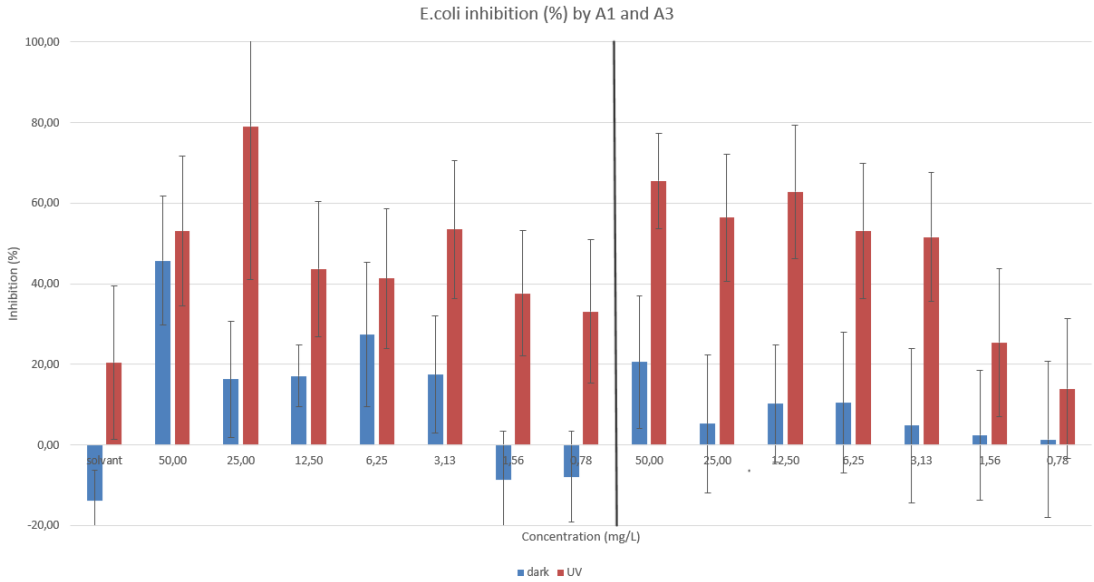

Escherichia coli is a gram-negative bacillus belonging to the Enterobacteriaceae family. Gram-negative bacteria are more difficult for antimicrobial substances to penetrate due to their complex cell wall structure, providing a more robust physical and chemical barrier than gram-positive bacteria.
The consistency of the data in the graph 3.33 is generally acceptable, except for some inhibition values that are higher at lower concentrations. For example, at a concentration of 25 mg/L, azobenzene A1 shows an inhibition rate of 79% (under UVA exposure), compared to a 53% inhibition rate at a higher concentration of 50 mg/L. The precipitation of the azobenzene might explain this discrepancy due to suboptimal solubility in the

solvent used (DMSO), leading to an inconsistency between the concentrations used and the results obtained.

In general, we can observe that the inhibition rates are higher than those obtained for *S.epidermidis*, despite the complex cell wall structure of *E.coli*. This could be because *E.coli*, unlike *S.epidermidis*, does not tend to form clusters, allowing for better diffusion of the antimicrobial substance and, consequently, higher inhibition rates. The formation of clusters prevents the azobenzene from penetrating the cells within the mass, leaving a significant percentage of bacterial cells uninhibited. This results in a reduction in the average inhibition rate.

Regarding the consistency of the results in confirming that the cis conformation is more effective than the trans, there are several results at different concentrations that can be considered valid. Specifically, the concentrations where the lower $\%_\sigma$ margin of the values under UVA light is higher than the upper $\%_\sigma$ margin of the values without UVA exposure.

Comparing the two antibacterial compounds used, the highest inhibition percentage is observed with azobenzene A1 at a concentration of 25 mg/L, but it is also necessary to consider the standard deviation propagation for each result. Taking this into account, we can see that azobenzene A3 at a concentration of 50 mg/L shows an inhibition percentage on *E.coli* of 65.5% with a standard deviation propagation of 11.8%. On the other hand, azobenzene A1 at a concentration of 25 mg/L exhibits an inhibition percentage on *E.coli* of 79% with a standard deviation propagation of 37.9%. Therefore, considering this factor, the most satisfactory result is that obtained with azobenzene A3. Overall, when looking at the results for A3 at lower concentrations, we can observe that most of them are more consistent and reliable than those obtained for A1.

Figure 3.34: *M.luteus* inhibition by A1 (left) and A3 (right) using microplate assays

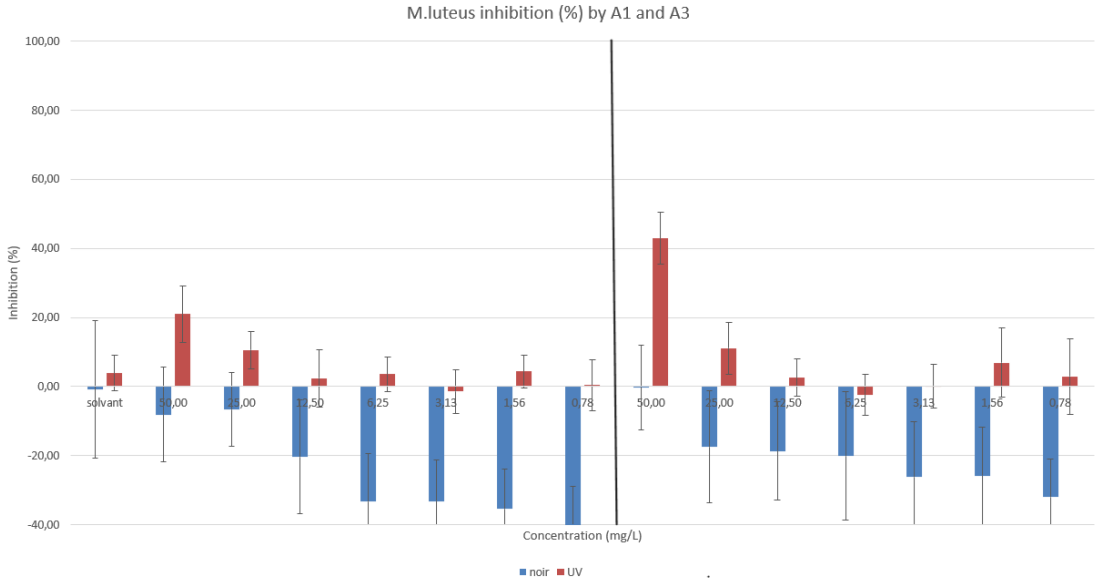

Micrococcus luteus is a saprotrophic, gram-positive, cocci-shaped bacterium. The cells are typically arranged in irregular clusters, which, like *S.epidermidis*, could potentially cause issues with the uniform diffusion of the antimicrobial substance within the cell walls of each bacterium in the aggregate.
In microplate tests, it is necessary to include both a positive control and a negative control to ensure the validity of the tests. The positive control should contain the culture medium with the bacteria but without the antimicrobial substance. The negative control should contain the culture medium without bacteria and the antimicrobial substance. In the optical density results, the positive control should show bacterial growth, while the negative control should show no growth. These controls will confirm that the test has been conducted correctly.
In this test, the negative control shows bacterial growth after 24 hours, with optical density values of 0.601, 0.322, and 0.227, starting from initial OD values of 0.105, 0.107, and 0.104, respectively. This is a clear sign of potential contamination by an external microorganism in the culture medium or during the automated inoculation procedure.
Moreover, the negative inhibition percentages in the absence of UVA light, as shown in the graph 3.34, is further evidence of possible contamination. This is because, according to the formula 2.2 for calculating the inhibition percentage, $OD_{var\ control}$ should be significantly larger to make the $\frac{OD_{var\ test}}{OD_{var\ control}}$ ratio less than 1. $OD_{var\ control}$ refers to the difference in optical density between the highest and lowest points of the bacterial growth curve in the control without an antimicrobial compound. The fact that it is smaller than expected indicates that the lowest point of the bacterial growth curve does not

have a sufficiently low OD value due to contamination of the culture medium by a microorganism.
Therefore, the test conducted on *Micrococcus luteus* cannot be considered valid and should not be used to draw conclusions about the activity of the analyzed azobenzenes.

Figure 3.35: *B.subtilis* inhibition by A1 (left) and A3 (right) using microplate assays

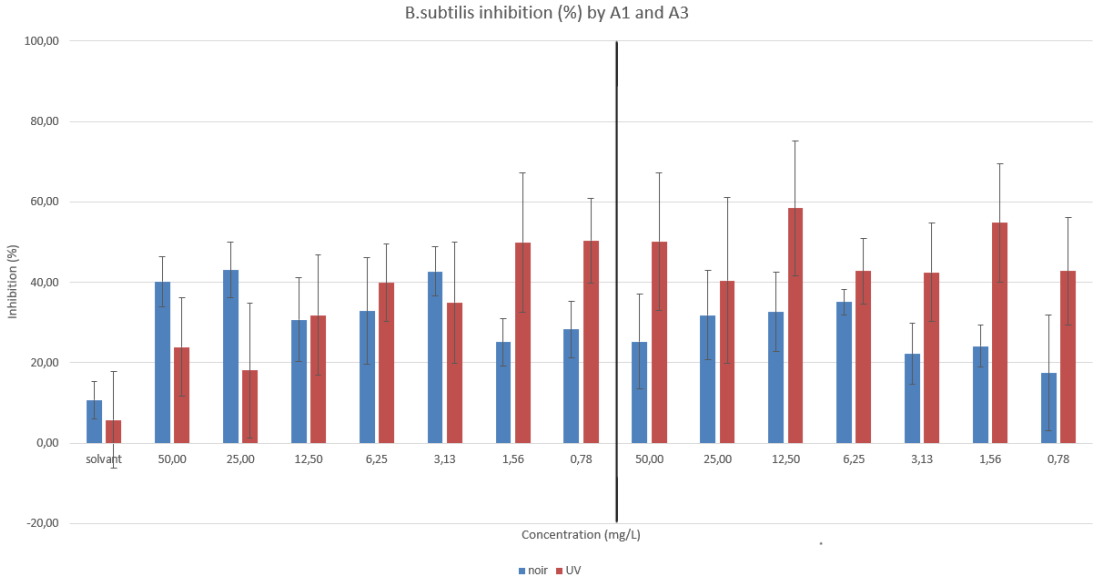

Bacillus subtilis is a gram-positive, rod-shaped bacterium belonging to the *Bacillaceae* family. It can form distinctly segmented three-dimensional colony biofilms. This could act as a barrier against the diffusion of the antimicrobial substance and hinder its inhibitory action.
It is evident that the consistency of the results relative to the concentrations used is not acceptable for either of the tested azobenzenes, as at higher concentrations, the inhibition percentages are very similar to or even lower than those at lower concentrations. This phenomenon may be attributed to the biofilm formed by *B.subtilis*, which could hinder the proper inhibitory action of the azobenzene on bacterial growth. Additionally, suboptimal solubility of the azobenzene in the solvent used, or potential errors during the automated liquid handling and inoculation process, could contribute to this outcome. In this case, we can exclude the possibility of contamination by an external microorganism, as the negative control shows no growth, while the positive control shows growth after 24 hours of incubation. From this perspective, the test was conducted correctly, but the potential issues mentioned above have compromised the results obtained.
For this reason, the test conducted on *Bacillus subtilis* cannot be considered valid and should not be used to draw conclusions about the activity of the analyzed azobenzenes.

3.3.2 Zone of inhibition test

Disk diffusion method
The results obtained using the disk diffusion method were unsatisfactory, as no inhibition zones were observed after 18 hours of incubation at 30°C. The issue may have been the diffusion of the antimicrobial substance from the paper disks through the agar gel. Therefore, a solution was proposed that does not involve the use of paper disks, with the hope of improving the diffusion of the substance through the agar gel.

Agar diffusion method
This method does not involve the use of paper discs to apply the antibacterial substance to the gel. Instead, 6 mm holes are punched into the agar surface with a glass capillary, and the azobenzene solution is directly inserted into them. Preliminary tests were conducted to ensure that the solution would properly diffuse through the gel before proceeding with the actual experiments.
The results obtained were consistent and more satisfactory compared to the previous experiment using the disk diffusion method. However, the precision of this method cannot be compared to that of tests conducted in microplates, as it can only provide qualitative or semi-quantitative results.

The effectiveness of antibiotics can be evaluated by their ability to suppress bacterial growth, described by the MIC (minimum inhibitory concentration), which is generally determined through tests in solid media. The MIC value is determined as the zero intercept of a linear regression of the squared size of the inhibition zones, x, plotted against the natural logarithm of the antibiotic concentration, c:

$$ln(MIC) = ln(c) - \frac{x^2}{4Dt} \tag{3.2}$$

D is the diffusion coefficient, presumed to be independent of concentration and t the time of antibiotic diffusion [72]. This analysis is based on a solution of a differential equation describing free diffusion in one dimension [35]:

$$D\frac{\partial^2 c(x,t)}{\partial x^2} - \frac{\partial c(x,t)}{\partial t} = 0 \tag{3.3}$$

where $c(x,t)$ describes the dependence of antimicrobial substance concentration on distance from the source and on time. This approach has been applied successfully to studies of two-dimensional diffusion of dyes and antibiotics [72].
The analysis of antimicrobial substance diffusion in solid agar reveals significant deviations from the expected behavior, as the inhibition zones increase linearly, rather than quadratically, with the logarithm of the azobenzene concentration. This behavior may be due to the fact that azobenzenes are relatively hydrophobic molecules. This observation led us to consider the possibility that these antimicrobial substances may diffuse through the agar medium more slowly than predicted by the free diffusion model. Therefore, a new theoretical model for data analysis is proposed, the dissipative diffusion model, which accounts for possible antimicrobial substance loss during diffusion [71].
The dissipative diffusion model allows for a more accurate quantitative assessment of bacterial susceptibility for antibiotics exhibiting free diffusion behavior deviations. It considers interactions with the diffusion medium, antibiotic degradation, or other losses during diffusion.
The alternative diffusion model includes a dissipative term to account for antibiotic loss through interactions with the diffusion matrix or other dissipative mechanisms. The proposed dissipative diffusion equation is:

$$D\frac{\partial^2 c(x,t)}{\partial x^2} + V\frac{\partial c(x,t)}{\partial x} - \frac{\partial c(x,t)}{\partial t} = 0 \tag{3.4}$$

where V is a coefficient characterizing the dissipation rate.
Using the method of separation of variables, the dissipative equation can be rewritten into two ordinary differential equations that describe the concentration's temporal and spatial dependence. The spatial part of the solution shows absorption-dominated diffusion that decays exponentially, which can be expressed as:

$$\ln(\mathrm{MIC}) = \ln(c) - \frac{2D}{V + \sqrt{V^2 - 4D}}x \tag{3.5}$$

This formula describes an exponential reduction in the amount of material available for diffusion, which may be due to the binding of the antibiotic to the agar matrix, degradation, or other mechanisms.
When the dissipative term is negligible ($V^2 \approx 4D$), the solution approximates that obtained from the free diffusion model via the separation of variables [32].

Experimental MIC values, determined using both the absorptive (linear) and free (quadratic) diffusion models, are summarized in table 3.1 and 3.2. The table also includes the corresponding R^2 values from the regression analysis, with R^2 values closer to 1 indicating

a better fit. The size of the inhibition zones is presented as a function, either linear or quadratic, of the natural logarithm of the antibiotic concentration, along with linear fits and regression residuals for each antimicrobial agent.

Table 3.1: Susceptibility of *E.coli* to A1 and A3: MIC [μg/mL] and R^2 values from linear regression analysis using quadratic or linear dependence of zone size [mm] on ln(c)

Parameter	**A1 (UVA)**	**A3 (UVA)**	**A1 (dark)**	**A3 (dark)**
$\frac{x^2}{ln(c)}$ model				
MIC	11.498	5.684	48.087	16.001
R^2	0.917	0.904	0.944	0.938
$\frac{x}{ln(c)}$ model				
MIC	0.147	0.034	4.570	0.329
R^2	0.947	0.912	0.921	0.946

Table 3.2: Susceptibility of *S.epidermidis* to A1 and A3: MIC [μg/mL] and R^2 values from linear regression analysis using quadratic or linear dependence of zone size [mm] on ln(c)

Parameter	**A1 (UVA)**	**A3 (UVA)**	**A1 (dark)**	**A3 (dark)**
$\frac{x^2}{ln(c)}$ model				
MIC	5.958	7.658	11.245	15.877
R^2	0.924	0.842	0.919	0.908
$\frac{x}{ln(c)}$ model				
MIC	0.047	0.068	0.149	0.274
R^2	0.923	0.863	0.922	0.933

Comparing the two models, it is evident that significantly lower MIC values were obtained with the linear absorptive diffusion model. Additionally, higher R^2 values for the absorptive diffusion model compared to the free diffusion model indicate that the measured data follow a linear trend rather than a quadratic one. This result is consistent with the theory, as azobenzenes are relatively hydrophobic compounds and may exhibit dissipative mechanisms, which align more closely with the absorptive diffusion model. Despite this, the MIC values obtained using the free diffusion model are more consistent

with the general concentration ranges reported for this class of antibacterial substances.

In general, we can observe that the MIC is higher in the absence of UVA exposure for both bacteria tested and for both substances used. This result is consistent with the outcomes obtained in microplate tests and aligns with the previous observations regarding the enhanced inhibitory action of the cis isomer.

Regarding *E.coli*, when comparing the inhibitory effect of the two azobenzenes, we can note that the lower MIC value in μg/mL was obtained for azobenzene A3. This indicates greater activity of azobenzene A3, as a smaller amount of the antimicrobial substance is required to achieve total bacterial inhibition. Once again, the results concerning the activity of the two azobenzenes are consistent with those obtained in the microplate tests.

Focusing on the results obtained for *S.epidermidis*, we notice that lower MIC values were observed for azobenzene A1. This is inconsistent with the results from the microplate tests, although, when comparing the two antimicrobial substances, the minimum inhibitory concentrations are quite similar. This discrepancy could be due to the lower precision and consistency of the present method compared to the microplate tests. In any case, it would be necessary to repeat the tests multiple times using both methods to verify the reliability of the obtained data.

When comparing the results obtained for the two bacteria, we observe that the minimum inhibitory concentrations (MICs) for *S.epidermidis* are lower than those for *E.coli*. This suggests that both azobenzenes used were more effective at inhibiting *S.epidermidis*, in contrast to the results obtained in microplate assays. This difference may be explained by the structural and behavioral differences between the two bacteria. As a Gram-negative bacterium, *E.coli* has a more complex cell wall structure, making it more difficult for azobenzenes to interact with.

Nevertheless, the inhibition results from the microplate assays were better for *E. coli* compared to *S.epidermidis*, likely because *S.epidermidis* tends to form floating agglomerates in liquid environments, which significantly reduces the inhibitory effect of azobenzene. However, on solid media (e.g., agar plates), *S.epidermidis* typically grows in discrete colonies rather than forming floating agglomerates.

Given this different behavior of *S.epidermidis* in liquid versus solid media, it is likely that on agar plates, the difficulty of interacting with *E.coli*'s more complex cell structure outweighs the issue of agglomeration in *S.epidermidis*. Therefore, it is consistent that azobenzenes exhibit a stronger inhibitory effect on *S.epidermidis* than on *E.coli*, due to *S.epidermidis*'s simpler cell wall structure and the absence of agglomeration in solid media.

Figure 3.36: *E.coli* inhibition by A1 under UVA using the agar diffusion method with dissipative diffusion model

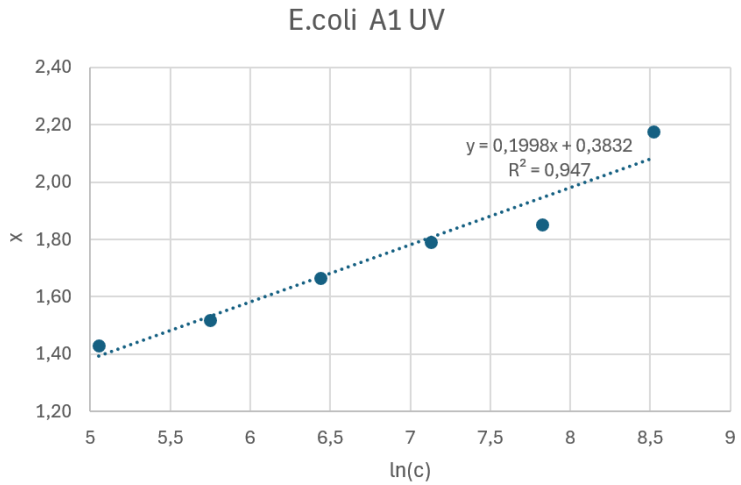

MIC = 0.147 μg/mL

Figure 3.37: *E.coli* inhibition by A1 under UVA using the agar diffusion method with free diffusion model

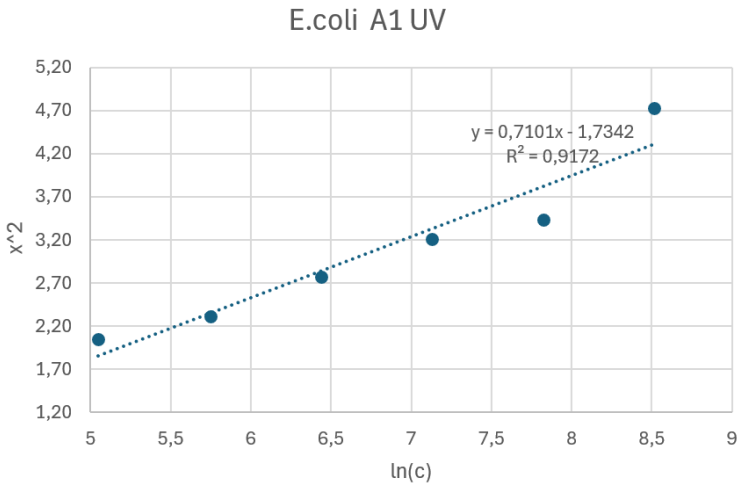

MIC = 11.498 μg/mL

Figure 3.38: *E.coli* inhibition by A1 without UVA using the agar diffusion method with dissipative diffusion model

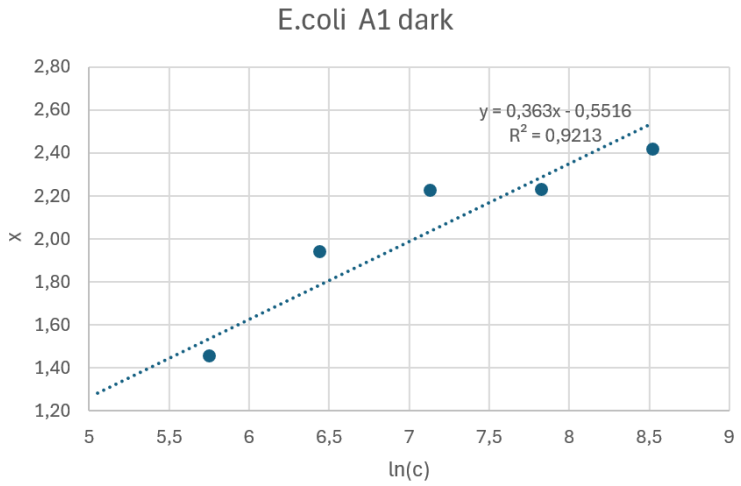

MIC = 4.570 μg/mL

Figure 3.39: *E.coli* inhibition by A1 without UVA using the agar diffusion method with free diffusion model

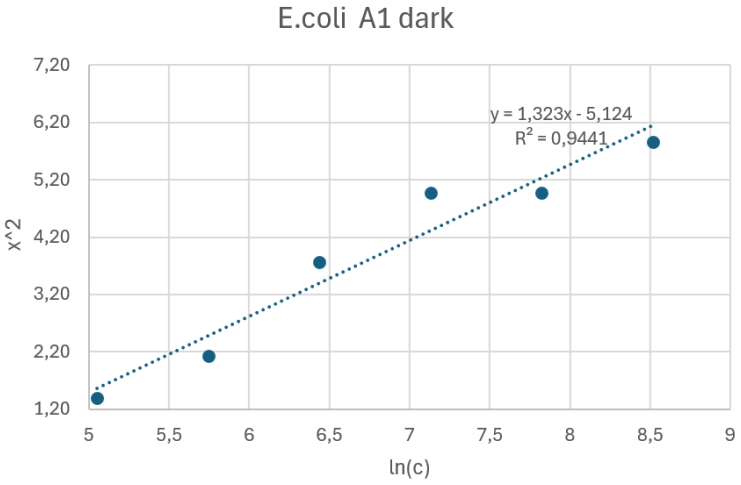

MIC = 48.087 μg/mL

Figure 3.40: *E.coli* inhibition by A3 under UVA using the agar diffusion method with dissipative diffusion model

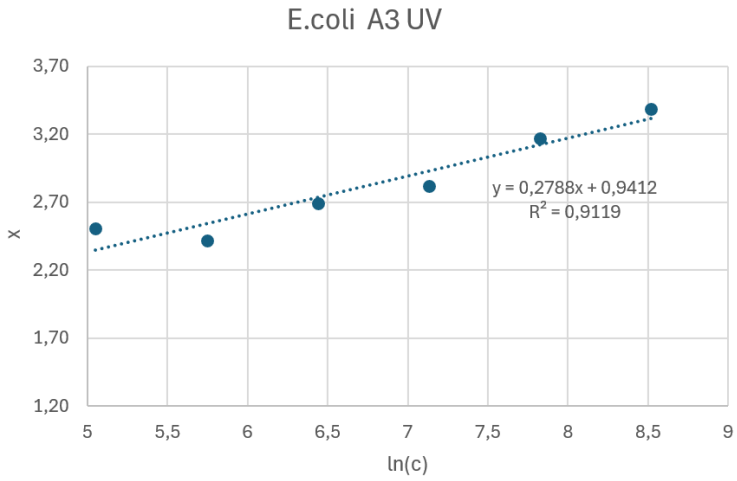

MIC = 0.034 μg/mL

Figure 3.41: *E.coli* inhibition by A3 under UVA using the agar diffusion method with free diffusion model

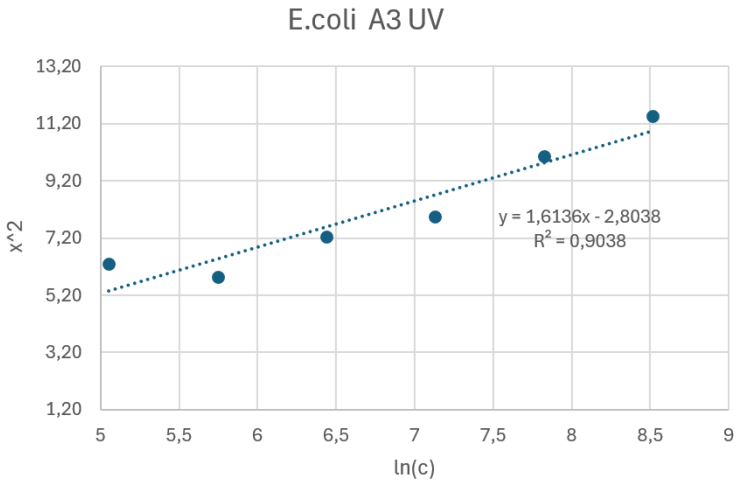

MIC = 5.683 μg/mL

Figure 3.42: *E.coli* inhibition by A3 without UVA using the agar diffusion method with dissipative diffusion model

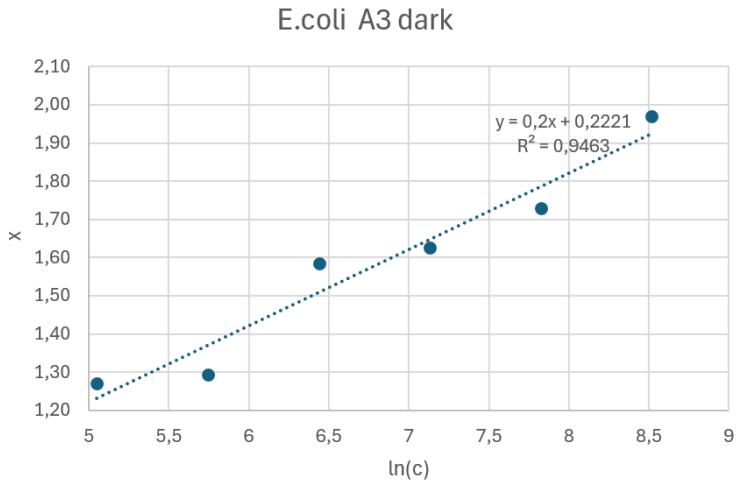

MIC = 0.329 μg/mL

Figure 3.43: *E.coli* inhibition by A3 without UVA using the agar diffusion method with free diffusion model

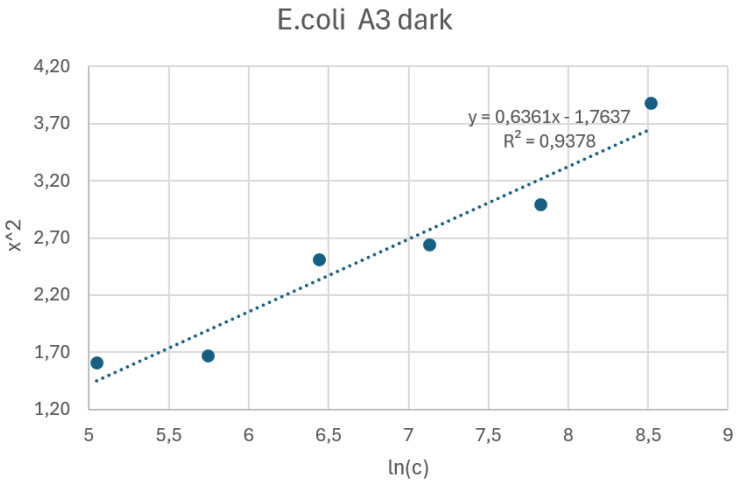

MIC = 16.001 μg/mL

Figure 3.44: *S.epidermidis* inhibition by A1 under UVA using the agar diffusion method with dissipative diffusion model

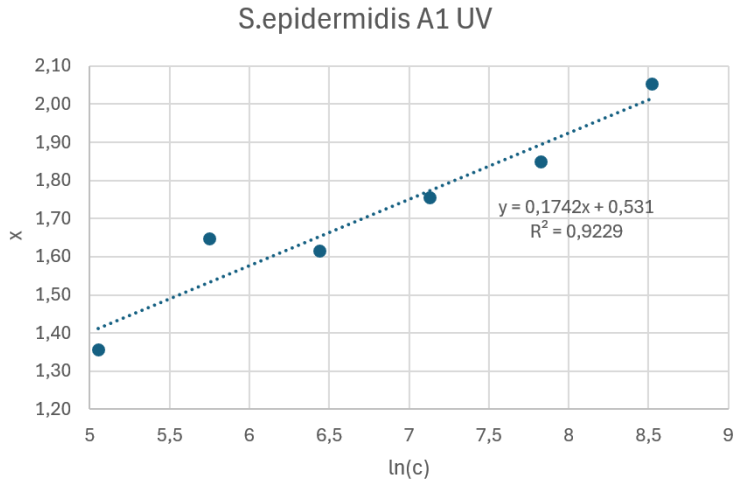

MIC = 0.047 μg/mL

Figure 3.45: *S.epidermidis* inhibition by A1 under UVA using the agar diffusion method with free diffusion model

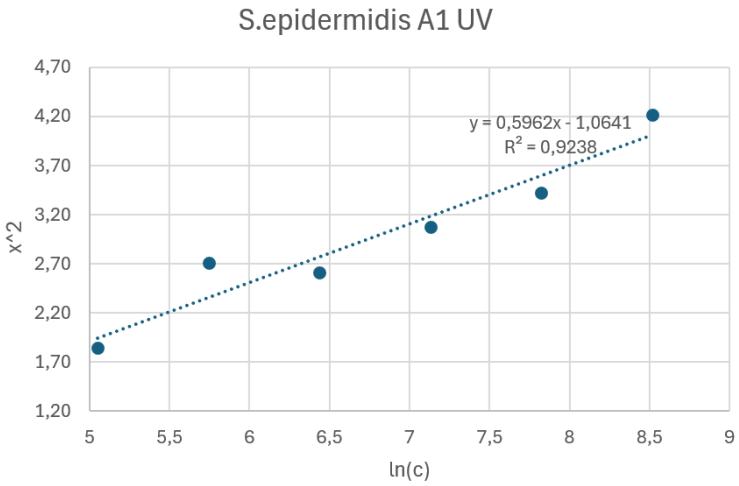

MIC = 5.958 μg/mL

Figure 3.46: *S.epidermidis* inhibition by A1 without UVA using the agar diffusion method with dissipative diffusion model

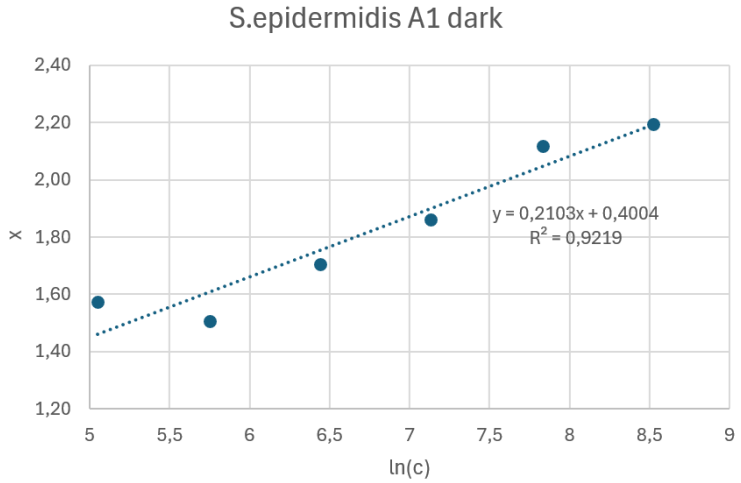

MIC = 0.149 μg/mL

Figure 3.47: *S.epidermidis* inhibition by A1 without UVA using the agar diffusion method with free diffusion model

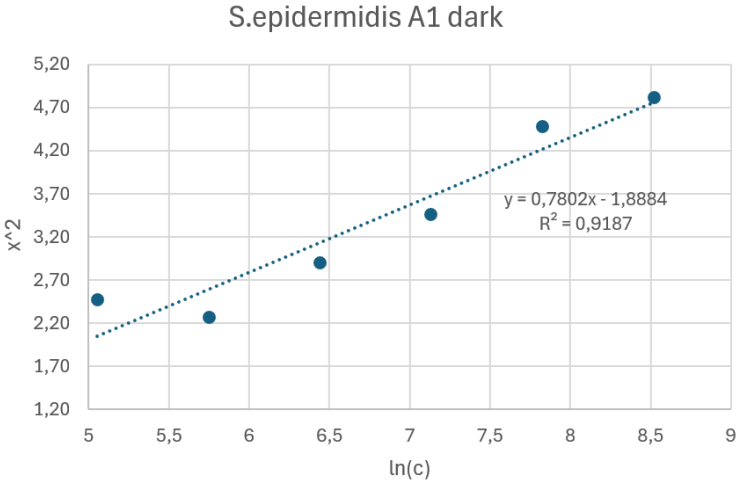

MIC = 11.245 μg/mL

Figure 3.48: *S.epidermidis* inhibition by A3 under UVA using the agar diffusion method with dissipative diffusion model

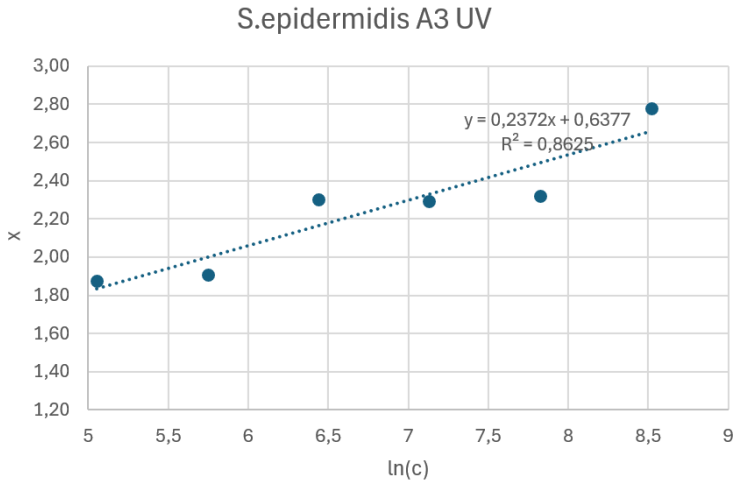

MIC = 0.068 μg/mL

Figure 3.49: *S.epidermidis* inhibition by A3 under UVA using the agar diffusion method with free diffusion model

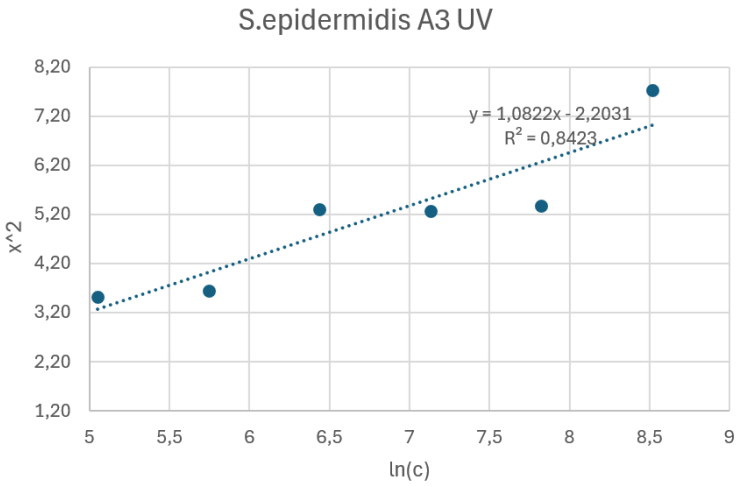

MIC = 7.658 μg/mL

Figure 3.50: *S.epidermidis* inhibition by A3 without UVA using the agar diffusion method with dissipative diffusion model

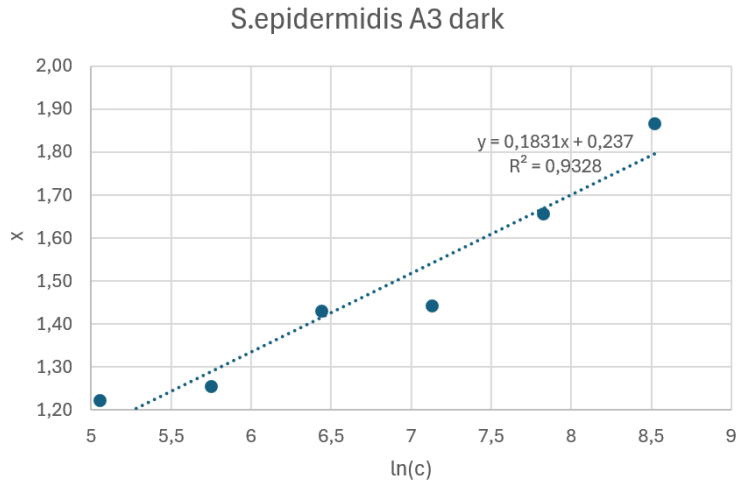

MIC = 0.274 μg/mL

Figure 3.51: *S.epidermidis* inhibition by A3 without UVA using the agar diffusion method with free diffusion model

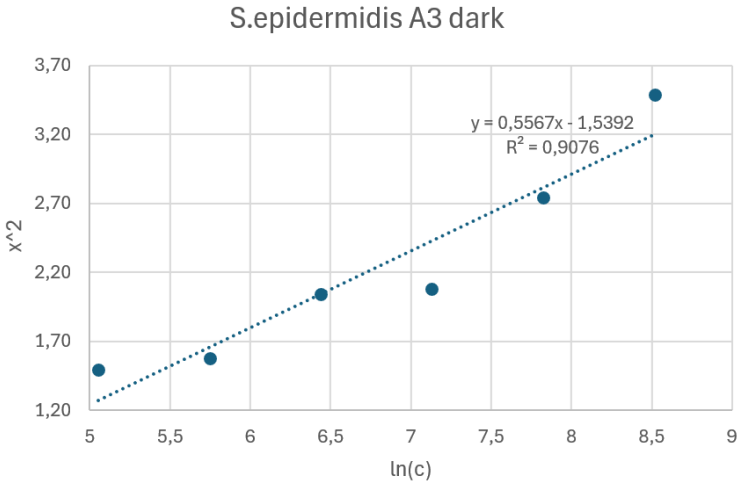

MIC = 15.877 μg/mL

Chapter 4

Conclusion

This research has underscored the importance of thoroughly analyzing the properties and mechanisms of action of azobenzenes as potential antimicrobial agents. The tests revealed the structural complexity of bacteria, such as *E.coli* and *S.epidermidis*, plays a crucial role in their susceptibility to these agents. Specifically, *E.coli* exhibited greater resistance to azobenzenes in agar diffusion tests, likely due to its complex cell wall structure, which hinders the diffusion of antimicrobial substances. In contrast, *S.epidermidis* showed higher sensitivity on solid media, where the formation of agglomerates is reduced.

The results obtained using the agar diffusion method highlighted the significance of selecting the appropriate theoretical model for accurate data interpretation. The dissipative diffusion model provided a more suitable explanation for the experimental observations compared to the free diffusion model, particularly considering the hydrophobic nature of azobenzenes. However, the discrepancies between the results from microplate tests and agar tests suggest that further studies are necessary to fully understand the behavior of these substances under different experimental conditions.

Another significant achievement from this research is the effect of UVA light exposure, capable of modulating the inhibitory activity of azobenzenes through photoisomerization, confirming the greater efficacy of the cis isomer. This result paves the way for potential photodynamic applications of azobenzenes in treating bacterial infections, where light could be used as a modulator of antimicrobial activity.

Finally, the research highlighted the importance of a rigorous experimental approach, with adequate controls to prevent contamination and ensure the validity of the results. The tests conducted on *Micrococcus luteus* and *Bacillus subtilis* emphasized the need to repeat experiments and employ various methods to verify the reproducibility and reliability of the data, especially when inconsistent results are observed.

In conclusion, this study has provided valuable insights into the potential of azobenzenes as antimicrobial agents, while also highlighting the challenges associated with their characterization and application. The complexity of biological systems and experimental variables requires careful attention in experimental design and data interpretation to ensure that the results can be effectively translated into clinical applications. Future research should focus on further refining theoretical models and optimizing experimental conditions with the goal of developing new antimicrobial treatments based on azobenzenes.

Appendix A

NMR spectra

The figures A.1, A.2, A.3 and A.4 below represent the H^1 NMR spectra of azobenzenes 1, 2, 3, and 4, with each peak indicating the corresponding proton it represents within the molecule.

Figure A.1: NMR spectrum 4-[(E)-(4-bromophenyl)diazenyl]-2,5-dimethylphenol

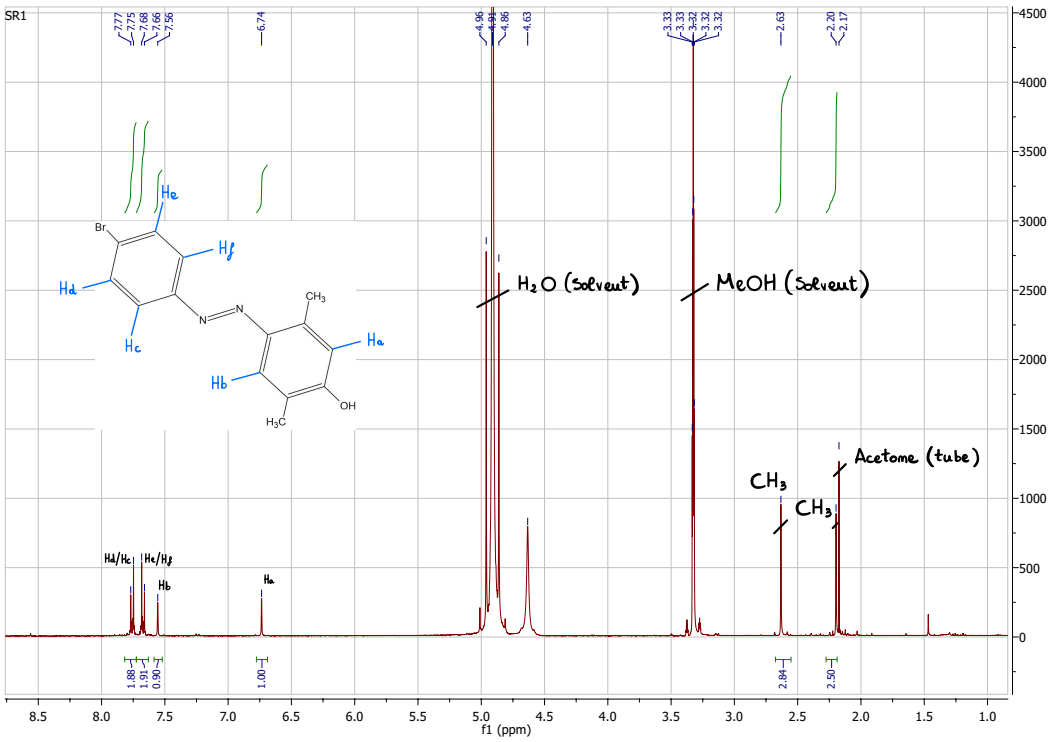

Figure A.2: NMR spectrum 4-[(E)-(4-bromophenyl)diazenyl]-5-methyl-2-(propan-2-yl)phenol

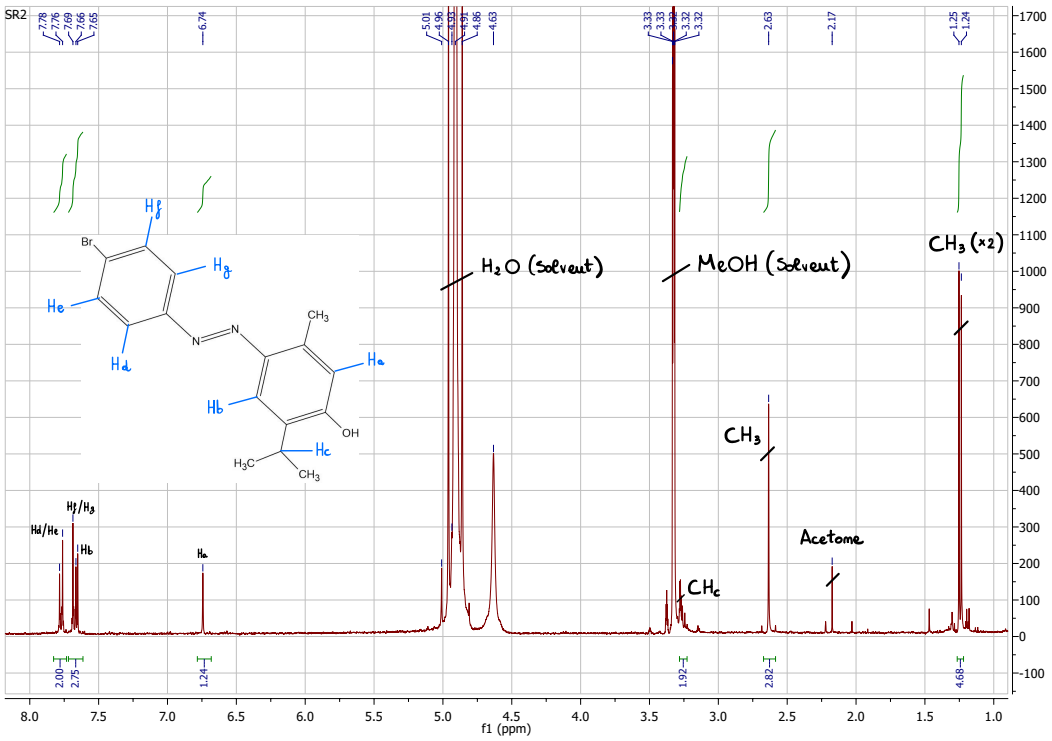

Figure A.3: NMR spectrum 4-[(E)-(3,4-dichlorophenyl)diazenyl]-5-methyl-2-(propan-2-yl)phenol

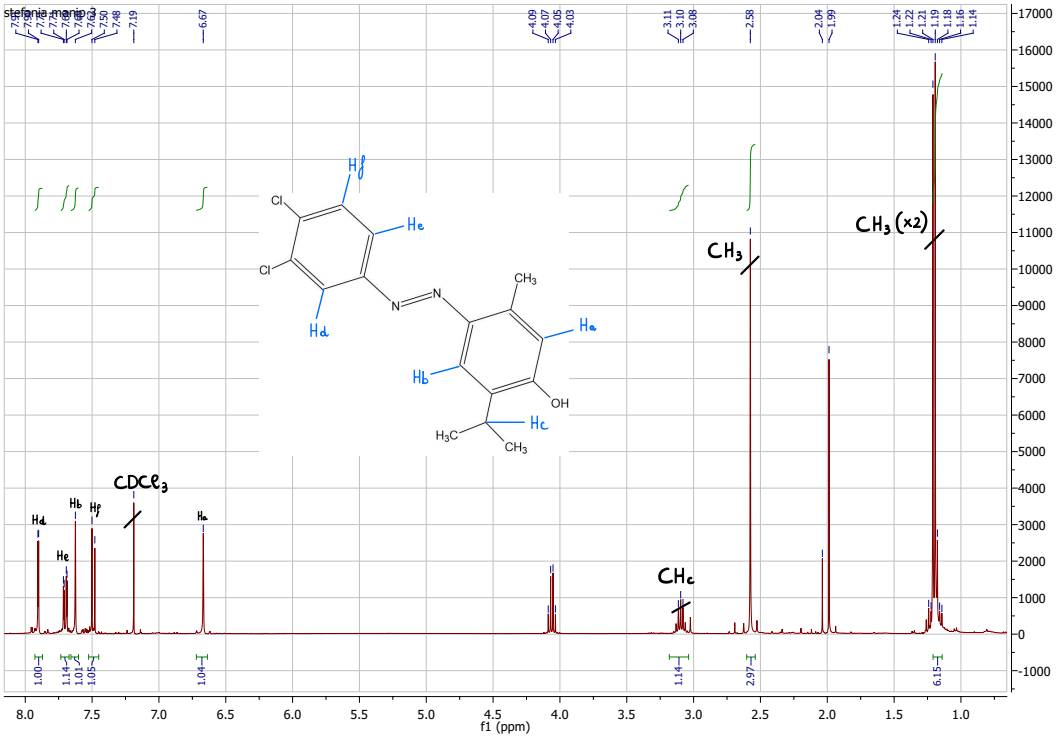

Figure A.4: NMR spectrum 2,5-dimethyl-4-[(E)-(4-nitrophenyl)diazenyl]phenol

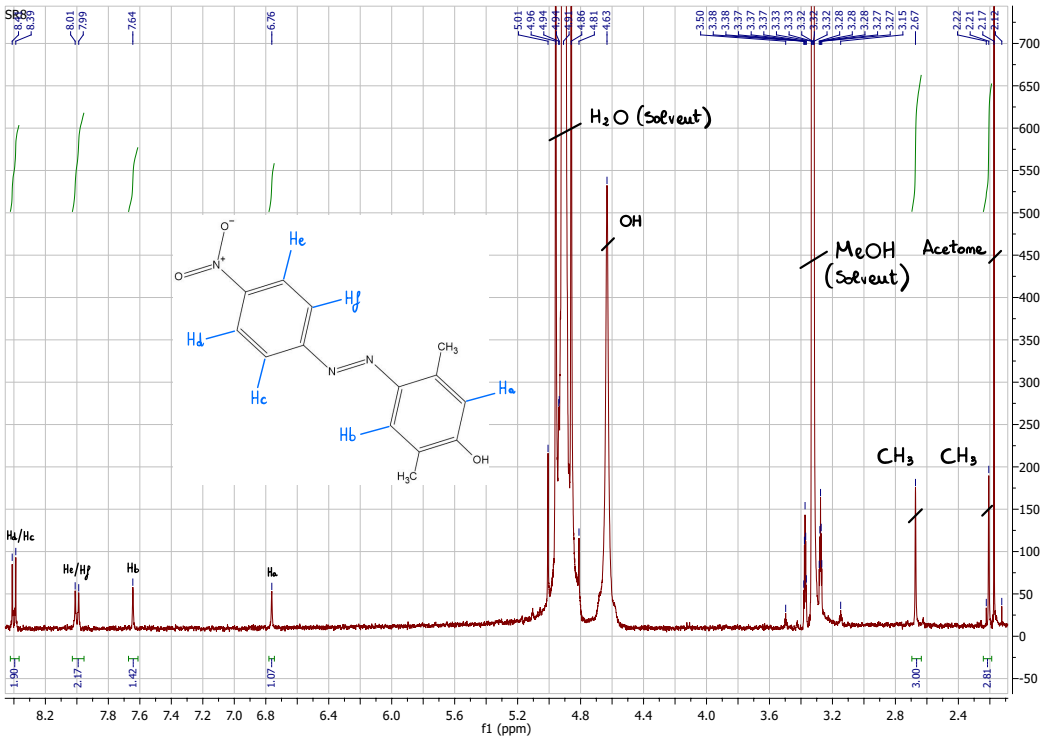

Bibliography

[1] Mayon-White RT; Ducel G; Kereselidze T and Tikomirov E. «An international survey of the prevalence of hospital-acquired infection». In: 20 (Feb. 1988), pp. 43–48 (cit. on p. 1).

[2] Hira Idrees; Samrah Tahir Khan; Maryam Aftab; Asmara Imtiaz. «Nosocomial Infections - A Review». In: *LGU Journal of Life Science* 5 (Mar. 2021) (cit. on p. 1).

[3] Sheila Eckenrode; Anila Bakullari; Mark L. Metersky; Yun Wang; Michelle M. Pandolfi; Deron Galusha; Lisa Jaser; Noel Eldridge. «The Association between Age, Sex, and Hospital-Acquired Infection Rates: Results from the 2009-2011 National Medicare Patient Safety Monitoring System». In: 35 (Oct. 2014) (cit. on p. 1).

[4] Teresa C. Horan; Mary Andrus and Margaret A. Dudeck. «CDC/NHSN surveillance definition of health care–associated infection and criteria for specific types of infections in the acute care setting». In: 36 (2008), pp. 309–332 (cit. on p. 2).

[5] Alemayehu Toma*; Serawit Deyno. «Overview on Mechanisms of Antibacterial Resistance». In: Vol.2, Issue 1 (Jan. 2015) (cit. on p. 2).

[6] Talapko J.; Meštrovi´c T.; Juzbaši´c M.; Tomas M.; Eri´c S.; Horvat Aleksijevi´c L.; Beki´c S.; Schwarz D.; Mati´c S.; Neuberg M. «Antimicrobial Peptides—Mechanisms of Action, Antimicrobial Effects and Clinical Applications». In: (Oct. 2022) (cit. on p. 3).

[7] Hiroshi Yoneyama and Ryoichi Katsu. «Antibiotic Resistance in Bacteria and Its Future for Novel Antibiotic Development». In: (2006) (cit. on p. 4).

[8] Kate P. Langton; Peter J. F. Henderson; Richard B. Herbert*. «Antibiotic resistance: multidrug efflux proteins, a common transport mechanism?» In: (June 2005) (cit. on p. 4).

[9] A.-P. Magiorakos; A. Srinivasan; R. B. Carey; Y. Carmeli; M. E. Falagas; C. G. Giske; S. Harbarth; J. F. Hindler; G. Kahlmeter; B. Olsson-Liljequist; D. L. Paterson; L. B. Rice; J. Stelling; M. J. Struelens; A. Vatopoulos; J. T. Weber and D. L. Monnet. «Multidrug-resistant, extensively drug-resistant and pandrug-resistant bacteria:

an international expert proposal for interim standard definitions for acquired resistance». In: *Clinical Microbiology and Infection* 18 (May 2011), pp. 268–281 (cit. on p. 4).

[10] W. BEREKET; K. HEMALATHA; B. GETENET; T. WONDWOSSEN; A. SOLOMON; A. ZEYNUDIN and S. KANNAN. «Update on bacterial nosocomial infections». In: *European Review for Medical and Pharmacological Sciences* 16 (2016), pp. 1039–1044 (cit. on p. 4).

[11] Shenoi S.; Friedland G. «Extensively Drug-Resistant Tuberculosis: A New Face to an Old Pathogen». In: *Annual Review of Medicine* 60 (2009), pp. 307–320 (cit. on p. 4).

[12] Urban-Chmiel R.; Marek A.; Stepien-Pysniak D.; Wieczorek K.; Dec M.; Nowaczek A.; Osek J. «Antibiotic Resistance in Bacteria—A Review». In: (Aug. 2022) (cit. on p. 4).

[13] Gram H.C. «Über die isolierte Färbung der Schizomyceten in Schnitt- und Trockenpräparaten». In: *Fortschritte der Medizin (in German)* 2 (1884), pp. 185–189 (cit. on p. 5).

[14] Tânia A.T. Gomes; Waldir P. Elias; Isabel C.A. Scaletsky; Beatriz E.C. Gutha; Juliana F. Rodriguesc; Roxane M.F. Piazzab; Luís C.S. Ferreirac; Marina B. Martinez. «Diarrheagenic Escherichia coli». In: *Brazilian journal of microbiology* (Nov. 2016) (cit. on p. 6).

[15] James P. Nataro; Theodore Steiner and Richard L. Guerrant. «Enteroaggregative Escherichia coli». In: 4 (1998) (cit. on p. 6).

[16] Dautzenberg MJD; Haverkate MR; Bonten MJM; et al. «Epidemic potential of Escherichia coli ST131 and Klebsiella pneumoniae ST258: a systematic review and meta-analysis». In: *BMJ Open* (Jan. 2016) (cit. on p. 6).

[17] Keith Poole. «Multidrug resistance in Gram-negative bacteria». In: *Elsevier Science Ltd* 4 (2001), pp. 500–508 (cit. on p. 6).

[18] Erko Stackebrandt; Cathrin Koch; Oxana Gvozdiak and Peter Schumann. «Taxonomic Dissection of the Genus Micrococcus». In: *INTERNATIONAL JOURNAL OF SYSTEMATIC BACTERIOLOGY* (Oct. 1995), pp. 682–692 (cit. on p. 6).

[19] Beata Mlynarczyk-Bonikowska; Cezary Kowalewski; Aneta Krolak-Ulinska and Wojciech Marusza. «Molecular Mechanisms of Drug Resistance in Staphylococcus aureus». In: (July 2022) (cit. on p. 6).

[20] Caillan Crowe-McAuliffe; Michael Graf; Paul Huter; Hiraku Takada; Maha Abdelshahid; Jirí Novácek; Victoriia Murinab; Gemma C. Atkinson; Vasili Hauryliuk and Daniel N. Wilson. «Structural basis for antibiotic resistance mediated by the Bacillus subtilis ABCF ATPase Vml». In: 115 (Sept. 2018), pp. 8978–8983 (cit. on p. 6).

[21] Michael Otto. «Staphylococcus epidermidis – the "accidental" pathogen». In: (Aug. 2009) (cit. on p. 7).

[22] Zhenfen Zhang and Zhibiao Nan. «Erwinia persicina, a possible new necrosis and wilt threat to forage or grain legumes production». In: *European Journal of Plant Pathology*. Springer, Feb. 2014 (cit. on p. 7).

[23] Gálvez L.; Gil-Serna J.; García-Díaz M. and Palmero D. «First report of a garlic bulb rot caused by Erwinia persicina in Europe». In: (May 2015) (cit. on p. 7).

[24] CAROLINE M. O'HARA; ARNOLD G. STEIGERWALT; BERTHA C. HILL; J. MICHAEL MILLER and DON J. BRENNER. «First Report of a Human Isolate of Erwinia persicinus». In: *JOURNAL OF CLINICAL MICROBIOLOGY* (Jan. 1998), pp. 248–250 (cit. on p. 7).

[25] LYSIANE HAUBEN; EDWARD R. B. MOORE; Luc VAUTERIN; MARIJKE STEENACKERS; JORIS MERGAERT; LINDA VERDONCK; and JEAN SWINGS. «Phylogenetic Position of Phytopathogens within the Enterobacteriaceae». In: *Systemtic and applied microbiology* 21 (Feb. 1998), pp. 384–397 (cit. on p. 7).

[26] X. Duarte; C.T. Anderson; M. Grimson; R.D. Barabote; R.E. Strauss; L.S. Gollahon; M.J.D. San Francisco. «Erwinia chrysanthemi strains cause death of human gastrointestinal cells in culture and express an intimin-like protein». In: *FEMS Microbiology Letters* (Mar. 2000), pp. 81–86 (cit. on p. 7).

[27] Karim Naghmouchi; Christophe Le Lay; John Baah; Djamel Drider. «Antibiotic and antimicrobial peptide combinations: synergistic inhibition of Pseudomonas fluorescens and antibiotic-resistant variants». In: *Elsevier Masson SAS* 163 (Nov. 2011), pp. 101–108 (cit. on p. 7).

[28] Harsh Kumar; Laura Franzetti; Ankur Kaushal and Dinesh Kumar. «Pseudomonas fluorescens: a potential food spoiler and challenges advances in its detection». In: *Annals of Microbiology* 69 (July 2019), pp. 873–883 (cit. on p. 7).

[29] *WHO publishes list of bacteria for which new antibiotics are urgently needed*. Tech. rep. World Health Organization, 2018 (cit. on p. 8).

[30] Zahid Mahimwalla; Kevin G. Yager; Jun-ichi Mamiya; Atsushi Shishido; Arri Priimagi and Christopher J. Barrett. «Azobenzene photomechanics: prospects and potential applications». In: *Polymer Bulletin* 69 (June 2012), pp. 967–1006 (cit. on p. 8).

[31] Miriam Di Martino; Lucia Sessa; Martina Di Matteo; Barbara Panunzi; Stefano Piotto and Simona Concilio. «Azobenzene as Antimicrobial Molecules». In: *Molecules* (Sept. 2022) (cit. on pp. 8, 10).

[32] H. M. Dhammika Bandara and Shawn C. Burdette. «Photoisomerization in different classes of azobenzene». In: *Chemical Society Reviews* 41 (2012), pp. 1809–1825 (cit. on pp. 9, 60).

[33] L ABD-ALREDHA R.AL-RUBAIE and R. JAMEEL MHESSN. «Synthesis and Characterization of Azo Dye Para Red and New Derivatives». In: *E-Journal of Chemistry* 9 (June 2011), pp. 465–470 (cit. on p. 10).

[34] Nagham Mahmood Aljamali. «Review in Azo Compounds and its Biological Activity». In: *Biochemistry Analytical Biochemistry* 4 (2015), pp. 1–4 (cit. on p. 11).

[35] Cooper KE. «Theory of antibiotic inhibition zones in agar media». In: *Nature* 176 (1955), pp. 510–1 (cit. on pp. 12, 59).

[36] Bregestovski P. D.; Maleeva G. V. «Photopharmacology: A Brief Review Using the Control of Potassium Channels as an Example». In: *Neuroscience and Behavioral Physiology* 49 (2) (2019), pp. 184–191 (cit. on p. 12).

[37] Leippe P.; Frank J. A. «Designing Azobenzene-Based Tools for Controlling Neurotransmission». In: *Current Opinion in Structural Biology* 57 (2019), pp. 23–30 (cit. on p. 12).

[38] Wegener M.; Hansen M.J.; Driessen A.J.; Szymanski W.; Feringa B.L. «Photocontrol of antibacterial activity: Shifting from UV to red light activation». In: *Journal of the American Chemical Society* 139 (2017), pp. 17979–17986 (cit. on p. 12).

[39] Ventura C.R.; Wiedman G.R. «Substituting azobenzene for proline in melittin to create photomelittin: A light-controlled membrane active peptide». In: *Biochimica et Biophysica Acta (BBA)* 1863 (2021) (cit. on p. 12).

[40] Prakash S.; Somiya G.; Elavarasan N.; Subashini K.; Kanaga S.; Dhandapani R.; Sivanandam M.; Kumaradhas P.; Thirunavukkarasu C.; Sujatha V. «Synthesis and characterization of novel bioactive azo compounds fused with benzothiazole and their versatile biological applications». In: *Journal of Molecular Structure* 1224 (2021) (cit. on p. 12).

[41] Kaur H.; Narasimhan B. «Antimicrobial activity of diazenyl derivatives: An update». In: *Current Topics in Medicinal Chemistry* 18 (2018), pp. 3–21 (cit. on p. 12).

[42] Peddie V.; Abell A.D. «Photocontrol of peptide secondary structure through non-azobenzene photoswitches». In: *Journal of Photochemistry and Photobiology C: Photochemistry Reviews* 40 (2019), pp. 1–20 (cit. on p. 12).

[43] Kaur H.; Lim S.M.; Ramasamy K.; Vasudevan M.; Shah S.A.A.; Narasimhan B. «Diazenyl schiff bases: Synthesis, spectral analysis, antimicrobial studies and cytotoxic activity on human colorectal carcinoma cell line (HCT-116)». In: *Arabian Journal of Chemistry* 13 (2020), pp. 377–392 (cit. on p. 12).

[44] Pałasz A.; Ciez D.; Trzewik B.; Miszczak K.; Tynor G.; Bazan B. «In the search of glycoside-based molecules as antidiabetic agents». In: *Topics in Current Chemistry* 377 (2019), p. 19 (cit. on p. 12).

[45] Nafeesa Naeem; Ehsan Ullah Mughal; Munirah M. Al-Rooqi; Nizar El Guesmi; Ziad Moussa; Saleh A. Ahmed Reem I. Alsantali; Qandeel Alam Raja; Abdullah Y.A. Alzahrani; Amina Sadiq d. «Miscellaneous azo dyes: a comprehensive review on recent advancements in biological and industrial applications». In: *Dyes and Pigments* 199 (2022) (cit. on pp. 12, 13).

[46] Sweeney EA; Chipman JK; Forsythe SJ. «Evidence for direct-acting oxidative genotoxicity by reduction products of azo dyes». In: *Environ Health Perspect* 102 (1994), pp. 119–22 (cit. on p. 13).

[47] Ali H.M.; Badr S.Q.; Al-Kinani M.F.H. «DNA Binding three Azo Dyes as new Antibiotics». In: *In IOP Conference Series: Materials Science and Engineering* 571 (2019) (cit. on pp. 13, 14).

[48] Hu Y.; Zou W.; Julita V.; Ramanathan R.; Tabor R. F.; Nixon-Luke R.; Bryant G.; Bansal V.; Wilkinson B. L. «Photomodulation of Bacterial Growth and Biofilm Formation Using Carbohydrate-Based Surfactants». In: *Chemical Science* 7 (2016), pp. 6628–6634 (cit. on p. 14).

[49] Piotto S.; Concilio S.; Sessa L.; Porta A.; Calabrese E. C.; Zanfardino A.; Varcamonti M.; Iannelli P. «Small Azobenzene Derivatives Active against Bacteria and Fungi». In: *European Journal of Medicinal Chemistry* 68 (2013), pp. 178–184 (cit. on p. 14).

[50] Piotto S.; Concilio S.; Sessa L.; Diana R.; Torrens G.; Juan C.; Caruso U.; Iannelli P. «Synthesis and Antimicrobial Studies of New Antibacterial Azo-Compounds Active against Staphylococcus Aureus and Listeria Monocytogenes». In: *Molecules* 22 (2017) (cit. on p. 14).

[51] Piotto S.; Concilio S.; Sessa L.; Iannelli P.; Porta A.; Calabrese E. C.; Galdi M. R.; Incarnato L. «Novel Antimicrobial Polymer Films Active against Bacteria and Fungi». In: *Polymer Composites* 34 (2013), pp. 1489–1492 (cit. on p. 14).

[52] Velema W.A.; Van Der Berg J.P.; Hansen M.J.; Szymanski W.; Driessen A.J.; Feringa B.L. «Optical control of antibacterial activity». In: *Nature Chemistry* 5 (2013), pp. 924–928 (cit. on p. 15).

[53] C. Sun; H. Li; H. Yin; Y. Li; Y. Shi. «Effects of the cyano substitution at different positions on the ESIPT properties of alizarin: A DFT/TD-DFT investigation». In: *Journal of Molecular Liquids* 269 (2018), pp. 650–656 (cit. on p. 15).

[54] P. Ezati; J.-W. Rhim; M. Moradi; H. Tajik; R. Molaei. «CMC and CNF-based alizarin incorporated reversible pH-responsive color indicator films». In: *Carbohydrate polymers* 246 (2020) (cit. on p. 15).

[55] P. Ezati; H. Tajik; M. Moradi; R. Molaei. «Intelligent pH-sensitive indicator based on starch-cellulose and alizarin dye to track freshness of rainbow trout fillet». In: *International Journal of Biological Macromolecules* 132 (2019), pp. 157–165 (cit. on p. 15).

[56] X. Si; L. Deng; Y. Wang; M. Han; Y. Ding. «An electrochemical sensor for the determination of Luteolin using an alizarin red/carboxylic acid group functionalized carbon nanotube». In: *Microchemical journal* 174 (2022) (cit. on p. 15).

[57] R. Singh; Geetanjali; S.M.S. Chauhan. «9,10-Anthraquinones and other biologically active compounds from the genus rubia». In: *Chemistry Biodivers* 1 (2004), pp. 1241–1264 (cit. on p. 16).

[58] Y. Cai; Q. Luo; M. Sun; H. Corke. «Antioxidant activity and phenolic compounds of 112 traditional Chinese medicinal plants associated with anticancer». In: *Life Science* 74 (2004), pp. 2157–2184 (cit. on p. 16).

[59] T.V. Kharlamova. «Synthesis and HIV-1 RNase H-activity of new alizarin acetonyl derivatives». In: *Chemistry of Natural Compounds* 45 (2009), pp. 629–633 (cit. on p. 16).

[60] J.M. Briggs J. Deng; T. Sanchez; N. Neamati. «Dynamic pharmacophore model optimization: identification of novel HIV-1 integrase inhibitors». In: *Journal of Medicinal Chemistry* 49 (2006), pp. 1684–1692 (cit. on p. 16).

[61] W. Lemlikchi; P. Sharrock; M. Fiallo; A. Nzihou; M.O. Mecherri. «Hydroxyapatite and alizarin sulfonate ARS modeling interactions for textile dyes removal from wastewaters». In: *Procedia Eng.* 83 (2014), pp. 378–385 (cit. on p. 16).

[62] I. Essaidi; A. Snoussi; H.B.H. Koubaier; H. Casabianca; N. Bouzouita. «Effect of acid hydrolysis on alizarin content, antioxidant and antimicrobial activities of Rubia tinctorum extracts». In: *Pigment Resin Technol.* 46 (2017), pp. 379–384 (cit. on p. 17).

[63] Archana A. Bele* and Anubha Khale. «An overview on thin layer chromatography». In: (Jan. 2010), pp. 2–3 (cit. on p. 21).

[64] A. B. Roge*; S. N. Firke; R. M. Kawade; S. K. Sarje and S. M. Vadvalkar. «Brief review on: flash chromatography». In: Vol.2, Issue 8 (July 2011), pp. 1930–1937 (cit. on p. 22).

[65] *Manuel d'utilisation instruments chromatographiques Pure*. BÜCHI. 2023 (cit. on p. 22).

[66] Santosh Kumar Bharti; Raja Roy. «Quantitative 1 H NMR spectroscopy». In: (2012) (cit. on p. 23).

[67] Dominique Marion. «An Introduction to Biological NMR Spectroscopy». In: (2013) (cit. on p. 23).

[68] D. Sue Katz. *The Streak Plate Protocol*. Tech. rep. American society for microbiology, 2008 (cit. on p. 25).

[69] *Instruction manual Eppendorf EpMotion 5070*. Eppendorf SE. 2023 (cit. on p. 30).

[70] Bhargav H. S.; Sachin D. Shastri; Poornav S. P.; Darshan K. M. and Mahendra M. Nayak. «Measurement of the Zone of Inhibition of an Antibiotic». In: (Feb. 2016), pp. 409–410 (cit. on p. 32).

[71] Boyan Bonev*; James Hooper and Judicae¨l Parisot. «Principles of assessing bacterial susceptibility to antibiotics using the agar diffusion method». In: (Feb. 2008) (cit. on pp. 32, 60).

[72] Cooper KE; Woodman D. «The diffusion of antiseptics through agar gels, with special reference to the agar cup assay method of estimating the activity of penicillin.» In: *Journal of pathology and Bacteriology* 58 (1946), pp. 75–84 (cit. on pp. 59, 60).